Dissertation

Role of Prostaglandin D_2 Receptors in Monocyte/Macrophage Function in Pulmonary Inflammation

Katharina JANDL, BSc. MSc.

For the Academic Degree of Doctor of Philosophy

(PhD)

at the Medical University of Graz

Institute of Experimental and Clinical Pharmacology

Under the supervision of Prof. Dr. Akos HEINEMANN

2016

Statuary Declaration

I hereby declare that this thesis is my own original work and that I have fully acknowledged by name all of those individuals and organisations that have contributed to the research for this thesis. Due acknowledgement has been made in the text to all other material used. Throughout this thesis and in all related publications I followed the "Standards of Good Scientific Practice and Ombuds Committee at the Medical University of Graz"

Graz, 18.07.2016

Table of content

ABSTRACT

Prostaglandin (PG) D_2 is released during the early-phase of inflammation. This lipid mediator exerts its bioactive potential via its two D-type prostanoid (DP) receptors, DP1 and DP2 (also called CRTH2 for chemoattractant receptor homologous molecule expressed on Th2 cells). Both receptors are reported to be associated with distinct biological effects, DP2 being clearly proinflammatory, while the role of DP1 in inflammation has still remained unclear. Up to now, the potential of PGD_2 in the regulation of macrophage function and its role in the early phase of experimental acute lung-injury has not been elucidated yet.

Here, we could show for the first time that human monocyte-derived macrophages express functional PGD_2 receptors. Activation of either PGD_2 receptors led to intracellular Ca^{2+} signaling that resulted in migration of macrophages. In contrast, stimulation of DP2, but not DP1 induced cytokine release in a NFκB-dependent fashion. These proinflammatory effects were transferable to *in-vivo* responses during the early phase of LPS-induced acute lung injury in mice. PGD_2 treatment, as well as the specific activation of either DP1 or DP2 receptors, led to aggravated pulmonary inflammation visible by increased neutrophilic alveolitis, myeloperoxidase activity and airway hyperreactivity in lung function testing. Alveolar macrophages could be identified as a driving source of increased cytokine secretion upon exogenous PGD_2 treatment and depletion of alveolar macrophages proved to inhibit the augmented inflammatory reactions caused by PGD_2. Furthermore, blockade of endogenous PGD_2 diminished neutrophil recruitment into both alveolar and pulmonary interstitial space. Most importantly, we could identify neutrophil migration and survival as two pathways in which activation of PGD_2 receptors on macrophages influences neutrophil function. Interestingly, we detected the presence of the hematopoietic prostaglandin D synthase (HPGDS) – the rate-limiting enzyme of PGD_2 production –and the receptors for PGD_2 on alveolar macrophages in humans. The increased expression of HPGDS in the lungs of patients with acute-respiratory distress syndrome suggests an autocrine feed-back loop of HPGDS-PGD_2-DP1-DP2 action on macrophages.

This study extents the existing knowledge of PGD_2 pharmacology and action on immune cells by showing the presence and functionality of PGD_2 receptors on human monocyte-derived macrophages. Activation of the latter increased pulmonary inflammation by enhancing neutrophil function. Thus PGD_2 receptors on macrophages might prove a potential therapeutic target during acute inflammatory pulmonary diseases.

ZUSAMMENFASSUNG

In der frühen Phase einer Entzündungsreaktion kommt es zur Freisetzung von Prostaglandin (PG) D_2. Dieser Lipidmediator entfaltet seine biologische Wirkung über zwei spezifische Rezeptoren, die D-Typ Prostanoid Rezeptoren DP1 und DP2 (auch genannt CRTH2 für "chemoattractant receptor homologous molecule expressed on Th2 cells"). Die Aktivierung beider Rezeptoren wurde bis jetzt mit unterschiedlichen biologischen Auswirkungen und Effekten assoziiert. Dabei nimmt DP2 eine eindeutig entzündungsfördernde Funktion wahr, wohingegen die Rolle der DP1 Aktivierung noch nicht vollständig geklärt wurde. Weiters wurde das Potential von PGD_2 in der Regulierung der Funktionen von Makrophagen sowie die Rolle von PGD_2 in der frühen Phase eines experimentellen Modells zu akutem Lungenversagen bis jetzt noch nicht erforscht.

In dieser Arbeit konnten wir zum ersten Mal zeigen, dass humane Makrophagen mit monozytärer Abstammung funktionale PGD_2 Rezeptoren exprimieren. Die gesonderte Aktivierung der jeweiligen PGD_2 Rezeptoren führt zu einer Aktivierung eines intrazellulären Ca^{2+} Signalwegs, der die Migration der Makrophagen zur Folge hatte. Im Gegensatz dazu führte nur die Stimulierung der DP2 Rezeptoren, nicht aber der DP1 Rezeptoren, zu einer NFκB-abhängigen Zytokin-Freisetzung. Diese entzündungsfördernden Prozesse waren auch in ein *in-vivo* Modell transferierbar, welches die frühe Phase des experimentellen akuten Lungenversagens nachahmt. PGD_2-Behandlung, sowie auch die selektive Aktivierung von DP1 und DP2 Rezeptoren, führte zu einer Erschwerung der pulmaren Entzündung, welche sich durch verstärkte neutrophile Alveolitis, Myeloperoxidase-Aktivität und Atemwegshyperreagibilität im Lungenfunktionstest zeigte. Zusätzlich weisen unsere Ergebnisse daraufhin, dass Makrophagen eine treibende Kraft in der erhöhten Zytokinproduktion darstellen, da Makrophagen-Depletierung die PGD_2-induzierte Verstärkung der Entzündungsreaktion verhindert. Zusätzlich verringerte sich auch die Neutrophilen-Infiltration sowohl in dem Alveolar- als auch in dem interstitiellen Bereich. Weiters konnten wir zwei mögliche Wege identifizieren, über die PGD_2 mittels Makrophagen die Neutrophilen-Funktion verstärkt,– nämlich über erhöhte Migration und eine verlängerte Überlebensdauer von Neutrophilen. Interessanterweise fanden wir auch eine beachtliche Expression der hematopoietischen Prostaglandin D Synthase (HPGDS) – das Schlüssel-Enzym der PGD_2-Produktion – und der dazugehörigen PGD_2 Rezeptoren auf humanen Alveolarmakrophagen. Die erhöhte

Expression der HPGDS in Patienten mit akutem Lungenversagen weist zusätzlich auf einen autokrinen Feedback-Mechanismus von HPGDS-PGD_2-DP1-DP2 hin.

Diese Studie erweitert damit das vorhandene Wissen über die Pharmakologie von PGD_2 und dessen Einfluss auf Immunzellen, indem sie sowohl die Präsenz als auch die Funktionalität von PGD_2 Rezeptoren auf humanen Makrophagen zeigen konnte. Die Aktivierung der Rezeptoren führte über Erhöhung der Neutrophilen-Aktivität zu einer Verstärkung der pulmonalen Entzündung. Daher könnten PGD_2 Rezeptoren auf Makrophagen einen neuen therapeutischen Angriffspunkt in der Behandlung akuter entzündlicher Prozesse der Lunge darstellen.

ABBREVIATIONS

ABC	ATP-binding cassette
ALI	Acute lung injury
AM	alveolar macrophage
ARDS	acute respiratory distress syndrome
BALF	bronchoalveolar lavage fluid
BMDM	bone-marrow-derived macrophages
cAMP	cyclic adenosin monophosphate
CRTH2	chemoattractant receptor homologous molecule expressed on Th2 cells
COPD	chronic obstructive pulmonary disease
COX	cyclooxygenase
CR	complement receptor
DC	dendritic cells
DP	D-type receptor
ERK	extracellular signal-regulated kinase
GM-CSF	granulocyte macrophage-colony stimulating factor
GPCR	G-protein-coupled receptor
GST	glutathions-s-transferase
HPGDS	hematopoietic prostaglandin D synthase
HSC	hematopoietic stem cell
ICAM	intracellular adhesion molecule

IFN	interferon
Ig	Immunoglobin
IL	interleukin
JAK	Janus kinase
JNK	JUN N-terminal kinase
LFA	lymphocyte functional antigen
LPS	lipopolysaccharide
MAPK	p38 mitogen-activated protein kinase
MARCO	Macrophage receptor with collagenous structure
MCP	monocyte-chemoattractant protein
M-CSF	granulocyte macrophage-colony stimulating factor
MDM	monocyte-derived macrophages
MMP	matrix metalloproteinase
MR	mannose receptor
MRP	multidrug resistance protein
P3C	Pam3CSK4
PAMP	pathogen-associated-molecular patterns
PBS	phosphate-buffered saline
PEEP	positive end-expiratory pressure
PG	prostaglandin
PLC	phospholipase C
PPARγ	peroxisome proliferator-activated receptor γ

PPR	pathogen recognition receptors
ROS	reactive-oxygen species
SNP	single-nucletoide polymorphism
SR	scavenger receptor
TGF	transforming growth factor
TLR	Toll-like receptors
TNF	tumor-necrosis factor
TREM	triggering receptor expressed on myeloid cells
Tx	thromboxane
VCAM	vascular cell adhesion molecule
VLA	very late antigen
7TM	seven-transmembrane

ACKNOWLEDGEMENTS

During my PhD studies, which I performed at the Institute of Experimental and Clinical Pharmacology, I have gained a deeper knowledge in the scientific field of inflammation. Although my learning experience will probably and hopefully continue through my entire life, I could not have gotten a better foundation than the one I received during my studies.

Especially, I want to express my dearest gratitude to my supervisor, Prof. Akos Heinemann, who made me the scientist that I am now. Using his deep knowledge, broad experience and useful guidance, he was a great supervisor – always helpful, always challenging. Furthermore, I would like to thank Prof. Rufina Schuligoi for her scientific support and help at any time I needed it.

All the work I enjoyed would not have been the same, if it weren't for the pleasant and inspiring atmosphere at the entire institute. My special thanks are reserved for Kathrin Rohrer, Iris Red, Martina Ofner, Wolfgang Platzer and Ilse Lanz.

I would also like to mention fellow PhD Students, Ida Aringer, Robert Frei and Anna Theiler with whom I had the pleasure to share an office.

I am more than greatly indebted to the perfectly organized PhD program DK-MOLIN, which has been generously supported by the Austrian Science Funds FWF (Grant W1241) and the Medical University of Graz. All classes, all lectures and all courses broadened my scientific knowledge. Furthermore, I had the opportunity of presenting my work at international scientific congresses – a priceless and important experience in scientific life.

I can truly count myself a lucky person, to have such a supporting and loving family. Each person contributed to the work that is summarized here. First of all my parents, Ari and Andrea, who not only made my former education possible but also continued their support during my PhD studies – I could not be more grateful. My grandparents need special mention in this section as well, as they are wonderful persons and always proud of their grandchild.

My boyfriend, Rainer, showed immense and never-ending emotional and physical support, whenever needed and without being asked – I truly appreciate it. And special thanks to my sister who, although still in training for a psychologist, already showed a great skill in being one!

1. INTRODUCTION

1.1 Macrophagesin inflammation

1.1.1 Macrophage origin

With the discovery of phagocytosis by Elie Metchnikoff in 1862 a new field in science emerged – the study of innate immunity and the study of macrophages. The finding of professional phagocytes, as well as the newly put emphasis on macrophages and other leukocytes as key players of inflammatory responses, was rewarded with a Nobel Prize in 1908. Macrophages were first described as cells that were able to ingest bacteria and other microbes (1) and thus act as a first line defense mechanism.

Declaring macrophages as professional phagocytes would only insufficiently describe them though. Amongst immune cells, macrophages play a pivotal role, due to their evolutionary, ontological as well as functional characteristics. Evolutionary, they are the oldest and most preserved immune cells, as they evolved around 500 million years ago (2–4). Additionally, research in the early 19th century led to a series of newly discovered cells, including several cells that later will have proved to be tissue specific macrophages, including Kupffer cells found in the liver or skin-specific Langerhans cells (5).

Their ontological origin was then described in the 1960 when van Furth and Crohn proposed that all tissue macrophages originate from circulating peripheral blood monocytes (6). This belief prevailed over the next four decades until only recently more evidence accumulated that there are different ontological origins of tissue macrophages. Amongst an entity of tissue macrophages that act together in performing specialized function, there can be a population that is replenished from circulating blood monocytes, as well as a population that is independent on the steady input from monocytes (7–10). This population of extraembryonic yolk-sac-derived macrophages expands during early gestation even before the appearance of hematopoietic stem cells (HSC). Transcription factor dependency and genetic fate-mapping can be used to study macrophage ontogeny. HSC progenitors and yolk-sac-derived progenitors show a differential dependence on transcription factors Myb as well as PU.1 (10–12). HSCs completely rely on Myb but are independent on PU.1 while yolk-sac-derived macrophages show the opposite pattern. Embryonic Myb-deficiency did not prevent the appearance of macrophages in a series of organs, such as liver, epidermis and brain (10) indicating a compartment of tissue

macrophages that is established prenatally and independent of definitive hematopoiesis. The inducible runt-related transcription factor Runx1is expressed in a proportion of adult microglia but its positive progenitors are found early in gestation before the appearance of definitive HSCs (13). A limitation in using Runx-1 tracking approaches is that labeling must happen in the early developmental stages. Labeling in later stages will obscure the findings as a mixture between yolk-sac-derived as well as HSCs-derived macrophages and blood monocytes will be tracked. Unlike Runx1, using the inducible $Csf1r^{CreER}$ for fate-mapping analysis does not result in labeled blood monocytes. $Csf1r^{CreER}$ experiments could confirm an almost exclusive yolk-sac origin of microglia but also suggested the presence of yolk sac-derived macrophages in the liver as well and the heart (7). The entity of adult-definitive-HSC-derived cells that will give rise to the different lineages – lymphoid, myeloid, erythroid and megakaryocyte – will all go through a FLT3+ stage and thus $FLT3^{Cre}$ can be used to specifically track definitive-HSCs-derived macrophages (14). While researchers have already accomplished huge progress in describing the origin of several specific types of macrophages, the ontological origin of alveolar macrophages still remains uncertain. Macrophages can only be found in the alveolar region of mice shortly after birth and have been described to originate from HSC-derived peripheral blood monocytes in a granulocyte macrophage-colony stimulating factor (GM-CSF)-dependent manner. Despite their monocyte-precursor ontology, their steady-state pool cannot completely be replenished by circulating monocytes (8). Taken together this recent evidence provides new knowledge about the origin of tissue macrophages. It is now clear, that not all macrophages are derived from a common hematopoietic stem-cell precursor, but that a 2^{nd} population arises early in gestation in a c-myb-dependent way prior to the development of definitive HSCs (Fig. 1). Although scientists were also able to describe a proportion of tissue macrophages that is independent of monocyte replenishment, it still remains unclear whether the self-sustaining capacity of tissue macrophages is due to self-renewal or through local proliferation (15).

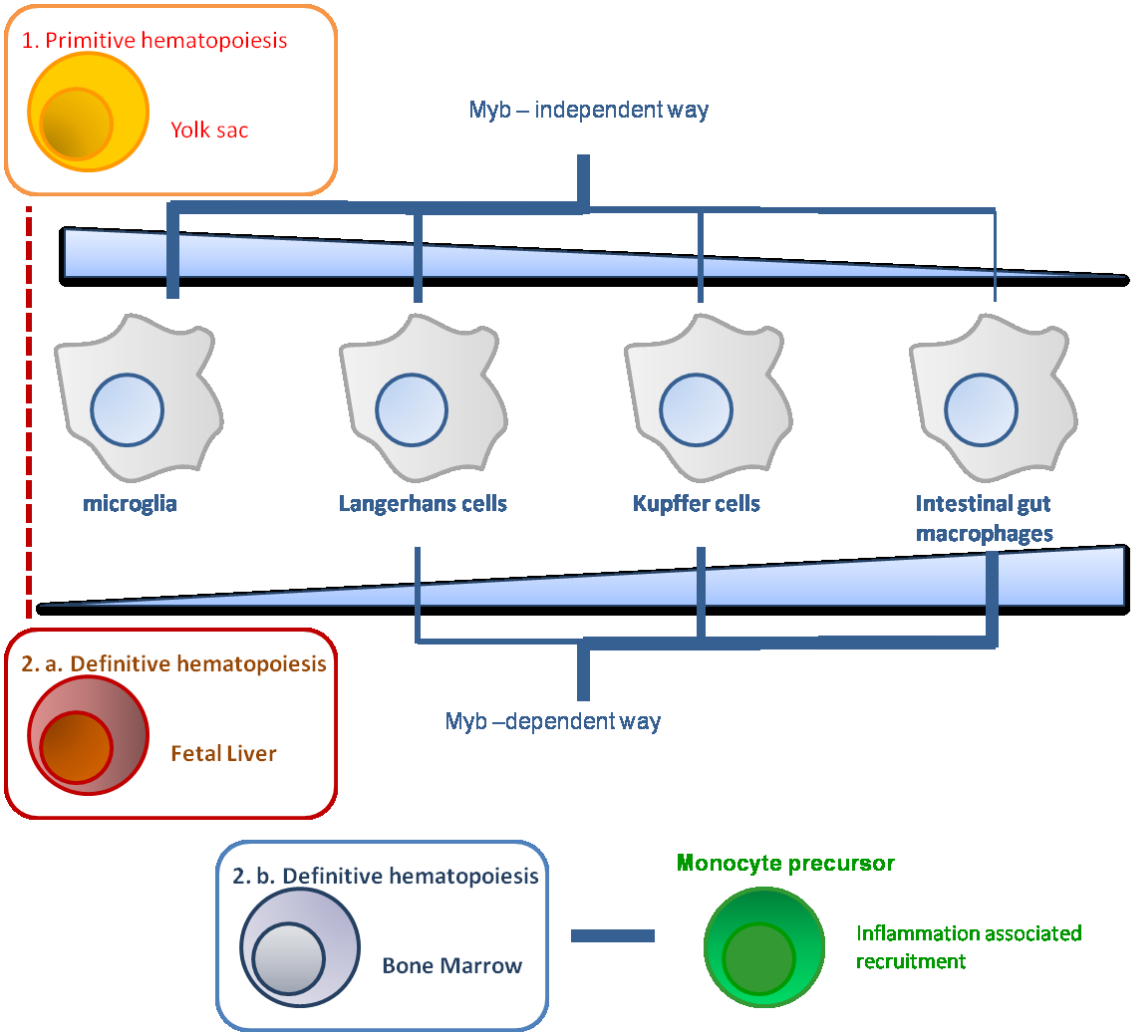

Figure 1. Macrophage origin. Development of macrophages starts in the yolk sac with a process known as primitive hematopoiesis, during which, in a c-myb-independent way, macrophages start to disseminate without a monocytic intermediate. After the colonolization of the fetal liver by aorto-gonad-mesonephors-derived HSCs, definitive hematopoiesis takes over. C-myb-dependent macrophages further colonize different tissues and the major hematopoietic lineages are generated. Myeloid-lineage-derived fetal liver monocytes give rise to tissue macrophages that either coexist with yolk-sac tissue macrophages or can even outcompete the latter. This population of tissue macrophages can be maintained without input from bone marrow-macrophages. Both yolk sac-macrophages as well as fetal liver-derived macrophages show a potential of self-renewal and/or proliferation that is absent in bone marrow-macrophages. The bone marrow is the subsequent organ of hematopoiesis and the source of blood monocyte-precursors that can then constantly replenish tissue macrophages under inflammatory conditions such as damage or infections. Figure adapted from (18).

1.1.2 Monocyte subsets and functions

Pathological processes can trigger extravasation of monocytes from the circulation into tissues and a subsequent differentiation into tissue macrophages (16). Although it is now generally accepted that the majority of tissue macrophages is independent of moncytic input, monocytes do show a capacity of replenishing tissue macrophages under inflammatory conditions. Thus in agreement with their function, monocytes should be viewed as a distinct compartment of effector cells (17,18). In 1989 Passlick et al. demonstrated two distinct monocyte subsets in humans according to their differential expression of CD16 and CD14 (19) that have been expanded into three subsets by Ziegler-Heitbrock et al. in 2010 (20) and are now officially recognized. The classical CD14++CD16-, the intermediate CD14++CD16+ and the non-classical CD14+CD16++ monocytes. Their function is, thus, related to their cell surface expression of CD14 and CD16. The pattern recognition receptor CD14 is a Toll-like receptor (TLR) 4 co-receptor and functions in bacterial lipopolysaccharide (LPS) signaling (21,22). CD14++ monocytes make up the majority of the monocyte pool and act as scavenger cells with a higher phagocytic capacity than non-classical monocytes (23). The classical CD14++/CD16- monocytes also highly express CCR2 and L-selectin (CD62L) which suggests a role in monocyte migration to the lymph nodes and a possible differentiation into dendritic subtypes (24). The CD16 antigen is identified as low-affinity Fc receptor for immunoglobin (Ig)G –FcγRIIIa – and is involved in innate immunity reactions such as immune-complex mediated immune cell activation and differentiation (25,26). The non-classical CD16++ monocytes are implicated in patrolling the endothelium, influencing angiogenesis, and responding to viral infections (21,23,27). CD16+ monocytes also express CCR2 but to a lesser extent than their CD16- counterpart (28,29). The intermediate CD14+CD16+ population is known to expand during inflammatory reaction, and shows a special implication in septic processes (30–32). Their pro-inflammatory role is further substantiated by their abundant tumor-necrosis factor (TNF)α production upon LPS stimulation as well as their inability of interleukin (IL)-10 production (33). In regard of IL-10 production CD14++CD16+ monocytes proved to be the main source (34). Both the classical as well as the intermediate monocytes can be recruited during inflammatory reactions in a CCR2/CCL2 and very late antigen-1(VLA1)/vascular cell adhesion molecule (VCAM)1-dependent way (35). The non-classical monocytes show a strong implication in autoimmune diseases such as rheumatoid arthritis (36,37) and transmigrate the endothelium in a CX3CR1/CCL3 and lymphocyte functional antigen

(LFA)1/intracellular adhesion molecule (ICAM)1-dependent manner (38,39). Following the classification into three main subtypes, it is now evident that along with distinct cell surface expression of CD14 and CD16 come functional differences (Fig. 2).

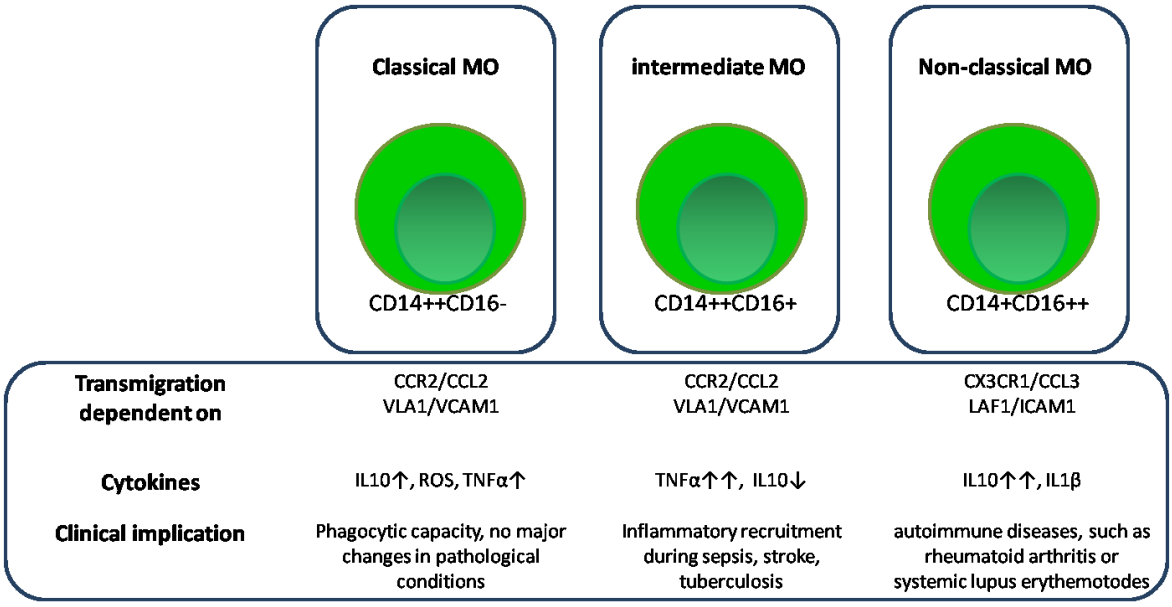

Figure 2. Differences in human monocyte (MO) subsets. Classical CD14++CD16- monocytes exit the bone marrow via a CCR2-dependent fashion and are able to produce IL10 as well as TNFα upon stimulation. Intermediate CCR2 dependent CD14++CD16+ monocytes are now regarded as the inflammatory monocytes that show the highest capacity of TNFα release amongst all subsets. Recruitment during inflammation of classical and intermediate monocytes is mediated by VLA1/VCAM1 interaction. Endothelial transmigration of the non-classical CD14+CD16++ monocytes is mediated by CX3CR1/CCL3 interaction via LAF1/ICAM1-dependent manner. The non-classical monocytes are able to produce large amounts of IL-10 as well as IL1β after inflammatory stimuli. Figure adapted from (35).

1.1.3 Plasticity and function of tissue macrophages

Almost every tissue hosts its own specific type of macrophages, sometimes at abundant levels of up to 10-15% of the total cells in quiescent state. Although tissue macrophages all belong to the same family of immune cells, they are highly specialized in response to their tissue microenvironment which is represented by completely different transcriptional profiles of distinct tissue macrophages (40,41). Despite their high specialization state they share some common functions. In order to maintain tissue homeostasis, they are specialized in phagocytosis and clearance of cellular debris as well as neutralization of

harmful agents or pathogens. It is now believed that tissue macrophages differ from dendritic cells (DCs) in the respect of mobility. While DCs act as sentinals and are highly mobile, tissue macrophages, such as microglia in the nervous system, are likely to only react to their surrounding environment and are mostly non-migratory (18,42). Tissue macrophages are equipped with a variety of receptors that facilitates their guarding and immune surveillance function. Although the expression levels differ in response to local adaption reactions, tissue macrophages express scavenger receptors (SR), pattern recognition receptors (including Toll-like receptors, TLRs, Nod-like receptors, C-type lectin receptors, RIG-I-like receptors), adhesion molecules and cytokine receptors (18). To fulfill their function in defense against pathogens, tissue macrophages show a high bactericidal activity that is attributable to proteases found in their lysosomal compartment (43). Alongside, macrophages rapidly react to inflammatory signals with a repertoire of cytokines and chemokines that orchestrate the inflammatory cascade by recruiting and activating other immune effector cells such as neutrophils, monocytes or lymphocytes. While a quick response is essential to a functional immune system, hyperactivation of macrophages would lead to tissue damage. Thus macrophage activation goes alongside with balancing and silencing reactions, such as deactivation (or alternative activation) of gut macrophages by IL-10 (44,45), transforming growth factor (TGF)-β-mediated silencing of microglia-cell activation (46) or maintenance of a resting state of alveolar macrophages by interaction of the glycoprotein OX-2, CD200, with the CD200 receptor (47,48).

The rapid adaption and response of tissue macrophages to external and internal stimuli leads to a classification of macrophages into classically activated M1 and alternatively activated M2 type macrophages that show proinflammatory and resolving features, respectively. This division is oversimplifying the broad spectrum of macrophage activation, though. It is now suggested to describe macrophages either by their source, by defining their activators – such as LPS, interferon (IFN)γ, IL-4 and so forth -, or by a collection of activation markers (49). Macrophage polarization and plasticity is a useful tool in an organism's defense function to inflammatory stimuli and can be carried out by both tissue macrophages as well as monocyte-derived macrophages (15). *In-vitro* studies mainly use microorganism-derived and/or inflammation–related molecules such as LPS and IFNγ, respectively, to drive macrophages into an activated M1 type, while Th2-related cytokines can be used to polarize macrophages into M2 type. This taxonomy does not truly mirror *in-vivo* processes, where the different activation states are rather merged, and thus

these stimuli should be used in full awareness of this limitation. Recent transcriptome analysis of human macrophages after stimulation with various activation signals by Xue et al. revealed at least 9 different macrophage subtypes, thus well exceeding the former dual classification (50). Therefore, characterization by the stimuli used appears a better choice in classifying the type of macrophages (Fig. 3). This *in-vitro* transcriptome analysis can be further used to study macrophage activation *in-vivo*. Xue et al. used pulmonary macrophages to apply the characterization based on transcriptome analysis on freshly isolated human alveolar macrophages (AM) from nonsmokers, smokers and chronic obstructive pulmonary disease (COPD) patients. AMs from each group revealed a distinct and specific transcriptional program. A glucocorticoid-associated gene module, but also gene-modules associated with IL-4 and IL-13 stimulation, was especially enriched in smokers.

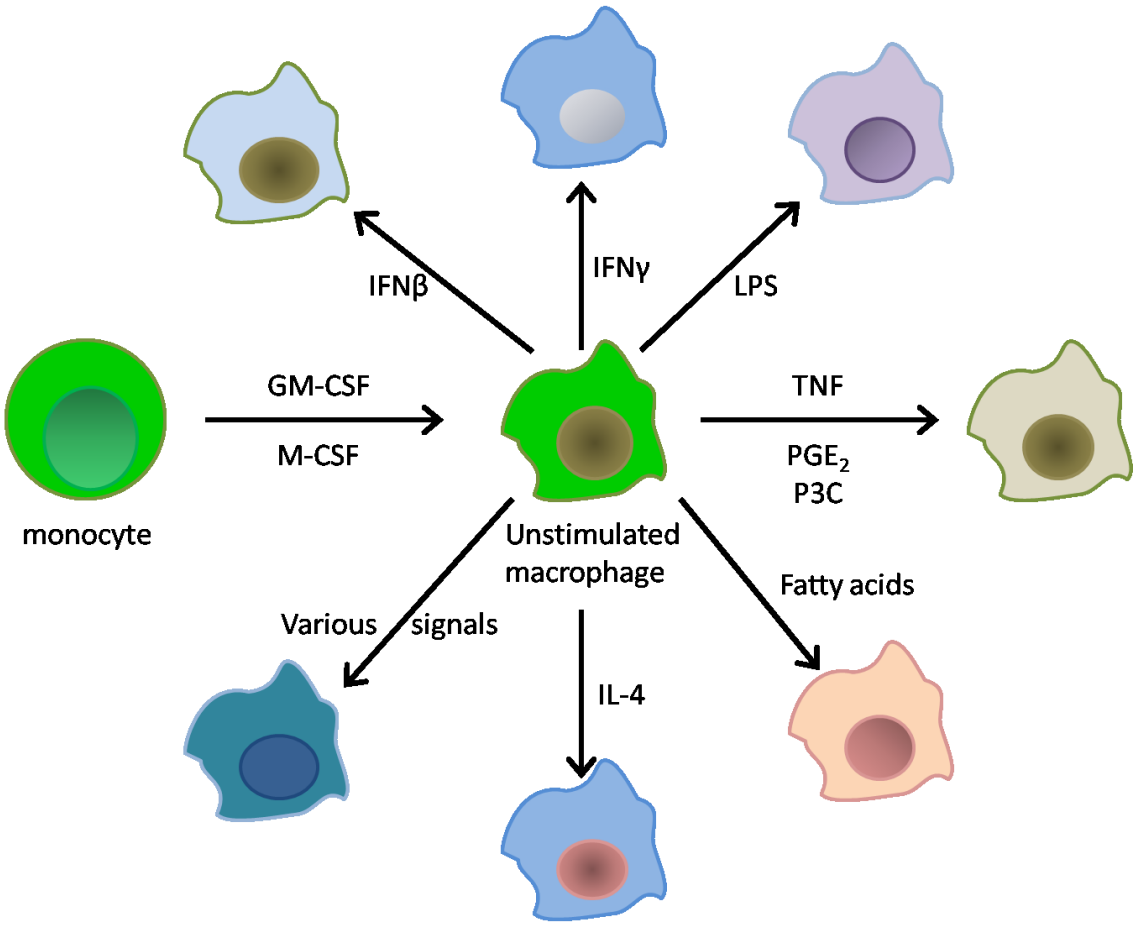

Figure 3. Spectrum of macrophage activation according to different stimuli and specific transcriptome programs. Macrophages react with specific transcriptional programs to a variety of stimuli. Signals that induce those macrophage programs include the classical LPS and IL4 stimulation, but the spectrum is extended and includes TNF, fatty acids, IFNγ, IFNβ,

PGE_2,TLR1/TLR2 agonist Pam3CSK4 (P3C), and other various signals. The specific programs that are induced include gene expression associated with chronic inflammatory responses, cell differentiation, apoptosis, negative regulation kinase activity, metabolic processes, immune responses, leukocyte activation, NFκB pathway activation and other cellular responses.

1.1.4 Pulmonary macrophages

Making up 95% of all cells in naïve bronchoalveolar lavage, macrophages form the majority of the cell load and act as sentinels in maintaining the alveolar integrity and tissue homeostasis. Apart from lymphocytes they are the only cell type found under homeostatic conditions in the alveoli with the constant aim on preventing inflammatory responses (51). In the respiratory tract, air that is drawn is freed from larger particles at the area of the nose and throat, while particles and pathogens of around 5μm diameter get deposited in the alveoli. This is where macrophages need to be located to keep airways clean and to exert their defense function of rapid phagocytosis and killing. This reaction is of fundamental importance as the inner epithelium in the alveoli is only protected by a thin layer of fluid lining the alveoli (52). This fluid, however, contains factors such as IgA, IgG, complement, surfactant and collectins that support the defense function alveolar macrophages and enhance their phagocytic capacity (53). Alveolar macrophages highly express immunoglobin receptor (FcR), complement receptor (CR), mannose receptor (MR or CD206) and other scavenger receptors that bind damage-associated pattern molecules and pathogen-associated pattern molecules (52,54). Thus, the high content of complement and collectins in the alveolar fluid leads to opsonisation of the pathogen and binding to the Fcγ, Fcα, CR and MR on alveolar macrophages. Furthermore, alveolar macrophages express MER tyrosine receptor kinases that are essential in efficient phagocytosis of apoptotic cells. Together with two other tyrosine receptor kinases, Tyro3 and Axl, Mer forms the TAM-receptor family which act as inhibitors of innate inflammatory response to pathogens (55–57). Phagocytosis of unopsonized material, such as non-biological particles, e.g. air pollutants, is mainly mediated by class A scavenger receptors (SR-A) and the macrophage receptor with collagenous structure (MARCO) (58–60). Toxic environmental particulate matter contains small amounts of microbial materials such as endotoxin and thus can activate Toll-like-receptor (TLR) signaling. TLR2 and TLR4 are the ones most associated with binding of particulate matter. While TLR4 signaling is activated after encounter of alveolar macrophages with LPS, which is present on the outer membrane of gram-negative

bacteria, TLR2 signaling is initiated by zymosan (beta-glucans) and peptidoglucan on gram-positive bacteria (58).

Unique among murine macrophages, lung macrophages express high levels of CD11c, but comparably low levels of CD11b – a molecule required in monocyte migration to inflammatory sites – compared to other tissue macrophages (61,62). Characterization of human macrophages proves more complicated because of the low accessibility of samples. Typical macrophage markers such as CD68, CD163 and CD206 are expressed on human alveolar macrophages, but are further upregulated under certain pathological conditions (63,64).

In healthy humans, alveolar macrophages promote tolerance of T-cells and limit immune responses because they constantly induce T cell antigen-specific unresponsiveness. This is due to their poor capability of presenting antigens to T-cells as well as their lack of expression of co-stimulatory molecules such as CD86 (51,65). A study using indomethacin, a cyclooxygenase inhibitor that simultaneously inhibits prostanoid production and shows agonistic features on the D-type receptor 2 (DP2), and neutralizing anti-TGF-β_1 suggests that alveolar macrophages suppress T-cell responsiveness via secretion of diffusible prostaglandins (66).

Ex-vivo human alveolar macrophages show a capability of polarization into IFNγ or IL-4/IL-13 activated macrophages, with a clear upregulation of genes associated with M1 and M2 polarization, respectively. While IFNγ treatment leads to increased expression of TLR2, TLR4, CXC-chemokine ligand 9 (CXCL9), CXCL10 and CC-chemokine ligand 5 (CCL5), IL-4-activated alveolar macrophages increase the expression of genes encoding for the mannose receptor (also known as CD206), several matrix metalloproteinase such as MMP2, MMP7 and MMP9, the tyrosine protein kinase MER, CD163, and the adenosine A3 receptor. As mentioned above, those include two extremes of activated macrophages, which are distinct from each other in respect to expression of gene-clusters, cell-surface markers and function. In healthy human alveoli, a skewing towards an M1 or M2-type is highly debatable. While only about 8% of all alveolar macrophages seem to express IL-13 (67), which is associated with alternative macrophage activation, 50% of them express CD206 (68), one of the most common markers used to characterize alternatively activated macrophages. Thus, so far there is no consensus about a dominant macrophage population in the healthy lung. Especially during pathological conditions, a fine-tuning of activating

and inhibitory signals will assure a macrophage phenotype that meets the immunological needs.

Inadequate macrophage activation is regulated in steady state via soluble factors and cell-cell interaction with the respiratory epithelium. CD200 receptor on alveolar macrophages interact with CD200 ligand expressed by type II alveolar epithelial cells, and inhibits extracellular signal-regulated kinase (ERK), p38 mitogen-activated protein kinase (MAPK) and JUN N-terminal kinase (JNK) inflammatory signaling pathways. IL-10 is found in abundance in the alveolar region of healthy lungs and acts as a repressor of inflammation via the induction of the Janus kinase 1 (JAK1)–signal transducer and activator of transcription 3 (STAT3) pathway that then block the expression of pro-inflammatory cytokines and in microRNA miR-146b-dependent way inhibits TLR4 signalling (69,70) . TGFβ is a regular component in the healthy lung, which is tethered to the epithelium – more specifically to type II alveolar cells – via αvβ6 integrin. TGFβ stimulation on alveolar macrophages then leads to anti-inflammatory signaling via SMAD4 (71).

Pulmonary macrophages are also critical early during development due to their function of phagocytosing apoptotic cells in the fetal lung. After lethal irradiation, monocytes can repopulate the macrophage pool, but furthermore, are also recruited to the site of inflammation following lung injury. This led to the assumption that alveolar macrophage originate from circulating blood monocytes. As with other macrophage populations, this proved only to be partially true. With the use of lineage tracking, investigators could show that alveolar macrophages develop from fetal monocytes and populate the alveoli only after birth. They then reside in the alveoli as long-lived cell with a capacity of self-renewel that are not essentially dependent on the pool replenishment of circulating blood monocytes (8,72,73). Only during injury, including constant exposure to air pollution and cigarette smoke, recruited peripheral blood monocytes differentiate into macrophages and populate the lung. Whether these peripheral blood monocyte-derived macrophages are long lived as well and whether they populate the lung alongside with the fetal monocyte-derived macrophages or even replace the latter still remains unclear.

1.1.5 Macrophages in airway disease

Alveolar macrophages are essential in maintaining lung tissue homeostasis and removing daily cellular debris in the process of efferocytosis. During inflammatory reactions their perfect positioning in the alveoli allows them to rapidly react to pathogenic signals. As

described above, the airway epithelium possesses a variety of tools in regulating and inhibiting macrophage activation. During inflammation, the bronchial epithelial layer may get destructed which results in the loss of dampening signals for macrophages. The absence of epithelial-derived mediators can be beneficial in altering macrophage response to pathogens from a regulatory to a pro-inflammatory state, but cannot solely induce it. For initiation of inflammatory signaling cascades, pro-inflammatory signals must overcome the repressive constitutive mechanisms. Often this is accomplished via multiple-receptor signaling. TLR-signaling requires the help of co-stimulatory molecules such as CD14 and MD-2 and further proinflammatory signaling is only efficient with simultaneous stimulation of receptors for inflammatory cytokines, such as tumor necrosis factor receptor (TNFR), IL-1β receptor (IL-1R) and interferon-γ receptor (IFNGR) (51). In cases when a pathogenic signal passes a certain threshold, the cellular structure gets shattered which results in the loss of regulatory signals and an upregulation of CD14 molecules (74,75) and the pro-inflammatory triggering receptor expressed on myeloid cells (TREM) 1 on alveolar macrophages (76). Furthermore, epithelial cell-derived IL-10R signaling is inhibited by agonistic action on TLR2, TLR4 and TLR9 (77) (Fig. 4).

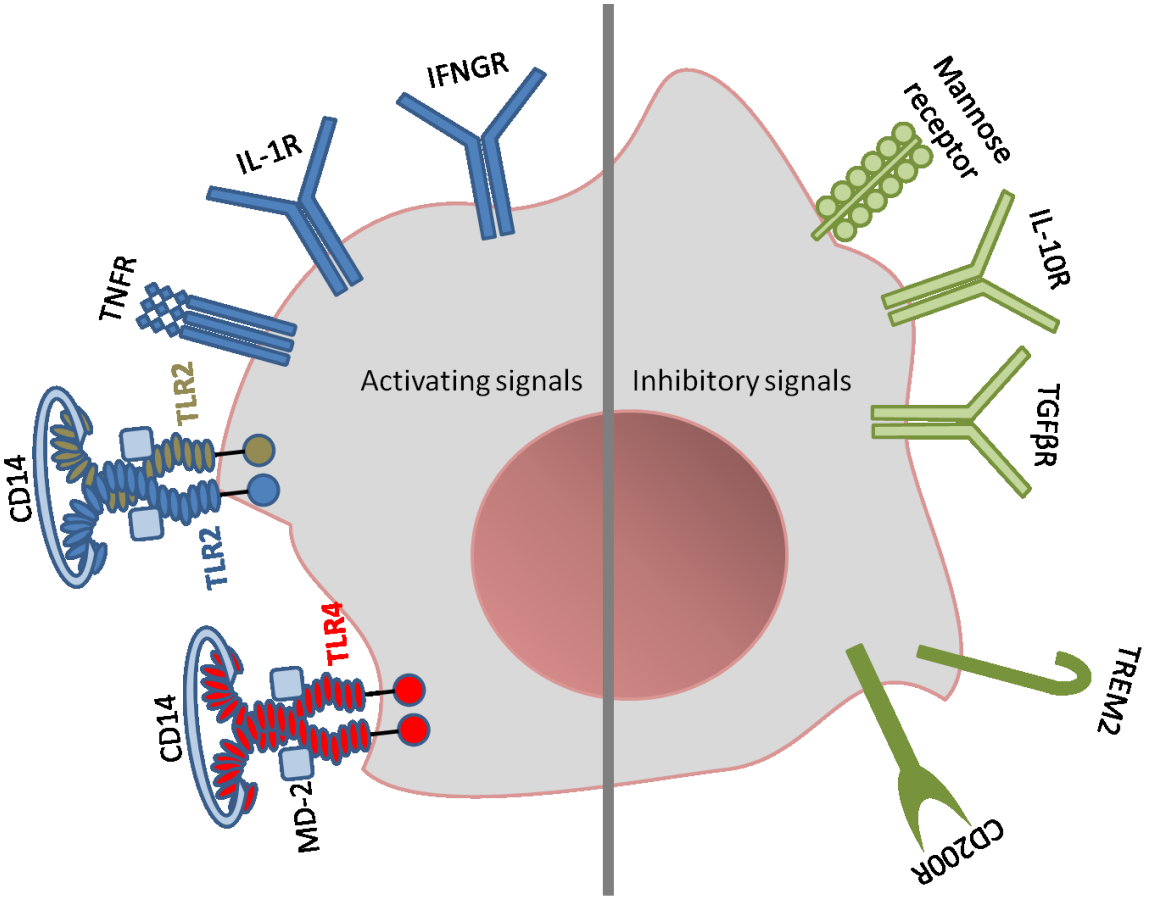

Figure 4. Interplay of pro- and anti-inflammatory signals acting on alveolar macrophages during the initiation of inflammation. Both activating and inhibitory signals are needed to balance appropriate macrophage activation. Cytokine receptors for TNFα, IL-1β and IFNγ are needed in cooperation with activation of TLR and their co-stimulatory molecules, CD14 and MD-2, are needed to perpetuate an initiated inflammation. With a loss of anti-inflammatory signals, such as the absence of macrophage-epithelial cell interaction that mediates signaling via CD200R and TREM2, the homeostatic balance can shift into the activating state. Figure adapted from (51).

Having overcome the immunosuppressive events acting on alveolar macrophages and having initiated a pro-inflammatory state, these cells show increased phagocytic capacity (78) as well as an enhanced production of pro-inflammatory cytokines and increased levels of oxidative burst (79).

With their high plasticity, macrophages can rapidly adapt their phenotype in response to their local microenvironment. Therefore, their role during disease is multifunctional. During certain inflammatory conditions, macrophages can contribute and enhance the inflammatory response. During severe influenza pneumonia, macrophages can produce high levels of IFNβ that lead to increased alveolar epithelial cell injury (80). Furthermore, recruited macrophages increase levels of alveolar epithelial cell apoptosis (81).

Macrophages are critical in clearing the airways from inhaled pathogens. This is achieved by means of phagocytosis/efferocytosis, production of reactive oxygen species and secretion of inflammatory cytokines and chemokines that further attract other immune cells (82). Their function in clearance comes with a damaging influence of alveolar macrophages on other cells. A variety of products are released into the lung microenvironment that lead to injuries of the surrounding cells. This is especially apparent in cystic fibrosis, where macrophage activation leads to a secretion of high levels of TNF, IL-1β, Il-6 and IL-8. Those factors influence the development and the increased inflammatory state in cystic fibrosis (83). A similar picture of hyperreaction by alveolar macrophages is seen during infection with B. cenocepacia (84,85). During idiopathic lung fibrosis, a disease characterized by excessive pulmonary remodeling and deposition of extracellular matrix, macrophages contribute to the fibrotic pathology. Especially initiation of fibrosis via the increased production of TGFβ, TNF, and IL-6 is influenced by alveolar macrophages (82,86,87). TGFβ as well as platelet-derived growth factor, both secreted by

alveolar macrophages, induce the proliferation of myofibroblasts and thus lead to increased collagen deposition (86,88).

But besides their ability to enhance the inflammatory reaction and actively damage surrounding cells, alveolar macrophages have a crucial role in limiting unwanted immune responses and in resolving pulmonary inflammation. Elimination of constitutive negative regulation of macrophages via CD200R or MARCO, immediately results in higher viral clearance of influenza (47,89), whereas the absence of macrophages aggravates influenza infection (90,91). Also during other respiratory tract infections, including Mycobacterium tuberculosis or Streptococcus pneumonia, pulmonary macrophages play a central role in eliciting inflammatory responses. Early stages of M. tuberculosis infection lead to a predominant pro-inflammatory phenotype of macrophages that produce high amounts of inducible nitric oxide (iNos) and proinflammatory cytokines (92,93). This interaction stage via complement, mannose and Fc receptors, of alveolar macrophages and the mycobacteria is critical as this enables the bacteria to enter the macrophage and live and replicate within. This leads then to a recruitment of Th1 lymphocytes and the formation of granulomas – a response that is meant to limit infection but can also cause tissue damage by itself (92). Phagocytosis of opsonized S. pneumonia by macrophages clearly is favorable during infection. Unfortunately, exceedingly high levels of efferocytosis by alveolar macrophages results in impaired phagocytic capacity by alveolar macrophages and thus impaired clearance of S. pneumonia. (94).

Ever more evidence is supporting the fact that pulmonary macrophages, although increasingly and abundantly found in COPD (95), are dysfunctional in the disease. This is evident by their decreased ability to phagocytose apoptotic cells (96,97) and bacteria (98) as well as their striking transcriptional pattern that has lost most proinflammatory signatures (50).

The high diversity of alveolar macrophages and their profound plasticity is reflected by the dual role of macrophages in allergic airway disease. In absence of alveolar macrophages, achieved by clodronate-depletion, allergic inflammation in mice is aggravated (99). Transfer of healthy unsensitized alveolar macrophages into asthmatic mice (100), also proved beneficial thus clearly serving a protective role. Furthermore, their regulatory ability to suppress T-cell proliferation has been reported in mice and humans (101). This dampening of immune responses is also reflected by their ability to decrease the antigen-

presenting capacity of dendritic cells (102). Furthermore, while the protective role of resident alveolar macrophages seems to dominate, recruited monocytes promote allergic lung inflammation (103). But, as in the virtue of this cell, alveolar macrophages are not exclusively protective against allergic asthmatic responses. As mentioned above, adoptive transfer of healthy macrophages protects against airway hyperresponsiveness in mice, the transfer of sensitized and primed alveolar macrophages into healthy mice results in eosinophilic inflammation in the latter (104). Besides eosinophils, alveolar macrophages also facilitate the recruitment of neutrophils into the alveoli (105,106) that undergo apoptosis only a few hours following activation. Functional alveolar macrophages quickly take up the apoptotic neutrophils in order to prevent exceeding pulmonary tissue damage caused by the toxic neutrophilic substances. In asthmatic subjects this process is deteriorated which results in enhanced pulmonary inflammation (107,108).

1.1.6 Macrophages in acute lung injury

Acute lung injury (ALI) or its severe clinical manifestation acute respiratory distress syndrome (ARDS) is a devastating pulmonary disease that can result in respiratory failure. Distinct pathological stages characterize the disease. Severe inflammatory processes in the lung can cause diffuse alveolar damage with subsequent ventilation perfusion-mismatch, hypoxemia and loss of lung compliance (109,110). Patients are usually hospitalized in the intensive care unit due to the likely need of mechanical ventilation. Although a variety of stimuli and causatives can underlie ARDS, several diagnostic criteria have to be met in order to diagnose ARDS (also called ARDS Berlin definition): 1) oxygenation levels defined as partial pressure arterial oxygen / fraction of inspired oxygen or PaO2/FiO2 classify the severity of the disease from mild (200 mm Hg < $PaO_2/FIO_2 \leq 300$ mm Hg), to moderate (100 mm Hg < $PaO_2/FIO_2 \leq 200$ mm Hg), and severe ($PaO_2/FIO_2 \leq 100$ mm Hg) with a positive end-expiratory pressure (PEEP) of 5cm H_20, 2) bilateral opacities visualized by chest imaging, and 3) pulmonary edema not caused by cardiac failure and 4) acute onset (less than 7 days) (111). Etiology can be divided into direct lung injury, with the most common causes being pneumonia and aspiration of gastric contents, and indirect lung injury, mostly with underlying sepsis and severe trauma with shock and multiple transfusions (110). Other less common causes include acute pancreatitis, inhalational injury, transfusion of blood products, near drowning and so forth. According to the causality, the age of the patient and the presence of other non-pulmonary organ dysfunctions, mortality is rather variable with sepsis patients having the highest rates and

trauma patients experiences the best outcomes (112,113). The majority of patients with ARDS will be found in the intensive care unit with invasive mechanical ventilation. Mortality predictions are hard to meet, as mortality rate depends on the severity of the disease. Recently, a large cohort study reported 35 % mortality with mild, 40 % with moderate and 46% with severe ARDS (114). Amongst survivors, cognitive, psychiatric and physical morbidities can manifest themselves. One third of all patients will suffer from cognitive dysfunction, depression and anxiety but also impaired lung function (up to 80%) and pulmonary obstruction (20%) are common (115).

The histological equivalent to clinical ARDS is defined as diffuse alveolar damage (DAD), which presents itself with neutrophilic infiltration, hemorrhages and protein-rich pulmonary edema. This cluster of appearance characterizes the first phase of the disease – the so-called exudative phase. Concomitantly, increased levels of cytokines such as TNFα, IL-1β and IL-8 are found in the bronchoalveolar lavage (BAL) fluid. This can be partially attributed to alveolar macrophages that react to the pulmonary injury and initiate and/or enhance also the neutrophilic influx via secretion of IL-1, IL-6, IL8, IL-10 and TNF-α by activated alveolar macrophages (109). To enter the alveolar region, neutrophils have to pass the alveolar-capillary barrier that is composed of both the microvascular endothelium as well as the alveolar epithelium. Both epithelial and endothelial injury contribute to the development and severity of ARDS with the epithelial barrier function being greater than the one of the endothelium under homeostatic conditions (116). This is why the degree of epithelial injury or even the loss of epithelial barrier integrity outweighs the endothelial injury as a predictor of the outcome of ARDS (117). During the acute phase of ALI and ARDS, an injury or trigger causes an increase in permeability of the alveolar-capillary barrier, which results in the an influx of protein-rich fluid into the alveolar space and subsequent edema formation (109,118). Beside proteins, neutrophils are found in excess in the edema fluid and BAL fluid of ARDS patients. After injury, immune cells such as macrophages but also lung epithelial cells and fibroblasts react with the secretion of a variety of cytokines – both pro and anti-inflammatory – that initiate and potentiate neutrophilic influx. Amongst others, macrophages stimulate neutrophil recruitment via the secretion of IL-1, -6,-8 and -10 as well as TNF-α (109). While the role of macrophages in ARDS seems crucial, only a limited number of studies have addressed the role of alveolar macrophages in human ARDS. Rosseau et al. compared cell populations found in BAL fluid of ARDS patients, cardiogenic pulmonary edema patients and healthy volunteers.

Strikingly, the total number of alveolar macrophages, as well as CD11b and CD14 expression on the aforementioned, was increased in ARDS-patients. This increase was not associated with enhanced proliferation, but rather with recruitment (119). Still, local proliferation should not be underestimated, as GM-CSF induces proliferation of human alveolar macrophages in vitro (120) and increased levels of GM-CSF is found in the BAL fluid of patients with improved outcome after ARDS incidents (121,122). However, in ARDS patients, a randomized critical trial using systemic application of GM-CSF could not show a beneficial effect neither on the amount of ventilator-free days nor mortality (123).

During inflammation, alveolar macrophages are prompt in initiating a proinflammatory immune response that includes secretion of cytokines such as INFγ, TNFα and IL-1β to recruit neutrophils and lymphocytes (124). Besides neutrophils, also exudative macrophages are recruited that are essential in the clearance of the trigger and for removing cell debris. Recruited macrophages are unique as they express both proinflammatory (125,126) and immunosuppressive gene clusters (121,127). During phases of considerable severe inflammatory conditions, e.g. caused by intratracheal administration of LPS, mouse alveolar macrophage numbers are elevated, with an increased percentage of recruited macrophages with bone-marrow origin (128). In earlier stages of the model disease, alveolar macrophages act both as guardians, resulting in clearance of the toxic or damaging particles from the airways, as well as amplifiers of inflammatory responses. In later stages of human ARDS, starting approximately at day 5 after onset, macrophages undergo a phenotype switch towards anti-inflammatory state.

Interestingly, Barr and colleagues investigated a human model of acute lung inflammation and found that monocyte depletion could not ameliorate blood and alveolar neutrophilia, increased cytokine levels in the BAL fluid or the degree of inflammation visualized by positron tomography (129). In animal models, however, monocyte depletion prior to the injury proved beneficial in protection against ALI (130). Furthermore, supporting data for a pro-inflammatory role for alveolar macrophages is provided by Taaska *et al.* (131) showing that primed alveolar macrophages can induce lung injury independent of neutrophils. Taken together, the role of alveolar macrophages, as well as the interaction between macrophages, monocytes and neutrophils remains, up to now, unclear.

1.2 Prostaglandin D2 in inflammation

Lipid mediators, such as prostaglandin (PG) D_2, play a prominent role in inflammation, by promoting self-defense mechanisms and inducing cell signaling. In acute inflammation, rapid reaction to tissue damage or inflammation is essential, and normally mediated via production of cytokines and other small signaling molecules – prostaglandins and other arachidonic mediators belonging to the latter.

1.2.1 Synthesis and Production of Prostaglandin D_2.

Prostanoids - a term that includes prostaglandins and thromboxane (Tx) A_2 - are commonly derived from arachidonic acid. Arachidonic acid is an unsaturated fatty acid of 20 carbon molecules (20:4, n-6) and is localized in an esterized inactive form of phospholipids in the plasma membrane of cells. Upon stimuli, phospholipase A2 induces a catalytic cleavage of arachidonic acid from the cell membranes (132). Following this conversion of the membrane glycerophospholipids to arachidonate, cyclooxygenases (COX) produce PGG_2 and subsequently the common precursor prostanoid, PGH_2. Two isoforms of cyclooxygenase (COX) are known – COX1 and COX2 that differ only in 2 aminoacid entities (COX1 consisting of 602 and COX1 of 604 amino acids). Furthermore, structurally both enzymes share around 80% similarity, and differ mostly in ther N-terminus. Both are localized at the membrane of the endoplasmatic reticulum and the nuclar membrane. Arachidonic acid binds to the cyclooxygenase active domain via a hydrophobic channel that is found adjacent to the site responsible for membrane binding. Acetylsalicylic acid inhibits prostanoid biosynthesis via an irreversible serine acetylation on the active sites – in COX1 on serine 530 and in COX2 on serine 516, while other cyclooxygenase inhibitors block the enzymes in a reversible manner. PG production by COX can occur in a biphasic manner. A rapid production of PGD_2 – for example seen in explosive PGD_2 synthesis by mast cells following IgE crosslinking – has been described to be due to the constitutive COX1, whereas the later, slower production of prostanoids following ligand stimulation can be attributed to the inducible COX2 isoform (133,134). Next, a variety of prostanoids can be produced from PGG_2 in a tissue and cell specific context via prostaglandin and thromboxane synthases. Early studies on prostanoid production from rat peritoneal macrophages changed in response to different stimuli. While a calcium ionophor stimulated COX1 activity and synthesis of thromboxane A_2 and PGD_2, endotoxin induced predominately PGI_2 and PGE_2 (135). The rate-limiting enzymes of the terminal prostanoids are the specific synthases. PGD_2 is produced by two distinct PGD_2 synthases – the

lipocaline-type (LPGDS) and hematopoietic (HPGDS) enzyme. Both differ in their amino acid moieties, 3D structure, tissue distribution as well as immunological relevance (136). While LPGDS is abundantly found in the central nervous system, retina, melanocytes, heart, and reproductive organs, HPGDS has mostly been implicated in an inflammatory context (137). HPGDS belongs to the class of the glutathions-s-transferase (GST), implicating its need for glutathione to exert its catalytic activity (138). HPGDS is described to be expressed by a variety of immune cells, including mast cells, dendritic cells, Langerhans cells and Th2 cells (139,140). Up to now, HPGDS has mostly been implicated in allergic responses contributing to a proinflammatory phenotype. Regulation of the homodimeric enzyme can occur via Ca^{2+} and Mg^{2+} ions, that are able to influence the affinity for glutathione (141). The enzymatic product of the PGD synthases, PGD_2, acts as a bioactive lipid mediator. Still, this molecule can be further enzymatically and non-enzymatically modified into downstream products. PGD_2 is enzymatically converted to 13,14-dihydro-15-keto prostaglandin D_2 (DK-PGD_2), and non-enzymatically via albumin-induced isomerization to Δ12-PGD_2. Furthermore, it can be converted to a F-series prostanoid, 9α, 11β-PGF_2. Although 11β-PGF_2 is a stereomer of PGF_2, its actions differ, because of the activation of D-type prostanoid receptors. Dehydration of PGD_2 leads to the production of J-series of cyclopentonone PGs such as PGJ_2, Δ^{12}- PGJ_2, and 15-deoxy-$\Delta^{12,14}$- PGJ_2, the latest one being a agonist for the peroxisome proliferator-activated receptor γ (PPARγ), a member of the nuclear receptor superfamily of ligand-dependent transcription factors (142,143) .

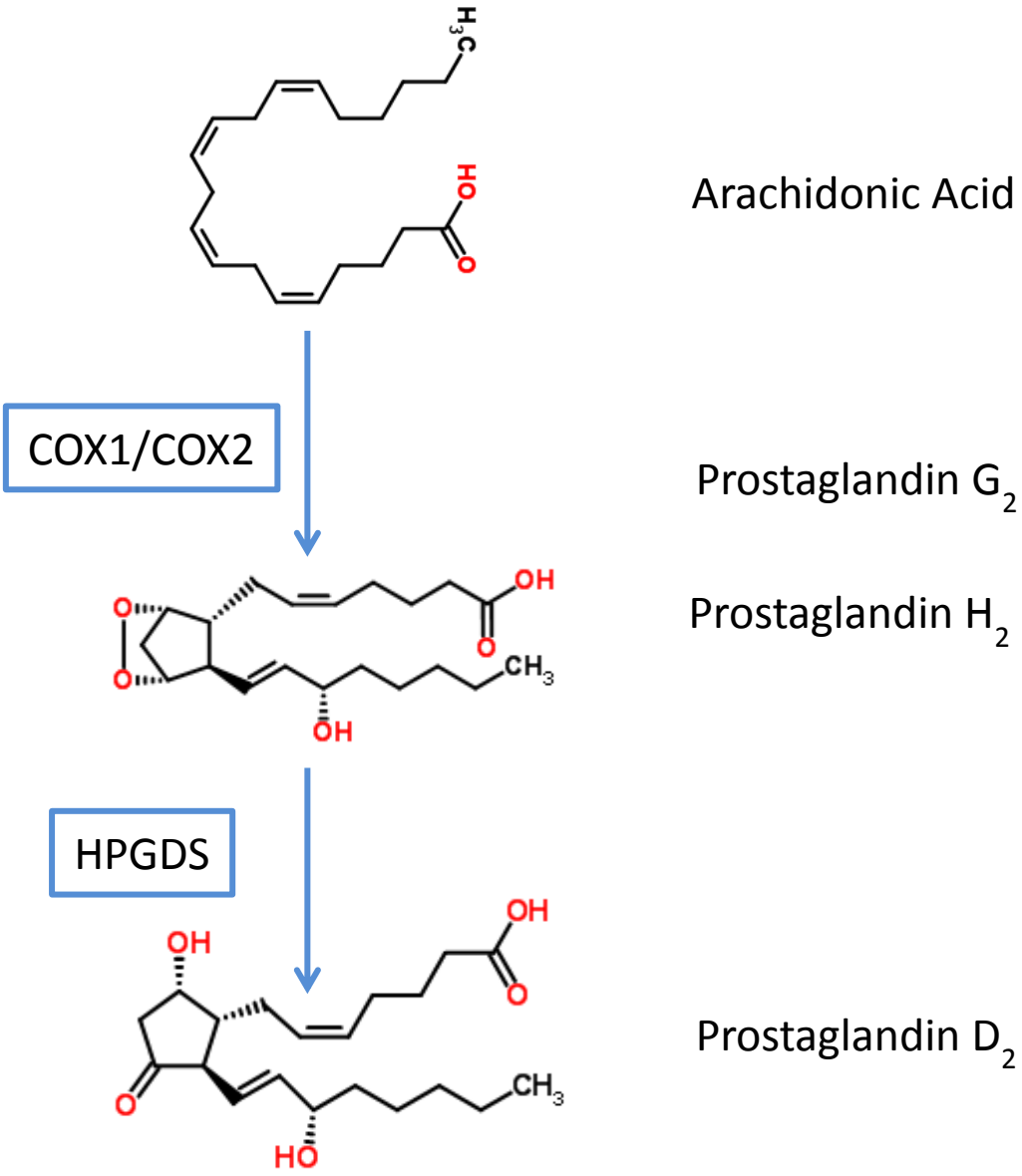

Figure 5. Synthesis of Prostaglandin D_2. Arachidonic acid is released from plasmamembrane glycophospholipids. Via the intermediate, PGG_2, the precursor molecule PGH_2 is enzymatically produced via the constitutive and inducible COX enzymes. Hemotopoietic PGD synthase (HPGDS), although coupled to COX production, is the rate-limiting enzyme in the terminal PGD_2 synthesis.

1.2.2 Prostaglandin D_2 release

After the biosynthesis of PGD_2, the prostanoid can either exit the site of production in a passive diffusion manner or via a facilitated transport using the constitutively expressed multidrug resistance protein 4 (MRP-4). MRP-4 belongs to the C subfamily of ATP-

binding cassette transporters (ABCC) and can transport a variety of endogenously produced molecules out of a cell. This transporter has been described to possess the unique ability of pumping out molecules that are involved in cellular communication and signaling, including cyclic nucleotides, steroids, but also prostanoids. The transporter, which is channel and pump at the same time, uses energy from adenosine triphosphate (ATP) hydrolysis to transport its substrates across the membranes against the diffusion gradient (144). Together with a high production rate of prostanoid, the expression of prostanoid transporters is increased in those cell types (145). Therefore, MRP-4-mediated PGD_2 efflux from the producing cell type can increase the paracrine activity of PGD_2.

1.2.3 Prostaglandin D_2 receptors

Prostaglandin D_2 exerts its bioactive potential predominantly on two distinct receptors, DP1 and DP2 (also known as CRTH2 – chemoattractant receptor homologous molecule expressed on Th2 cells) that both belong to the class of G-protein-coupled receptors (GPCRs). At higher concentrations (1 μM and above) PGD_2 is also an agonist on the thromboxane receptor TP (146).

1.2.3.1 G-protein-coupled receptors

Another ground-breaking discovery that was awarded with the Nobel Prize in 2012 was the description and unraveling on the mechanics of GPCRs by Robert Lefkowitz. The importance in GPCR-mediated signaling lies in their function in sensing the environment, reacting to changes and alterations and the consequential adaption of cells following the receptor signaling. This is further undermined by the fact that more than 50% of all medications pharmacologically target GPCRs.

Sequencing of the human genome revealed that around 1000 genes encoded for signaling receptors (147). Due to their location in the plasma membrane, and because the polypeptide chain spans seven times through the plasma membrane, GPCRs are also known as seven-transmembrane (7TM) receptors. The ternary complex model was proposed by Lefkowitz and co-workers in 1980 and described the general mechanism of GPCR activation (148). The ternary complex is formed by the 7TM domane that binds its ligand (agonist) on the extracellular part and on the intracellular parts interacts G-proteins that mediate the signaling.

The signal from outside the cell membrane is transferred to the inside only via receptor conformation changes (inactive and active), without the ligand passing through the

membrane. Normally one GPCR shows an affinity for a variety of extracellular ligands (agonists and antagonists, endogenous and synthetic ones). Activation of the receptor following ligand binding changes the conformation to a favorable active manner and thus leads to increased affinity for the heterotrimeric G-proteins inside the cells. The G-protein in the intracellular compartment is then responsible for the further transfer of information. This is accomplished by the dissociation of the receptor into its three subunits - Gα, Gβ and Gγ. There are four major subtypes found of the Gα subunit - Gα s, Gα i, Gα q and Gα 12. One GPCR is not limited to only one type of G-protein but instead can be associated to different subtypes. The family of Gα subunit determines its downstream effector functions (Fig.6). Gαs is likely to be coupled to adenylyl cyclase and stimulates enzyme activity (thus the s in Gαs). Gαi (i for inhibiting) inhibits adenylyl cyclase which results in decreased cyclic AMP (cAMP) levels inside the cells. Gα q is known to bind and activate phospholipase C (PLC), resulting in the cleavage of phosphatidyinositol bisphosphate into diaglyceral and inositol triphosphate and thus further in increased Ca^{2+} levels. $G\alpha_{12}$ is a described to activate small GTP-binding proteins, such as Rho. But information transfer of GPCRs is not limited to the Gα subunit. Gβ and Gγ subunits, which normally act as dimers, further activate phospholipases and ion channels and thus are important second-messenger molecules as well.

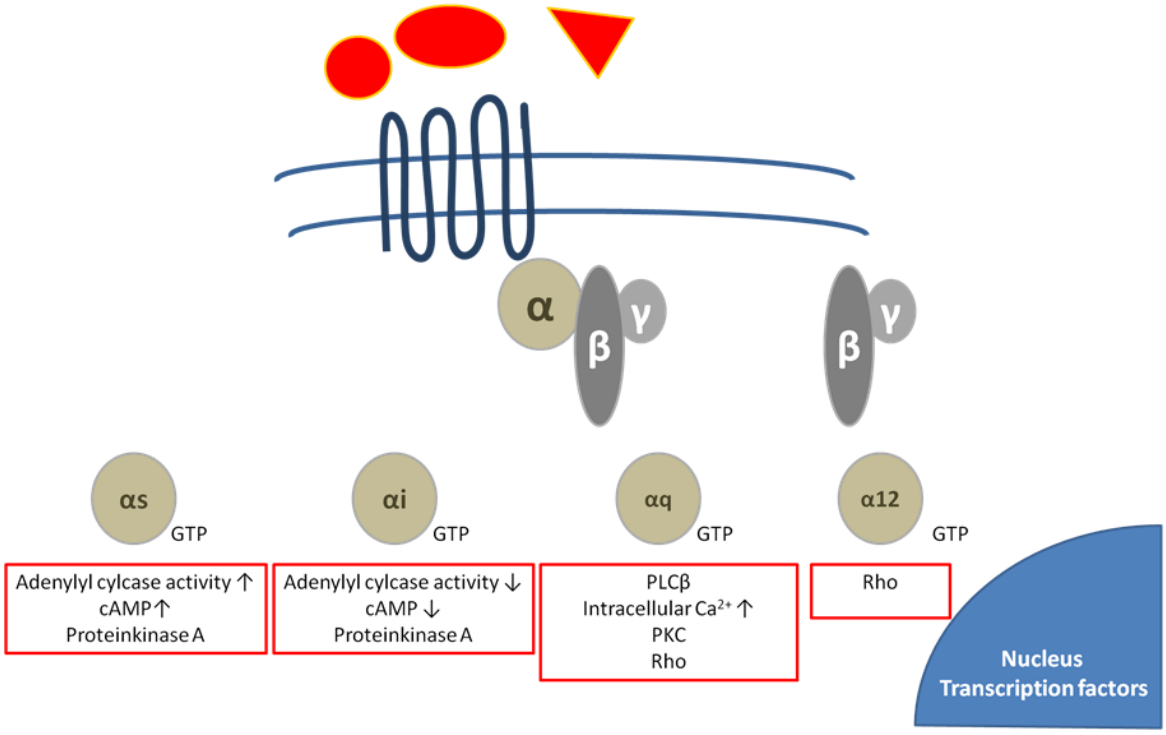

Figure 6. Signaling of GPCRs. Following agonist binding (red), the 7TM undergoes conformational changes to increase affinity for G-protein. G-proteins then act as second messengers that further mediate the signal. Finally, the signaling cascade ends with the activation of transcription factors that mediate cellular responses such as proliferation, survival, migration and others functional reactions.

1.2.3.2 Prostaglandin D_2 DP1 receptor

The D-type prostanoid receptor 1 (DP1) was the first receptor to be discovered as a target of PGD_2 (149). It belongs to the class of 7TM GPCRs and is expressed ubiquitously in almost all tissues, including inflammatory cells. DP1 has mostly been described to be associated to Gαs proteins. Thus ligand activation of the DP1 receptors has been stimulates adenylylcylcase and increases cAMP levels (150). Stimulation of DP1 receptors in the pulmonary vascular system appears very clear – its activation induces vasodilatation and bronchodilatation (151). Furthermore, BW245c – a selective DP1 agonist – has been described to inhibit platelet aggregation *in-vivo* (151). Taken together, this suggests a beneficial role for DP1 activation in pulmonary vascular diseases.

Unfortunately, as PGD_2 receptor DP1 is widely expressed on a variety of inflammatory cells, its role in inflammation has remained unclear. When a group established DP1 knock-out mice, the asthmatic response of these animals, as measured by eosinophil infiltration and airway hyperreactivity, was decreased, suggesting a pro-inflammatory effect of DP1 receptor (152). Consequently, DP1 antagonists were tested for their potential in regulation asthmatic responses, and indeed oral administration of DP receptor antagonis S-5751 decreased eosinophil recruitment and bronchial hyperresponsiveness in rats, by the suppression of expression of inflammatory cytokines IL-1β and IL-6 (153). On eosinophils, DP1 activation via both PGD_2 as well as the specific agonists could prolong survival and inhibit apoptosis – both mechanisms that can contribute to the severity of allergic reactions (154). But opposing studies also postulated an anti-inflammatory effect of DP1 receptor activation. BW245c potently inhibited basophil migration as well as IgE-mediated basophil degranulation (155). A DP1 agonist showed a similar potential in suppressing ovalbumin-induced asthma in mice via the suppression of lung dendritic cells and the induction of regulatory T-cells (156). This further highlights the controversial role of DP1 in mediating asthmatic responses.

Investigation on human subjects showed (i) a direct correlation between single-nucletoide polymorphisms (SNPs) in the PTGDR gene encoding DP1, resulting in decreased transcription of DP1 and the occurrence of asthma and (ii) distinct methylation and increased expression patterns of PTGDR in asthmatic patients (157,158).

1.2.3.3 Prostaglandin D_2 DP2 receptor

The second receptor for PGD_2 was discovered 1999, as a gene (GPR 44) that encodes for a GPCR that also shares a homology to chemoattractant receptors and was first described as on orphan receptor (159). Simultaneously, a new Th2 cell surface marker was identified and named "chemoattractant-receptor homologous molecule expressed on Th2 cells (CRTH2)" (160). Both molecules turned out to be the DP2 receptor. Due to its primary aminoacid sequence, the DP2 receptor shares more homology with other chemoattractant receptors – the formylmethionylleucylphenylalanine receptor subfamily – than with classical prostanoid receptors (161). Beside differences in structure, DP1 and DP2 also appear to be coupled to distinct G-proteins. DP2 receptor activation, does not lead to increased intracellular levels of cAMP levels, but Ca^{2+}. The DP2-mediated rise in intracellular Ca^{2+} levels were also shown to be sensitive to Pertussis toxin, suggesting an involvement of Gαi subunits. DP2 receptors are more selectively expressed – probably owing to their structure-equals-function properties. Being structurally related to chemoattractant receptors, its expression is predominately limited to inflammatory cells. Naturally, Th2 cells express DP2 – and on humans it discriminates them from Th1 cells. Furthermore, other inflammatory cells, such as eosinophils, basophils, mast cells, macrophages and dendritic cells express DP2 receptors and its expression has mostly been associated with migratory capacities (161–166). But PGD_2 is not only able to induce migration via the DP2 receptor, it also shows influential capacities on chemotaxis elicited by other stimuli. For example, LPS-induced chemotaxis on monocytes seems to depend on DP2 receptors (163). Interestingly, the expression of DP2 – as well as DP1- has only been investigated on murine macrophages, while we are up to now devoid of any information on the presence of PGD_2 receptors on human macrophages.

While the role of DP1 in inflammation remained controversial, DP2-mediated responses seem to induce predominantly pro-inflammatory actions. Selective DP2 agonism has been described to enhance allergic skin and airway inflammation via their action on eosinophil migration (167–169). Furthermore, DP2 activation biases the production of cytokines by lymphocytes into a Th2 polarization, including enhanced synthesis and secretion of IL-4, -

5 and -13 (170). Because of their ability in inducing migration both *in vitro* as *in vivo*, blocking of DP2 hypothetically should reduce inflammatory allergic reactions. And indeed, the application of DP2 antagonists proved to be beneficial in the pathogenesis of both cutaneous and pulmonary allergic inflammation by reducing eosinophil recruitment in murine ovalbumin-induced allergy model, by reversing airway hyperreactivity in a house-dust mite-induced model and reduction of IgE levels in chronic allergic skin inflammation (171–175). Besides airway and skin inflammation, DP2 antagonism showed beneficial effects in a dextrane sodium-sulphate-induced colitis model by ameliorating both inflammatory effects as well as consecutive weight loss (176).

1.2.4 PGD_2 metabolites and their selectivity on PGD_2 receptors.

PGD_2 as an endogenous ligand for both DP1 and DP2 receptors, shows a similar affinity for both receptors with an EC50 in the nanomolar range for both (166,177). Given that PGD_2 most likely is not the final product, end-stage metabolites derived from PGD_2 can act on either or both PGD_2 receptors, making the functional actions of PGD_2 more complex. PGD_2 has a reported *in-vitro* plasma half-life of 30 min, but as its metabolites are rapidly formed and are biological active, the loss of PGD_2 action is counterbalanced (178). The enzymatically formed 13,14-dihydro-15-keto-PGD_2 is a high affinity ligand for DP2 receptors, with no activity on DP1 receptors (177). Furthermore, the isomerization product Δ12-PGJ_2 and 14-deoxy- Δ12,14-PGD_2 show potent activity on DP2, without acting on DP1. On the other hand, PGJ_2 preferentially binds and acts on DP1 receptors comparable to PGD_2, but with lower magnitude on DP2 receptors. PGH_2 has also been described as a potent DP1 and DP2 agonist (179). Acting on both receptors is the PGD 11-ketoreductase product 11β-$PGF_{2\alpha}$ and the J-series metabolite 15-deoxy- Δ12,14-PGJ_2 and the most abundantly found plasma metabolite Δ12-PGJ_2 (177). Also derived from the common prostanoid precursor PGH2, the TxB_2 metabolit – 11-dehydro-TxB_2 – can act as a full agonist for DP2 (180).

1.2.5 HPGDS in airway inflammation

Given the differences in receptor distribution and signaling, as well as downstream metabolites that can mediate DP1 or/and DP2 associated responses, the role of PGD_2 in inflammatory reaction is complex, and often depends on the specific disease and the microenvironment which PGD_2 is acting in.

Initially, HPGDS activity has mainly been attributed to mast cells, activated via IgE crosslinking (181). As mast cells are primary effector cells in allergic inflammation, PGD_2 has strongly been linked to those diseases. The importance of PGD_2 in asthmatic responses has further been substantiated when another group identified eosinophils – another crucial effector cell in allergy - as a potential source of PGD_2 production (182). Immunohistochemical staining also showed that antigen-presenting cells such as histiocytes, dendritic, and Kupffer cells are positive for HPGDS. Furthermore, gene-expression was identified in human Th2 subsets, and accordingly, detectable levels of PGD_2 release from a Th2 cell line were found (183). Together with mast cells, eosinophils, Th2 cells and dendritic cells could thus contribute to PGD_2 synthesis during asthmatic reactions. In another experimental *in-vivo* setting, murine bone-marrow-derived macrophages (BMDM) produced PGD_2 in response to LPS treatment in a reactive-oxygen species (ROS)-dependent manner (184). Thus, several cell types have been identified as potential sources of PGD_2, further substantiating the assumption that production as well as action of PGD_2 is cell-type and disease specific.

During phases of allergic reactions, mast cells can react with PGD_2 production within 2 min after activation (134), which then acts as a bronchoconstrictor in mice and men (185). Furthermore, mild asthmatic patients display a 10 fold increase in bronchoalveolar lavage fluid PGD_2 levels compared to non-asthmatic subjects (186) and its levels also positively correlate with disease activity and severity (187). A recent study observed that HPGDS expression is induced in asthmatic patients in the epithelial compartment (188)

Therefore, both PGD_2 receptors as well as the terminal enzyme PGD_2 synthase are highly associated with airway diseases.

Therefore, this thesis aimed to

- investigate the presence of PGD_2 receptors on human macrophages with a special translational focus on pulmonary alveolar macrophages.

- elucidate the functional responses of macrophages that are elicited by PGD_2 stimulation.

- gain more insight into the influential capacities of PGD_2 in LPS-induced effects.

- investigate the role of PGD_2 receptor activation in pulmonary inflammation by the use of an *in-vivo* model of acute lung injury in mice

- explore the mechanism of how PGD_2-treated macrophages may influence pulmonary inflammation

2. Materials

2.1 Chemicals and Reagants

PBS - phosphate-buffered saline, pH 7.4 (with and without Ca^{2+} and Mg^{2+})	GIBCO Invitrogen, Paisley, Scotland, UK
CellFix	Becton Dickinson Immunocytometry Systems, Vienna, Austria
FACSFlow	Becton Dickinson Immunocytometry Systems, Vienna, Austria
HBSS - Hank's balanced salt solution)	GIBCO Invitrogen, Paisley, Scotland, UK
RPMI 1640 with stable glutamine	GIBCO Invitrogen, Paisley, Scotland, UK
HEPES buffer solution 1M	GIBCO Invitrogen, Paisley, Scotland, UK
amino acids (100x) non-essential	GIBCO Invitrogen, Paisley, Scotland, UK
sodium pyruvate solution	GIBCO Invitrogen, Paisley, Scotland, UK
Accutase	GIBCO Invitrogen, Paisley, Scotland, UK
penicillin/streptomycin (100x)	GIBCO Invitrogen, Paisley, Scotland, UK
Ultra V Block	Thermo Scientific, Fremont, CA
Dako antibody ailuent with background reducing components	Dako Österreich GmbH, Vienna, Austria
fetal bovine serum standard quality	GIBCO Invitrogen, Paisley, Scotland, UK
human serum, from human male AB plasma	Sigma Aldrich, Steinheim, Germany
lipopolysaccharide from Escherichia coli	Sigma Aldrich, Steinheim, Germany
o-dianisidine dihydrochloride	Sigma Aldrich, Steinheim, Germany
hydrogen peroxide solution 30%	Sigma Aldrich, Steinheim, Germany

H_2O_2 (w/w)	
dextrane T500	Sigma Aldrich, Steinheim, Germany
D(+)-glucose-monohydrate	Merck KGaA, Darmstadt, Germany
albumin, from bovine serum	Sigma-Aldrich, Steinheim, Germany
Histopaque -1077	Sigma-Aldrich, Steinheim, Germany
hematoxylin	
Ketasol (115,3mg/ml Ketaminhydrochlorid)	aniMedica, OGRIS Pharma V, Wels, Austria
xylazine Rompun (20mg/mL Xylazine)	Bayer, Vienna, Austria
Collagenase/Dispase	Sigma-Aldrich, Steinheim, Germany
evans blue	Sigma-Aldrich, Steinheim, Germany

2.2 Cytokines/ Chemokines/ Lipidmediator agonists and antagonists

human recombinant macrophage-colony stimulating factor (M-CSF)	PeproTech, Rocky Hill, NJ
human recombinant IFN-γ	PeproTech, Rocky Hill, NJ
human recombinant IL-4	PeproTech, Rocky Hill, NJ
human recombinant IL-8	PeproTech, Rocky Hill, NJ
human recombinant IL-10	PeproTech, Rocky Hill, NJ
human recombinant MCP-1/CCL2	PeproTech, Rocky Hill, NJ
PGD_2	Cayman Chemicals Ann Arbor, MI, USA
DK-PGD_2	Cayman Chemicals Ann Arbor, MI, USA

BW245C	Cayman Chemicals Ann Arbor, MI, USA
CAY 10471	Cayman Chemicals Ann Arbor, MI, USA
MK0524	Cayman Chemicals Ann Arbor, MI, USA

2.3 Kits

ProcartaPlex mouse cytokine & chemokine detection kit	eBioscience, San Diego, US
annexin V-FITC Apoptosis Detection Kit I	BD Pharmingen, Mountain View, CA
Vectastain ABC kit and 3-amino-9-ethycarbazole (AEC)	Vectorlabs, Burlingame, CA
macrophage depletion kit (Standard)	Clodrosome Encapsula NanoSciences LLC, Brentwood, TN
murine KC standard ABTS ELISA development kit	PeproTech, Rocky Hill, NJ
murine MCP-1 standard ABTS ELISA development kit	PeproTech, Rocky Hill, NJ
murine IL-6 standard ABTS ELISA development kit	PeproTech, Rocky Hill, NJ
murine TNF-α standard ABTS ELISA development kit	PeproTech, Rocky Hill, NJ

2.4 Antibodies

DP goat polyclonal antibody	Santa Cruz

PE mouse anti-human CD163, clone GHI/61	BD Pharmingen, Mountain View, CA
PE mouse IgG1 κ isotype control	BD Pharmingen, Mountain View, CA
PE mouse anti-human CD 80	BD Pharmingen, Mountain View, CA
PE mouse anti-human CD206	BD Pharmingen, Mountain View, CA
IgG from rabbit serum	Sigma Aldrich, Steinheim, Germany
Alexa Fluor 647 rat IgG2 κ isotype control	BD Pharmingen, Mountain View, CA
Alexa Fluor 647 anti-human CD 294 (CRTH2), clone BM16	BD Pharmingen, Mountain View, CA
Rabbit anti-goat Alexa Fluor 647	Invitrogen, Vienna, Austria
rabbit anti-CRTH2 (DP2) (1:200)	Acris Antibodies
rabbit anti-DP1 (1:100)	Cayman Chemicals, Ann Arbor, MI, US
HPGDS	LifeSpan Biosciences, Inc, Seattle, US
anti-Ly6g antibody	Abcam, Cambridge, UK
anti-Mouse NOS2 PE	eBioscience, Inc., Affymetrix company, Vienna, Austria
anti-Mouse F4/80 antigen FITC	eBioscience, Inc., Affymetrix company, Vienna, Austria
anti-RELM alpha antibody	Abcam, Cambridge, UK
Anti-mouse MHC-II	BD Pharmingen, Mountain View, CA
anti-mouse Siglec F	BD Pharmingen, Mountain View, CA
anti-mouse CD3ε	eBioscience, Inc., Affymetrix company, Vienna, Austria
anti-mouse B220	eBioscience, Inc., Affymetrix company,

	Vienna, Austria
anti-mouse CD11c	BD Pharmingen, Mountain View, CA

2.5 Equipment

Axiocert 40 CFL microscope	Carl Zeiss Microscopy GmbH, Germany
ORCA-03G digital camera	Hamamatsu, Japan
petri dishes (small/big)	Greiner, Frickenhausen, Germany
FACS Calibur	BD Biosciences (Bredford, MA, USA)
48-well plates	Greiner, Frickenhausen, Germany
24-well plates	Greiner, Frickenhausen, Germany
12-well plates	Greiner, Frickenhausen, Germany
6-well plates	Greiner, Frickenhausen, Germany
Nunc™ Lab-Tek™ II Chamber Slide™ System	Thermo Scientific, Fremont, CA
8 µm transwell chambers	Corning, Sigma Aldrich, Steinheim, Germany
200M inverted epifluorescence microscope	Carl Zeiss Microscopy GmbH, Germany
PolyChrome V monochromator	TILL Photonics GmbH, Gräfeling, Germany
RC-21B chamber	Warner Instruments, Hamden, USA
Olympus BX41 microscope	Olympus Optical Co. Ltd., Tokyo, Japan
flexiVent apparatus	SCIREQ, Montreal, QC, Canada
Precellys	Bertin Instruments, Saphymo GMBH,

	Frankfurt, Germany

2.6 Media and buffer formulations

Washing Buffer	PBS without Ca^{2+} and Mg^{2+} 90mM Glucose-Monohydrate 0.008mM Bovine serum albumin 10mM HEPES pH 7.4

Assay Buffer	PBS with Ca^{2+} and Mg^{2+} 90mM Glucose-Monohydrate 0.008mM Bovine serum albumin 10mM HEPES pH 7.4

Fixative Solution	2.5% CellFix 75% FacsFlow 22.5% Aqua dest.

Ringer Solution	5.8mM KCl 141mM NaCl 0.5mM KH_2PO_4 0.4mM NaH_2PO_4 11.1mM glucose 10mM Hepes 1.8mM $CaCl_2$ 1mM $MgCl_2$ pH 7.4

Adherence media for monocytes	RPMI 1640 with stable Glutamin 1x Penicillin/Streptomycin 1x Aminoacids non essential 1% Sodium Pyruvate 5mM HEPES Buffer Solution 5% human AB serum

Differentiation media for monocyte-derived-macrophages	RPMI 1640 with stable Glutamin 1x Penicillin/Streptomycin 10% FBS 20ng/mL human recombinant M-CSF

3. Methods

3.1 Experiments using human samples and cells.

Ethical approvals. All procedures involving human subjects as well as the usage for human tissue samples were conducted under the ethical approval of the Institutional Review Board of the Medical University of Graz.

Isolation of peripheral blood mononuclear cells. Whole blood from healthy volunteers was drawn and divided into two 50mL tubes each containing 4.4 mL sodium citrate. Platelet-rich plasma was removed by spinning the cells at 400 g with low brake for 20 min at room-temperature. Dextrane dissolved in saline was added to a final dextran concentration of 0.72 % and erythrocytes were allowed to sediment for 30 min. The remaining cells in the upper phase were layered on Histopaque gradients and spinned at 400 g with low brake for 20 min. Peripheral mononuclear cells were found in the buffy coats and cell number was determined.

Differentiation of monocytes to monocyte-derived-macrophages. Human PBMCs from buffy coats were seeded at a density of 10 Mio PBMCs/mL in prewarmed adherence media. Monocytes were allowed to adhere for 1 hour at 37° C in a humidified atmosphere containing 5% CO2. Then, non-adherent lymphocytes were removed by gentle washing with pre-warmed PBS and the remaining adherent monocytes, which normally make up around 10% of the PBMC fraction, were supplied with differentiation media containing 10 % FCS, 1 % penicillin/streptomycin and 20 ng/mL human M-CSF and incubated in an atmosphere of 5 % CO_2 at 37 °C. Media was changed every second or third day. After 7 – 10 days full differentiation was reached (189,190). Cells were detached with accutase and used for subsequent experiments.

Activation of human MDM. Full differentiation into resting macrophages was judged by visual observation of the microscopic appearance of human MDM, i.e increased size, granularity and branched and extended morphology. Cells were activated with either 100 ng/mL LPS or 20 ng/mL IL-4.

DP1 and DP2 cell surface receptor flow cytometric staining. Monocytes were used immediately after isolation from buffy coat and stained with PerCP-labeled anti-CD14

1:100 for 10 min at room temperature to discriminate from remaining cell populations. Macrophages were detached from cell culture plates using accutase and washed with 10mL of washing buffer. U937 cells were collected from culture flasks, and washed with washing buffer before staining. In order to inhibit unspecific binding of antibodies, Fc receptors on cells were blocked using 100 µL of UV block (for monocytes and U937 cells) or 100 µL of UV block containing 100 ng/mL human IgG (for DP2 staining on human macrophages) or 100 µL of UV block containing 100 ng/mL human IgG and 100 ng/mL rabbit IgG (for DP1 staining on human macrophages). DP2 staining was performed using a directly labeled rat anti-human Alexa Fluor 647 DP2 antibody and used at 20 µg/mL for 30min at room temperature. DP1 was stained using a primary polyclonal goat anti-human DP1 antibody at 20 µg/mL incubated for 30 min room temperature. The secondary rabbit anti-goat IgG secondary antibody was Alexa Fluor 647 labeled and used at a concentration of 2 µg/mL for 30 min room temperature. Following two washing steps, cells were taken up in 300 µL fixative solution and samples were measured on a FacsCalibur flow cytometer. Specificity was assured by the use of appropriate isotype-matched control antibodies used at the same concentrations.

Immunohistochemistry of DP1 and DP2 receptors. Human lung tissue samples derived from 5 patients with diffuse alveolar syndrome, which is the histological correlate to acute respiratory distress syndrome (ARDS) as has been identified by the American European Consensus Conference definitions (191), sarcoidosis, respiratory bonchiolitis and organizing pneumonia (192), as well as 5 healthy control tissues (the latter obtained from resection specimens for trauma) were used for immunohistochemical characterization of DP1, DP2 and HPGDS. Samples were cut to four µm sections, and placed at 65° C for one hour. Then samples were deparaffinized and hydrated with decreasing alcohol concentrations. Antigen retrieval was performed by microwaving slides for 2 × 5 min cycles in 10 mM citrate buffer. Samples were then processed by ABC method (Vectastain ABC kit; Vector Laboratories), according to the manufacturer's protocol. Sections were incubated with anti-DP2 (rabbit anti-human used 1:200) (193) or anti-DP_1 (rabbit anti-human used 1:100) (194) or anti-HPGDS (rabbit anti-human 1:200, LifeSpan Biosciences, Inc, Seattle, US) over night at 4°C. Staining was visualized with 3-3′-diaminobenzidine and counterstained with hematoxylin for 40 sec. Images were taken with a high-resolution digital camera (Olympus DP 50), processed, and analyzed by Cell^A imaging software (Olympus, Vienna, Austria). Contrast and brightness adjustment was performed.

Calcium ion (Ca^{2+}) flux. Isolated human peripheral blood monocytes were analyzed for changes in intracellular Ca^{2+} levels as previously described (195,196). $1x10^7$ isolated peripheral blood mononuclear cells were taken up in 500 µL assay buffer including Ca^{2+} and Mg^{2+} and loaded with 2 µM Fluo-3 in the presence of 0.02% pluronic F-127 for 60 min at room temperature. After washing off not incorporated Fluo-3, monocytes were labeled with CD14-PerCP for 10 min at room temperature. Following a washing step, cells were resuspended in assay buffer with Ca^{2+} and Mg^{2+} at a density of 1 Mio/mL. For each measurement, 500µL aliquots were taken. Changes in intracellular Ca^{2+} levels were then monitored on a FACScalibur flow cytometer. After recording baseline for 60 sec, cells were stimulated with 1 µL of agonists (prepared 500x concentrated) and Ca^{2+} levels were further measured for another three min. Increased fluorescent intensities corresponded to rises in intracellular Ca^{2+} concentrations. Data were normalized to increases in fluorescent intensities with respect to baseline levels.

Live cell Ca^{2+} imaging. Monocytes were seeded on glass cover slides (25 mm diameter) and differentiated to macrophages. On the day of the experiment, macrophages usually showed 50-70% confluence. Cells were then loaded with the ratiometric fura-2/AM (2 µM) for 40 min at 37°C in the dark and then carefully washed twice with Ringer solution (5.8 mM KCl, 141 mM NaCl, 0.5 mM KH_2PO_4, 0.4 mM NaH_2PO_4, 11.1 mM glucose, 10 mM Hepes, 1.8 mM $CaCl_2$, 1m M $MgCl_2$, pH 7.4). The slide was then mounted on a Zeiss 200M inverted epifluorescence microscope coupled to a PolyChrome V monochromator (Till Photonics) light source in a sealed, temperature-controlled RC-21B chamber (Warner Instruments). Cells were excited alternatively at 340 and 380 nm and fluorescent images were obtained. The emitted light was collected at 510 nm using an Andor Ixon camera. For data storage and subsequent offline analysis, the TillVision software (Till Photonics) was used. Baseline was recorded for 5 mins and cells were subsequently perfused with 1 µM PGD_2 or selective DP1 and DP2 specific agonists, DK- PGD_2 or BW245c both 1 µM in the presence of extracellular Ca^{2+}, respectively. Images were taken every 3s and before calculation, background fluorescence was recorded from each covers slide and subtracted. Maximal and minimal ratio values for $[Ca^{2+}]_i$ were determined at the end of each experiment by perfusion with 10 µmol/L ionomycin to obtain the maximal ratio following chelating all free Ca^{2+} with 20mmol/L EGTA to obtain the minimal ratio. Cells that did not show a response to ionomycin were discarded. $[Ca^{2+}]_i$ was calculated as described by Grynkiewicz et al (197,198). For analysis of the live-cell Ca^{2+} imaging data, the basal level

of Ca^{2+} was determined as an average value of the first 50 seconds of the curve. Afterwards, the agent-induced Ca^{2+} peak height was quantified for each individual cell after subtracting the baseline.

Macrophage migration. Migration of human MDM was assessed as described previously. Before assessing migration towards PGD_2, production of endogenous PGD_2 was blocked overnight using the cyclooxygenase inhibitor diclofenac (10 μM). Then, human MDM ($2x10^5$ per insert in RPMI 1640 medium containing 5 mM HEPES, 1 % non-essential amino acids, and 1 % sodium pyruvate) were allowed to migrate into the lower part of a Transwell compartment (Corning) with an 8 μm filter for 18 h at 37°C. Cells that had migrated through the insert onto the lower surface of the filter were fixed with 3.7 % paraformaldehyde for 30 min at 4°C. Filters were then cut and cell nuclei were fluorescently labeled with DAPI and mounted on microscope slides. Migration was analyzed using a Zeiss Axiovert 40 CFL microscope and Zeiss A-Plan 10×/0.25 Ph1 lens. For each condition five images of 20 x magnification were acquired per filter using a Hamamatsu ORCA-03G digital camera. Migration was quantified by counting the cell nuclei using ImageJ software (National Institutes of Health, US). The chemotactic index was then determined by assessing the number of cells that migrated in response to agonist divided by the number of cells that migrated spontaneously towards vehicle.

Cytokine release from MDM. The levels of TNF-α in cell culture supernatants were determined either by a commercially available ELISA (Peprotech) following the manufacturer's protocol or by using a commercially available multi-analyte immunoassay as recommended (Bender Medsystems, Vienna, Austria). In the latter, supernatants of each sample were incubated with a bead mixture and a biotin-conjugate responsible for the cytokine binding to obtain immuno-complexes. Addition of streptavidin-PE results in binding to the biotin-conjugate and in the emission of fluorescent signals as detectable by flow cytometry.

U937 cells. U937T NF-κB reporter cells were a kind gift from Herbert Strobl (Institute of Pathophysiology and Immunology, Medical University of Graz, Austria), which were generated by retroviral transduction of U937T cells with a self-inactivating vector containing a GFP-NFκB reporter cassette. Cells were prepared as previously described (199). In brief, cells were generated by retroviral transduction of U937T cells with a self-inactivating vector containing a NFκB reporter cassette.

Neutrophil migration. To assess neutrophil migration, $10x10^3$ neutrophils in PMNL were suspended in 200 µL of RPMI and put on top of a Transwell insert with a pore size of 5 µm. In the lower compartment, 600 µL of vehicle or increasing concentrations of the chemoattractant IL-8 dissolved in RPMI was placed. Neutrophils were allowed to migrate from the upper compartment into the lower compartment of this modified Boyden chamber. Cells that migrated through the filter into the bottom well were collected. Following centrifugation, neutrophils were resuspended in 150 µL fixative solution and enumerated by measuring for 60 sec on a FACScalibur flow cytometer. When neutrophil migration was assessed in the presence of macrophages, MDM were seeded on inserts bearing 5 µm filters 24 hours before the migration assay was performed and treated with vehicle or 1 µM PGD_2 1 hour before neutrophils were added and allowed to migrate.

Neutrophil apoptosis. Freshly isolated neutrophils in PMNL were resuspended at a density of 1 Mio/mL in RPMI +1 % Pen/Strep and treated with vehicle or 1 µM PGD_2. Cells were cultured for up to 24 hours. At 0, 1, 3 and 24-hour time points, neutrophils were harvested and apoptosis was determined. Staining was performed according to the manufacturers protocol by incubation with PI and FITC anti-Annexin V antibody for 15 min in the presence of Ca^{2+} and Mg^{2+}. Viable, non-apoptotic cells are characterized as being negative for both Annexin V and PI during the flow cytometric analysis. When neutrophil apoptosis was assessed in the presence of macrophages, MDM were seeded in 24 well plates 24 hours before neutrophils were added. MDM were treated with vehicle or 1 µM PGD_2 dissolved in RPMI +1 %Pen/Strep 1 hour before neutrophils were added.

3.2 Animal experiments.

All studies involving animal experiments were approved by the Animal Ethics Committee of the Austrian Federal Ministry of Science and Research (BMWFW-66.010/0046-II/3b/2013) and were carried out in line with the European Community's Council Directive.

Mice. Mice were purchased from Charles River Laboratories (Sulzfeld, Germany). Generally, for all experiments, 6-10 week old male wild-type BALB/c mice were used. Mice were housed and acclimatized at least one week before the start of all experimental handling. Mice had access to water and food ad libitum and were kept in a 12-hour light-dark cycle.

LPS-induced lung injury. For all agonist experiments, mice were pretreated with PGD_2, DK- PGD_2, BW245c or vehicle 1 day before LPS administration at given concentrations. Agonists were dissolved in 0.9 % saline and were injected subcutaneously in 200 µL volume. Solvents did not exceed a concentration of 0.1 %. Treatment was performed every 12 hours. For all antagonist experiments, MK0524 and CAY10471 were injected subcutaneously 1 day before LPS challenge every 12 hours. Antagonists were dissolved in 0.9% saline and were injected in 200 µL volume. Solvents did not exceed a concentration of 0.1 %. LPS was dissolved in saline to a dose of 1 mg/kg and administered in 50 µL volume. For intranasal administration of LPS, mice were lightly anesthetized by intraperitoneal injection of ketamine (50 mg/kg) and xylazine (5 mg/kg). Duration of LPS treatment depended on the experiments and was either 4 hour or 24 hours.

Bronchoalveolar lavage. Mice were injected with a lethal dose of of ketamine (150 mg/kg) and xylazine (15 mg/kg) via intraperitoneal injection. Then trachea was exposed and BAL was performed by intratracheal administration of a total of 4.5 mL PBS + 1 % EDTA. Initially, 0.5 mL of buffer was installed, followed by 4 x 1 mL of buffer. Lavage fluid was collected and stored on ice. Then BALF was spinned 400 g, 7 min, 4° C and supernatants were aliqoted and stored at -80° C for the following measurements of cytokines and lipid mediators. Cells were subsequently stained for differential BAL leukocyte markers.

Leukocyte staining on BALF cells. BALF cells obtained from lavage were immediately processed for subsequent staining. Erythrocytes were lysed on ice using an isotonic solution of ammonium chloride. Remaining cells were then stained with the following antibodies and at given concentrations: (all antibodies are anti-mouse) MHC II (5µg/mL), Siglec F (5µg/mL), CD3ε (5µg/mL), B220 (2µg/mL) and CD11c (2µg/mL). Staining was performed in 50µL volume per conditions. Following a washing step, cells were resuspended in 200µL fixative solution and then counted for 30 sec on a FACSCalibur flow cytometer. Cell populations were identified with adaptions as described elsewhere (200). In detail, lymphocytes were first identified via FSC and SSC properties as FSC^{low}/SSC^{low}, followed by cell surface staining of CD3 and B220. $CD3^{high}/B220^{high}$ cells were identified and further divided into MHC-II^{neg} T- and MHC-II^{high} B-lymphocytes. Then the FSC^{med}, SSC^{med}, $CD3^{neg}/B220^{neg}$ granulocytes were further classified into $CCR3^{neg}$ neutrophils and $CCR3^{high}$ eosinophils. FSC^{high}/SSC^{med} alveolar macrophages were

classified as CD11c^{high}/MHC-II^{high} and monocytes were gated as CD11c^{med}/MHC-II^{neg} cells.

Myeloperoxidase (MPO) assay. MPO activity from was measured as indirect parameter for the neutrophil recruitment into the interstitial space. Furthermore, it directly correlates with disease severity. Activity was determined as described before (201). In brief, following BAL, lungs were perfused with 10 mL of ice-cold PBS +1 mM EDTA via the right ventricle until lungs appeared white and cleared from blood. Tissue was sampled and kept frozen at -80° C. Then, frozen lung samples were cut, weighed and homogenized in phosphate buffer with 0.5 % hexadecytrimenthyl ammonium bromide using ceramic beads and the precellys homogenizier (Peqlab). Homogenized lung tissue was then spinned and 10 µl of supernatant was added to 200 µl of 50 mmol/l potassium phosphate buffer (pH 6.0) containing the substrate 0.167 mg/ml of O-dianisidine hydrochloride and 0.5 µl of 1% H_2O_2/ml. The kinetics of MPO activity was measured at 450 nm (xMark^{TM}, Bio-Rad, Austria).

Lung histology. Mice were injected with a lethal dose of ketamine (150 mg/kg) and xylazine (15 mg/kg) intraperitoneally. Following lung perfusion with 10 mL PBS + 1 mM EDTA, lungs were prefixed via perfusion with 4 % paraformaldehyde. Lungs were then dissected and stored in paraformaldeyde at 4° C for further 24 hours, and were then embedded in paraffin. For immunohistochemistry, lungs were cut at 5 µm sections and deparaffinized and hydrated using decreasing concentrations of alcohol. Following that, sections were stained with hematoxyllin/eosin. Visual examination was performed using an Olympus BX41 microscope (Olympus) and an Olympus U Plan Apo x40/0.8 lens. Pictures were taken with an Olympus DP50 camera (2776 x 2074 pixels). Photographs were then further processed with CELL^{P} software (Olympus) and additional white balance, contrast, and brightness was adjusted.

Ly6G staining on murine lung samples. Five µm lung sections were prepared as described above and deparaffinized and hydrated using decreasing concentrations of alcohol. Sections were stained with anti-Ly6G used at 1:1000 and incubated over night at 4°C. Detection was achieved using the Vectastain ABC kit and 3-amino-9-ethycarbazole (AEC). Samples were then counterstained with hematoxylin for 40 secs and mounted. Visual examination was performed using an Olympus BX41 microscope (Olympus) and an Olympus U Plan Apo x40/0.8 lens. Pictures were taken with an Olympus DP50 camera

(2776 x 2074 pixels). Photographs were then further processed with CELL^P software (Olympus) and additional white balance, contrast, and brightness was adjusted.

Measurement of murine lung function. Mouse lung function was measured using a computer-controlled ventilation system, known as flexiVent (SCIREQ, Montreal, QC, Canada). Mice were first anesthetized with ketamine (50 mg/kg) and xylazine (5 mg/kg) by intraperitoneal injection. Next, the trachea was cannulated and connected to a flexiVent apparatus. A pump connected to the trachea is used for mechanical ventilation of the animals. The computer-controlled ventilation was performed with the use of a tidal volume of 10 mL/kg at a rate of 150 breaths/min. Responsiveness to inhaled methacholine – applied via a nebulizer that did not interfere with the ventilation pattern – was determined via the measurement of lung resistance and compliance.

Evans blue dye extravasation. As a measurement of vascular permeability and edema formation, Evans blue dye (60 mg/kg) was administered into the tail vein three hours after LPS treatment and was allowed to circulate for another 60 mins. Then, mice were subjected to a lethal dose of ketamine (150 mg/kg) and xylazine (15 mg/kg) via intraperitoneal injection. Lungs were then perfused with 10mL PBS + 1mM EDTA until lungs were cleared from erythrocytes. Whole lungs were then weighed and homogenized in PBS (1mL/100µg wet lung weight) using a Precelly device. Another 2 volumes of formamide were added to the homogenized tissue and incubated at 60°C for 24 hours. Following the incubation, samples were centrifuged. Evans Blue dye in supernatants was measured photometrically using the absorption of Evans blue at 620nm, corrected for the presence of heme pigments using the following equation: Absorption620 (corrected) = Absorption620 – (1.426 x Absorption740 + 0.030) and calculated against a standard curve (202,203).

Isolation of murine alveolar macrophages. Murine alveolar macrophages were isolated from BALF of treatment-naïve mice. BAL was performed as described above, but with the use of a total of 10mL of fluid to be sure to yield the majority of all present alveolar macrophages. Single cell suspension was counted and then cells were seeded at a density of $10x10^6$ cell/mL in RPMI +10 %FBS +1 % Pen/Strep. Following 1 hour of incubation at 37° C, non-adhesive cells – the majority being lymphocytes – were washed off with pre-warmed PBS. Remaining cells, being over 90 % alveolar macrophages, were supplied with

fresh media (RPMI +10 % FBS + 1 % Pen/Strep). Cells were mainly used to examine their cytokine secretion profile. An aliquot was also seeded on chamber slide for subsequent staining for macrophage markers. By examination, these cell preparations contained around 90 % macrophages.

Isolation of murine interstitial pulmonary macrophages. Following a bronchoalveolar lavage to yield alveolar macrophages, lungs were perfused with 10 mL PBS + 1mM EDTA until cleared from erythrocytes, followed by perfusion with PBS supplemented with 1 µg/µL collagenase/dispase. Then lungs were dissection and minced into 1x1x1 mm pieces. Digestion of minced lung tissue was achieved by incubation with RPMI + 20 % FBS + 1 µg/µL collagenase/dispase for 60 min at 37° C on a shaker. The digested material was then put through a cell strainer with a pore size of 60 µm followed by 2 washing steps. Cells were resuspended to give a single cell suspension that was then put on ice for 5 min. All particulate matter settled during the 5 min incubation on ice, and pulmonary macrophages remained in the supernatant. Then, cells were taken up and washed 3 times with PBS. Following enumeration of cells, pulmonary macrophages were seeded at $1x10^6$ cells/mL. Pulmonary macrophages were isolated using their adhesiveness to cell culture plastic surfaces. Following 1 hour of incubation at 37° C, non-adhesive cells – the majority being lymphocytes – were washed off with pre-warmed PBS. Remaining cells, being over 90 % alveolar macrophages, were supplied with fresh media (RPMI +10 % FBS + 1 % Pen/Strep). Cells were mainly used to examine their cytokine secretion profile. An aliquot was also seeded on chamber slide for subsequent staining for macrophage markers. By examination, these cell preparations contained around 90 % macrophages.

Immunofluorescence staining on alveolar and interstitial pulmonary macrophages. For microscopic immunofluorescence staining, freshly isolated alveolar or interstitial pulmonary macrophages were seeded on chamber slides, then the cells were fixed and blocked for 30 min with Ultra V Blocking solution. Incubation with the directly labeled antibody F4/80-FITC lasted for 30 min at room temperature. For both iNOS and RELM-α staining cells were permeabilized with 0.1 % Triton X-100 in PBS for 15 minutes at room temperature, followed by incubation with Ultra V Blocking solution for 40 min at room temperature. Cells were then incubated with directly PE-labeled anti-iNOS or primary anti-RELMα antibody. For RELMα staining AF-488-labeled goat anti-rabbit secondary antibody was incubated with the cells for further 30 min in dark at 4° C. After being mounted with Vectashield/DAPI medium, the samples were analyzed with an Olympus

UPlanApo–60x/1.20 lens using an Olympus IX70 fluorescence microscope, an Olympus DP50-CU digital camera and Olympus Cell^P software (Olympus, Lake Success, NY).

Depletion of murine lung macrophages. For intranasal administration of clodronate or control liposomes, mice were lightly anesthetized by intraperitoneal injection of ketamine (50 mg/kg) and xylazine (5 mg/kg). 300 µg of clodronate or control liposome in 60 µL volume were intranasally administered to anesthetized mice. To evaluate the kinetics of macrophage depletion, mice were killed 24, 48 and 72 hours post clodronate administration. In the final experiments, LPS was administered 72 hours after clodronate depletion.

Cytokine in BALF. The levels of TNF-α, IL-6, MCP-1, KC and IL-10 in the BALF were measured using commercially available ELISA kits (Peprotech) following the manufacturer's protocol.

Cytokine release from alveolar and interstitial pulmonary macrophages. Cytokines released from freshly isolated alveolar and interstitial pulmonary macrophages were quantified using ProcartaPlex Mouse Cytokine & Chemokine Detection Kit using the luminex technology. According to the manufacturer's protocol, a custom mixed panel of cytokines that included of TNF-α, IL-6, MCP-1, KC and IL-10 was investigated in this bead-based ELISA.

Proteins in BAL. Protein concentrations in BALF were colorimetrically determined using a BCA (bicinchoninic acid) assay. Here, bincinchoninic acid is used as the detection reagent. Peptide bonds in the samples act reducing on Cu^{2+}. The freshly generated Cu^{+} ion then forms a Cu^{+}- bincinchoninic acid chelate which can be measured at 562 nm wavelengths. According to a standard curve, sample concentrations are determined.

Lipid mediator analysis. For detection of lipidmediators, a stable isotope dilution liquid chromatography-mass spectrometry (LC-MS/MS) method was applied, as previously described elsewhere (204,205). To quantify the lipid mediators, PGD_2, PGE_2, 6-*keto*-$PGF_{1\alpha}$, TBX_2 and 12-HHTrE, slight modifications were applied to the protocol. Lipid mediator nomenclature is provided in Table 1. In general, BAL fluid samples were incubated with a mixture of deuterated internal standards (10 µL) in concentrations according to Table 1. Samples were then loaded onto Waters Oasis HLB solid phase extraction (SPE) cartridges. After allowing the PE cartridges to air-dry, lipid mediators

were eluted. The solution was consequently evaporated under vacuum and reconstituted in 60 µL of methanol and 10 µl of water. The solution was then spin-filtered, and 7.5 µL were injected onto an Acquity UPLC with a BEH C18 column (2.1x150 mm, 1.7 µm, Waters) and analyzed on a Waters Xevo TQS-MS in negative electrospray ionization mode.

Table 1. Nomenclature for lipid mediators.

Abbreviation	**Common name**	**Systematic name**
PGD_2	prostaglandin D_2	9α,15S-dihydroxy-11-oxo-prosta-5Z,13E-dien-1-oic acid
PGE_2	prostaglandin E_2; dinoprostone	9-oxo-11α,15S-dihydroxy-prosta-5Z,13E-dien-1-oic acid
6-keto-PGF1α	6-keto-prostaglandin $F_{1\alpha}$	6-oxo-9α,11α,15S-trihydroxy-prost-13E-en-1-oic acid
TxB_2	thromboxane B_2	9α,11,15S-trihydroxythromba-5Z,13E-dien-1-oic acid
12-HHTrE	12-HHT	12-hydroxy-5Z,8E,10E-heptadecatrienoic acid

Table 2. Calibration levels of the lipid mediators analyzed.

	Calibration level concentration (nM)							
Compound	8	7	6	5	4	3	2	1
PGD_2	526.84	166.16	40.54	12.16	3.40	1.13	0.45	0.23
PGE_2	526.84	166.16	40.54	12.16	3.40	1.13	0.45	0.23
6-keto-PGF1α	501.24	158.08	38.57	11.57	3.24	1.08	0.43	0.22
TxB_2	1445.92	347.02	88.68	25.06	6.94	1.93	0.67	0.27
12-HHTrE	662.32	208.89	50.95	15.28	4.28	1.43	0.57	0.29

$[^2H_4]$-PGD_2	51.29
$[^2H_4]$-PGE_2	28.53
$[^2H_4]$-8-epi-$PGF_{2\alpha}$	51.01
$[^2H_4]$-TxB_2	88.50
$[^2H_4]$-13-HODE	38.03

SPE extraction. Analytes were extracted in 3cc/60 mg HLB Oasis SPE cartridges (Waters) that were conditioned with 2 mL of methanol followed by 2 mL of water. A mixture of deuterated internal standards (10 µL; Table 2) was added to 750 µL BALF sample, followed by 10 µL BHT/EDTA solution (0.2 mg/mL, dissolved in methanol/water 50:50, v/v) and 750 µL extraction buffer (citric acid: 0.2 M NaH_2PO_4, pH5.6). This was consequently sampled onto the SPE cartridge. Samples were washed with 2 mL of water/methanol (80:20, v/v) and the cartridges were dried in the manifold under vacuum-induced air stream at −30 kPa for 30 min. After the elution of the analytes with 2.5 mL of methanol in cryotubes containing 10 µL of glycerol 30% in methanol, eluents were evaporated under vacuum, and finally samples were resuspended in 60 µL of methanol plus 10µL of water. Solution was 0.1 µm filtered (PVDF, Millipore) and injected (205).

UPLC-MS/MS measurement. Liquid chromatography coupled to mass spectrometry (LC-MS/MS) separation and quantification was carried out on a UPLC Acquity-Xevo TQS mass spectrometer system (Waters, Milford, MA). The autosampler and columns were temperized at 5° C and 60°C, respectively, and 7.5 µL of sample was injected. Separation was carried out using an Acquity UPLC BEH C18 (2.1 × 150 mm, 1.7 µm, Waters) and a gradient of solvents A (water with 0.1% of acetic acid) and B (acetonitrile/isopropanol 90:10, v/v) at a flow of 0.5 mL min^{-1}. The gradient started with 80% of A, and linearly decreased to 65% at 2.5 min, to 60% at 4.5 min, to 58% at 6 min, to 50% at 8 min, to 35% at 14 min, to 27.5% at 15.50 min and to 0% at 16.60min. After washing the column with solvent B for 0.9 min, it was equilibrated to initial conditions. Data was collected on a Waters Xevo TQS-MS mass spectrometer using negative electrospray ionization and scheduled multiple reaction monitoring (MRM) mode. Dwell time was automatically

adjusted in order to acquire 20 points per chromatographic peak; capillary voltage was 2.20 kV in negative. Desolvation temperature and gas flow were set according to the instrument recommendations for the chromatographic flow (205). Detailed MRM transition and chromatographic retention time for each compound is provided Table 3.

Table 3. Analytical characterization of the standards of the lipid mediators. Chromatographic retention time (RT), parent ion, product ion, the internal standard (IS) assigned to each lipid mediator and the on-column injected linear range are reported.

Lipid mediator	RT (min)	Parent ion $[M-H]^-$ (m/z)	Product ion (m/z)	IS	Linear range (fmol)
PGD_2	4.87	351.1	271.1	$[^2H_4]$-PGD_2	1.7-3951
PGE_2	4.61	351.2	271.1	$[^2H_4]$-PGE_2	1.7-3951
6-keto-$PGF_{1\alpha}$	3.13	369.2	162.9	$[^2H_4]$-8-epi-$PGF_{2\alpha}$	1.6-3759
TxB_2	3.98 (broad peak)	369.2	168.9	$[^2H_4]$-TxB_2	1.6-3780
12-HHTrE	9.29	279.2	179	$[^2H_4]$-13-HODE	2-10844
$[^2H_4]$-PGD_2	4.84	355.2	193.1		
$[^2H_4]$-PGE_2	4.58	355.3	275.1		
$[^2H_4]$-8-epi-$PGF_{2\alpha}$	3.95	357.2	197		
$[^2H_4]$-TxB_2	3.95 (broad peak)	373.2	173		
$[^2H_4]$-13-HODE	11.27	299.2	198.1		

4. Results

Most data presented in this thesis have been published in:

Jandl K, Stacher E, Bálint Z, Sturm EM, Maric J, Peinhaupt M, Luschnig P, Aringer I, Fauland A, Konya V, Dahlen SE, Wheelock CE, Kratky D, Olschewski A, Marsche G, Schuligoi R, Heinemann A.

Activated prostaglandin D2 receptors on macrophages enhance neutrophil recruitment into the lung.

J Allergy Clin Immunol. 2016 Mar;137(3):833-43. doi: 10.1016/j.jaci.2015.11.012. Epub 2016 Jan 12.

4.1 PGD_2 DP1 and DP2 receptors are expressed on human monocyte-derived macrophages

The first part of the study was concerned with the expression of PGD_2 receptors on human monocytes and human monocyte-derived macrophages. The expression of PGD_2 receptors on macrophages was assessed to get first insights into delineating the physiological role of PGD_2 on macrophages. To this end, a flow cytometric staining on the cell surface was performed. Either human monocytes – freshly isolated from buffy coats – or fully differentiated human MDM were detached, and immediately stained for the cell surface expression of DP1 and DP2 receptors. Analysis showed that monocytes expressed both DP1 and DP2 receptors at basal levels and their expression was approximately equal to each other (Fig 7A). After differentiation to human MDM, expression of PGD_2 receptors appeared more heterogeneous with increased levels of DP2 found on the cellular surface (Fig 7B). Concomitant, DP2 expression on human macrophages was elevated compared to freshly isolated monocytes, while DP1 expression only showed a tendency of increased expression on MDM (Fig. 7B). Since both receptors appeared to be abundantly found on human MDM, a physiological role was likely to be expected.

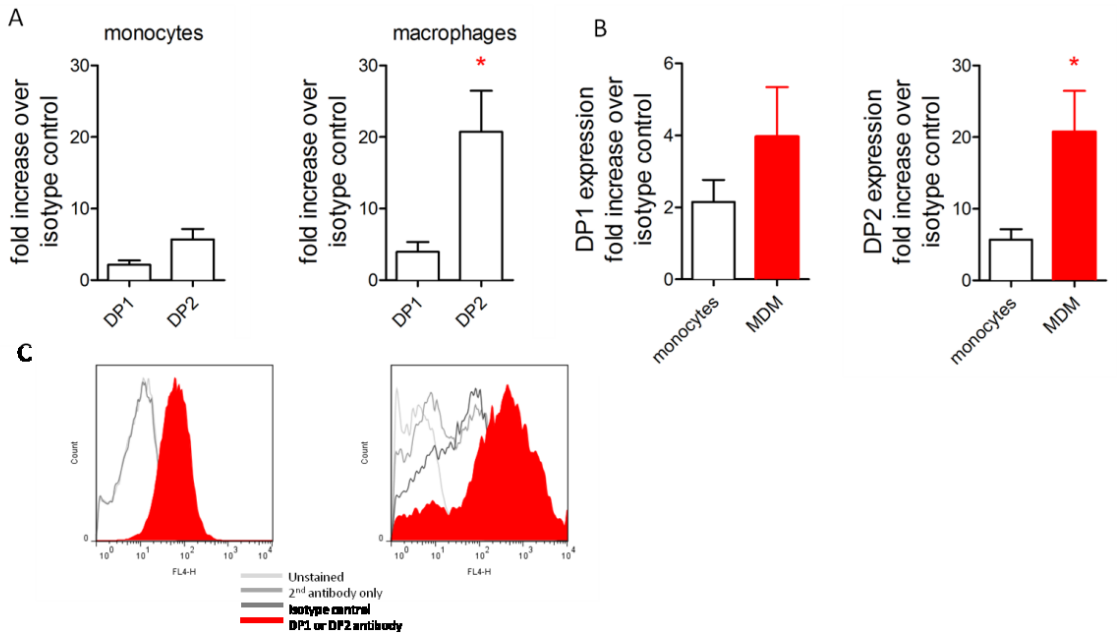

Figure 7. Cell surface expression of DP1 and DP2 receptors determined by flow cytometric analysis. (A, B) CD14 positive monocytes isolated from buffy coats and differentiated human MDM were used for direct (DP2) or indirect (DP1) flow-cytometric staining.; n=3-6, each from a different donor. * $p \leq 0.05$ as determined by two-tailed student's t-test. (C) Representative flow cytometric histograms of direct and indirect staining with DP1 and DP2 specific antibodies (filled histogram), respectively, on MDM.

PGD_2 plays a prominent role in pulmonary diseases, as it is considered an early phase mediator, released in high amounts upon stimulation. Therefore, we next probed for the expression pattern of DP1 and DP2 in human tissue samples derived from healthy donors. Human lung tissue samples were obtained from resection specimen from trauma and were not associated with any underlying diagnosed pulmonary disease. Therefore, these lung samples can be considered to represent the physiological state. In the healthy lung, DP1 and DP2 receptors stained positive on alveolar macrophages (Fig.8A, B). Quantification revealed that both DP1 and DP2 receptors were expressed on more than half of all macrophages found in the lung samples (Fig 8C).

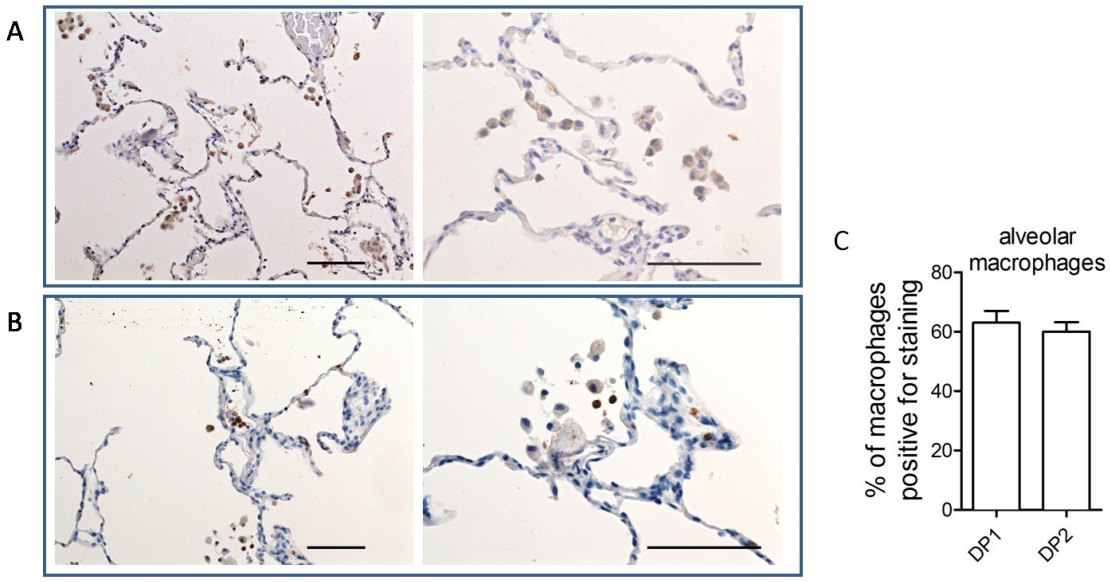

Figure 8. Immunohistochemical staining of (A) DP2 and (B) DP1 staining in 200x (left panels) and 400x magnification. Bar indicates 100µm. Paraffin-embedded tissues samples derived from control lungs were stained for DP1 and DP2 receptors. Note the specific staining of both receptors on alveolar macrophages. Pictures are representative of 5 donors. (C) Quantification of DP1 and DP2 positive pulmonary macrophages (n=5).

Next, we wanted to determine whether expression of DP1 and DP2 on alveolar macrophages was influenced by an underlying pulmonary pathology and, therefore, we probed for DP1 and DP2 expression on human lung tissue samples derived from ARDS, respiratory bronchiolitis, sarcoidosis and organizing pneumonia.

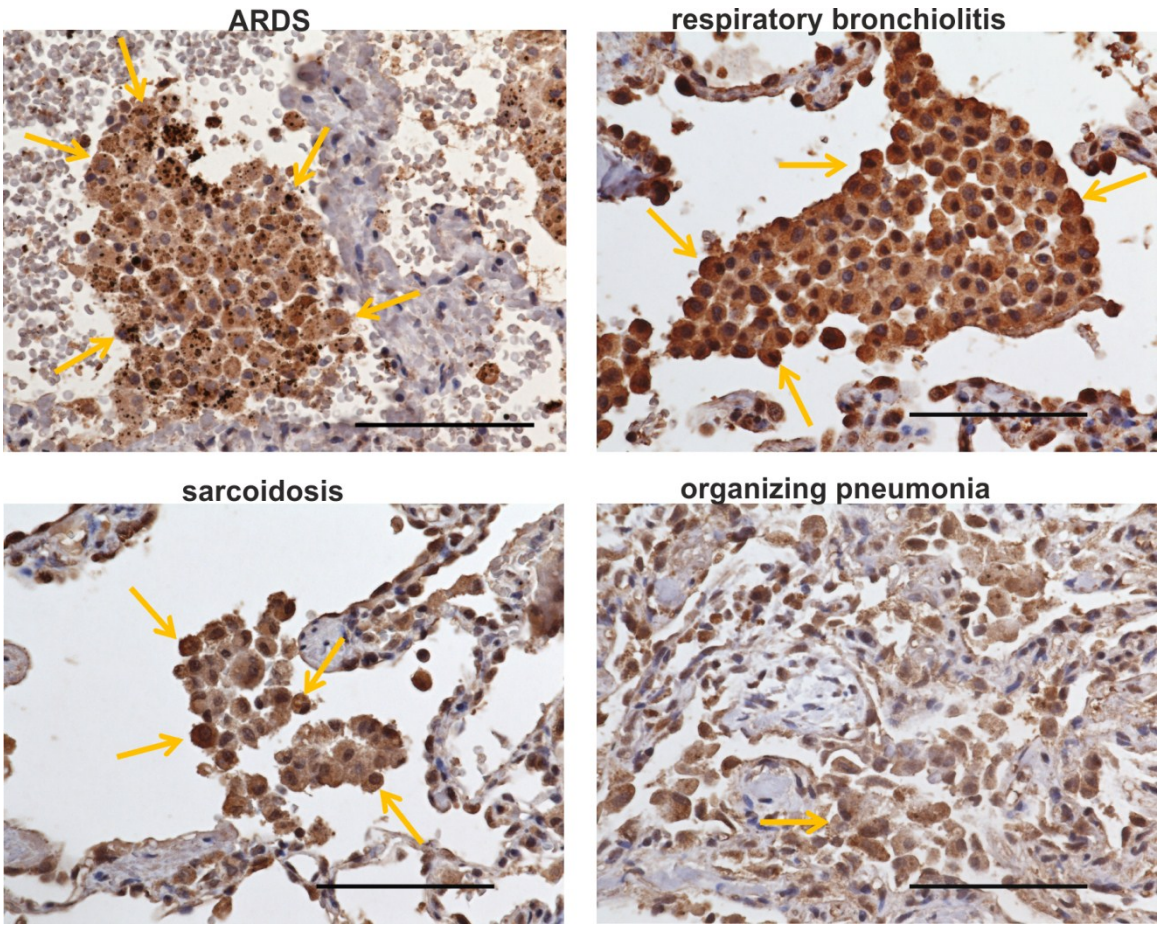

Figure 9. Immunohistochemical staining of DP1 staining in 400x magnification. Bar indicates 100µm. Paraffin-embedded tissue samples derived from ARDS, respiratory bronchiolitis, sarcoidosis and organizing pneumonia lungs were stained for DP1. Note the staining on alveolar macrophages as indicated with arrows. Pictures are representative of 5 patients per group.

Immunohistochemistry could not show alterations in the expression pattern of DP1 and DP2 in the various diseases or control samples (Fig.9 and Fig.10). This suggests that expression was conserved and homogeneous in the lung. Both receptors were highly expressed on pulmonary macrophages in each disease as well as in the healthy lung. This expression pattern suggested a possible role for the PGD_2-DP1-DP2 axis in the modulation of macrophage biology in pulmonary diseases.

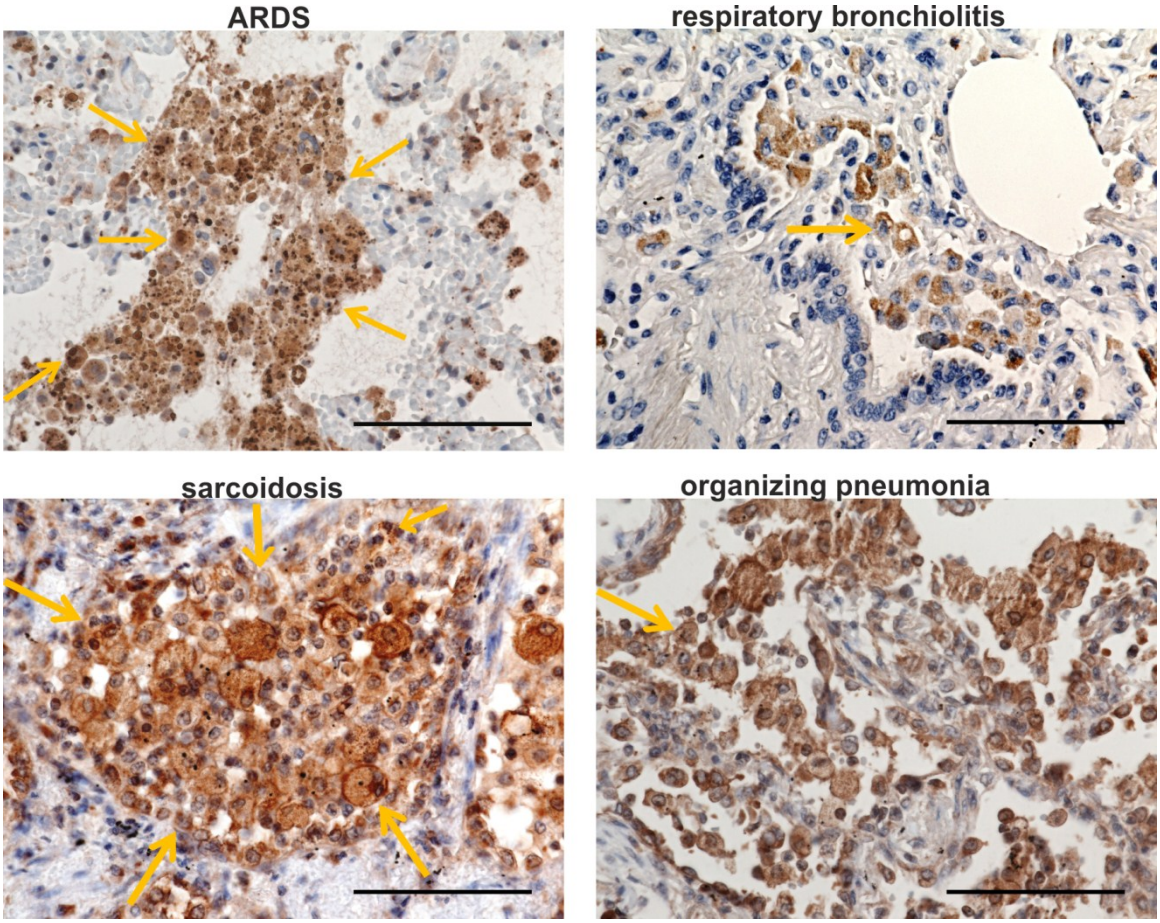

Figure 10. Immunohistochemical staining of DP2 staining in 400x magnification. Bar indicates 100µm. Paraffin-embedded tissues samples derived from ARDS, respiratory bronchiolitis, sarcoidosis and organizing pneumonia lungs were stained for DP1. Note the staining on alveolar macrophages as indicated with arrows. Pictures are representative of 5 patients per group.

4.2 Activation of PGD_2 receptors, DP1 and DP2, on human monocyte-derived macrophages leads to receptor-induced Ca^{2+} flux

Next we set out to determine the signaling and physiological importance of PGD_2, we assessed activation of macrophages via the measurement of intracellular Ca^{2+} levels. The release of Ca^{2+} from intracellular stores often precedes functional responses such as migration, growth, differentiation and proliferation. To this end, macrophages were seeded on coverslips and loaded with the ratiometric Ca^{2+} indicator fura-2/AM. Perfusion and live-cell imaging revealed that PGD_2 was able to elicit a strong Ca^{2+}response on human MDM (Fig.11A). To determine which receptor was able to induce the release of $Ca^{2+}$from internal stores, MDM were stimulated with either DP2 specific DK-PGD_2 or DP1 specific BW245C, respectively (Fig. 11B). Activation of both receptors led to a rise in intracellular

Ca^{2+}, although to a lesser extent than PGD_2 itself (Fig. 11C). To prove specificity and also substantiate that both receptors act independently of each other, we pharmacologically antagonised either DP1 or DP2 receptors using the specific antagonists CAY10471 or MK0524, respectively (Fig.11D). Single blocking of one receptor was able to diminish the Ca^{2+} response elicited by PGD_2, and dual use of both antagonists almost completely blocked the PGD_2 induced Ca^{2+}-flux (Fig. 11D and E).

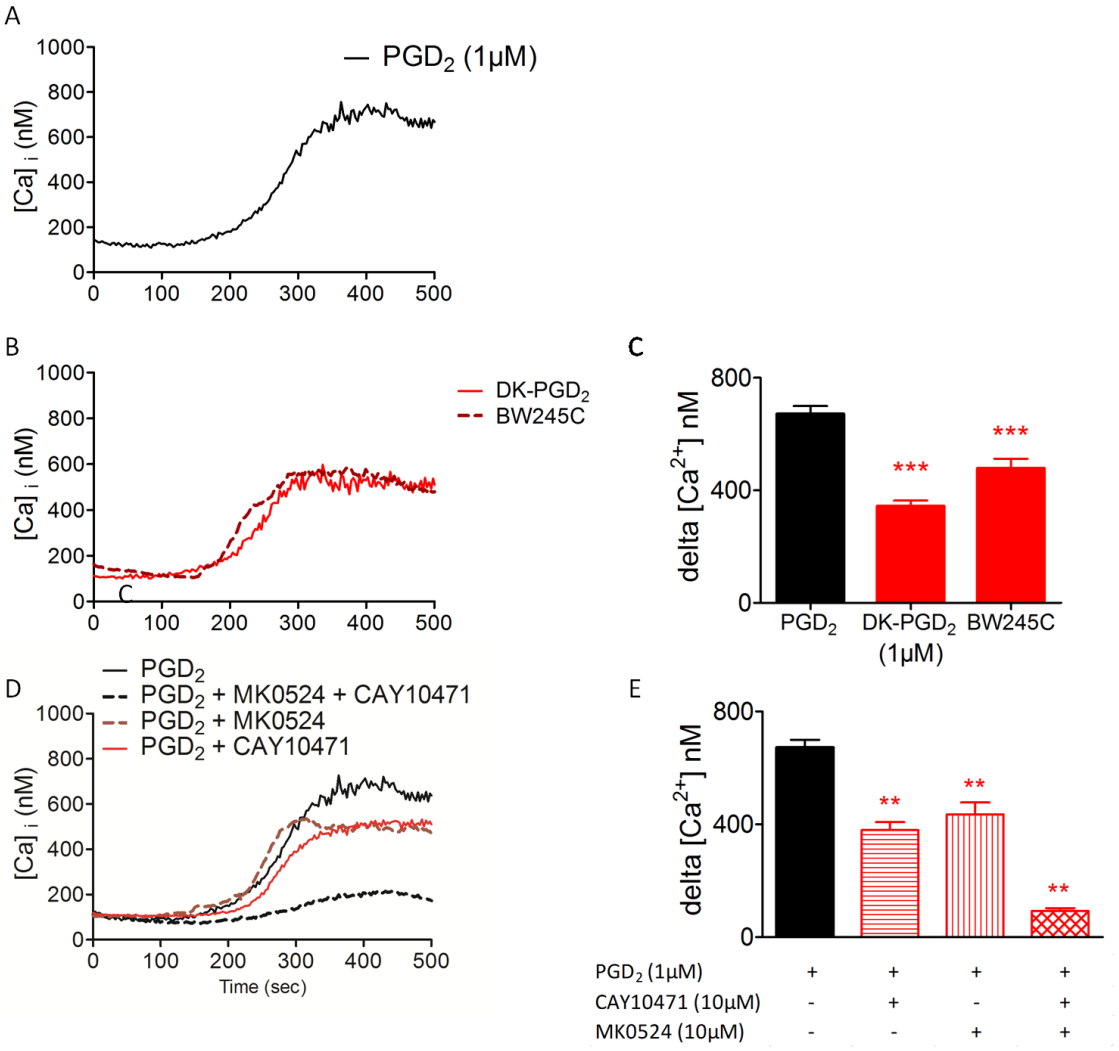

Figure 11. Receptor induced Ca^{2+} flux in human monocyte-derived macrophages. Ca^{2+} mobilization was measured using live-cell fluorescent microscopy. Cells were cultured on glass-coverslips until full macrophage differentiation. Baseline was recorded for 5 min, and then agonist perfusion was performed. In the respective experiments, cells were perfused with antagonists for 7 min while recording baseline. Graphs depict the last 2 min before agonist treatment. Fluorescence was measured for at least 20 cells per experiment and results are presented as means + SEM for 3-7 independent experiments, each with an individual donor. (* $p<0.05$, *** $p<0.001$ versus vehicle for

one-way ANOVA of followed by Bonferroni's multiple comparison test.) (A) sample graph of PGD_2-mediated Ca^{2+} response over time. (B) Representative Ca^{2+} responses to the DP1-specific agonist DK-PGD_2 and DP2 agonist BW245C. Agonists were used at 1 µM. (C) Quantification of Ca^{2+} responses after stimulation with PGD_2, DK-PGD_2 and BW245C. Simultaneous activation of both DP1 and DP2 receptors by PGD_2 showed the most prominent effect (mean + SEM, *** $p<0.001$ versus PGD_2 as determined by one-way ANOVA followed by Bonferroni's multiple comparison test). (D) Representative Ca^{2+} responses of PGD_2 in the presence of either DP1 or DP2-specific antagonists, CAY10471 and MK0524, alone or in combination. (E) Both DP1 and DP2 selective antagonists could diminish the PGD_2-induced Ca^{2+} influx, and simultaneous blockade of both receptors almost abolished any release of intracellular Ca^{2+} flux by PGD_2 (mean + SEM, ** $p<0.01$ versus PGD_2 as determined by one-way ANOVA followed by Bonferroni's multiple comparison test).

The rise in intracellular Ca^{2+} levels upon stimulation with PGD_2 indicated an involvement of either Gαq or Gαi subunits in the signalling capacities of the two GPCR. To delineate the downstream pathway of PGD_2 receptor signalling we blocked Gαi heterotrimers by preincubation with pertussis toxin (Fig. 12A). Indeed, the PGD_2 response as well as DK-PD_2 was blocked to baseline levels by Gαi inhibition (Fig. 12B). As the PGD_2 response was completely blocked, it is assumable that both DP1 and DP2 receptors acted via an involvement of Gαi heterotrimers.

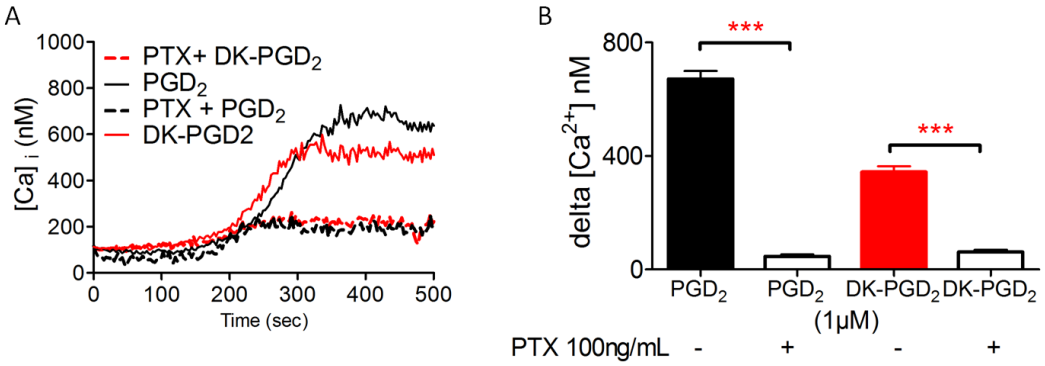

Figure 12. Overnight incubation with 100ng/mL PTX inhibited Ca^{2+} flux by PGD_2 and DK-PGD_2. (A) Representative Ca^{2+} response over time. (B) Quantification shows an almost complete abolishment of the PGD_2 and DK-PGD_2 induced Ca^{2+} release by inhibition of Gαi subunits (mean + SEM, *** $p<0.001$ as determined by one-way ANOVA followed by Bonferroni's multiple comparison test).

As we were able to delineate an expression of PGD_2 receptors on human monocytes as well – although to a substantially lesser extent than on macrophages – we also examined the ability of PGD_2 to induce Ca^{2+} flux. Freshly isolated CD14 positive monocytes from buffy coats were loaded with the Ca^{2+} sensitive dye Fluo-3. Following 60 sec of baseline measurement, cells were treated with PGD_2 or MCP-1 – used as a positive control – in increasing concentrations. While MCP-1 showed a strong increase in fluorescent intensity corresponding to a rise in intracellular Ca^{2+} levels, PGD_2 failed to elicit a comparable response. There was only a negligible release of Ca^{2+} at higher concentrations (Fig.13). As the effect of PGD_2 seemed to be limited on macrophages, we subsequently focused on this cell type.

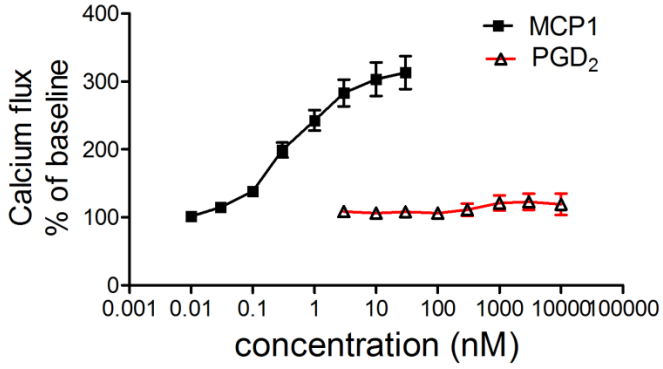

Figure 13. Receptor-mediated intracellular Ca^{2+}- changes in human peripheral blood monocytes. MCP-1 leads to a concentration-dependent Ca^{2+} -flux, whereas PGD_2 only slightly induces Ca^{2+} mobilization starting at 1 µM. Ca^{2+} flux was measured by flow cytometry as an increase in fluorescent intensity following agonist treatment. Results are represented as % of baseline fluorescence as means ± SEM of 3 independent experiments, each with a different donor.

4.3 PGD_2 induces migration of human MDM

Driven by the strong response to PGD_2 treatment in the Ca^{2+} flux experiment, we wanted to delineate if this subsequently leads to further effects of PGD_2 in the modulation of MDM function. Therefore, we evaluated the chemotactic potential of PGD_2 towards MDM using Transwell inserts followed by enumeration of fluorescent-labeled cell nuclei of the migrated cells on the lower surface of the filter. We found that PGD_2 acted as a potent human MDM chemoattractant. We observed a concentration-dependent chemotactic

activity towards MDM, with PGD_2 exerting its highest response at 100 nM (Fig. 14A and C). To delineate the specific involvement of the two PGD_2 receptors in the chemotactic response, we assessed PGD_2-mediated chemotaxis in the presence of DP1 and DP2 specific antagonists, CAY10471 and MK0524, alone or in combination. Single blocking of DP1 or DP2 could only partially inhibit the migratory activity of PGD_2, while inhibition of both receptors almost abolished any chemotactic response (Fig. 14B and C). Together with the Ca^{2+} release, these results suggested that on human MDM, DP1 and DP2 receptors are able to act independently of each other, while inducing comparable responses.

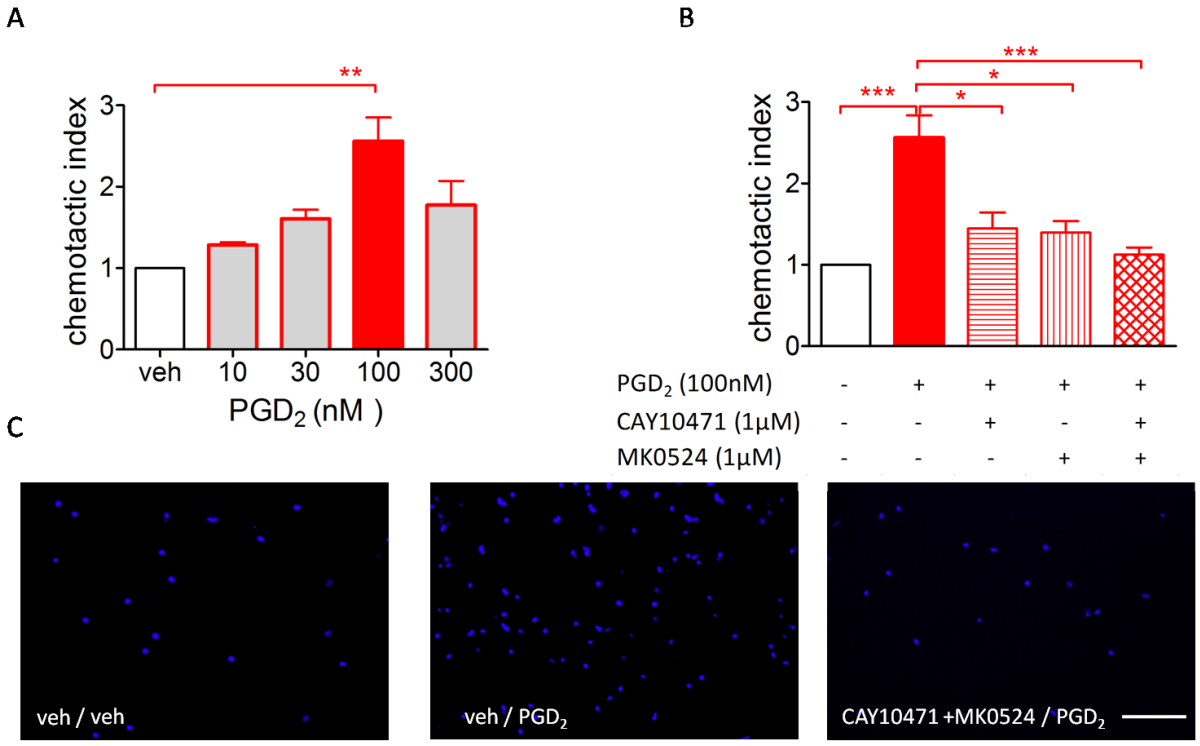

Figure 14. PGD_2 exerts a chemotactic potential towards macrophages via both receptors. Fully differentiated human MDM were treated with the cyclooxygenase inhibitor diclofenac (10 µM) overnight to inhibit endogenous PGD_2 production. Then cells were added on the top wells of a Transwell plate (8 µM pore size) and allowed to migrate to vehicle or increasing concentrations of PGD_2 in the bottom wells. After 18 hours nuclei of cells that migrated to the lower surface of the insert were fluorescently labeled with DAPI. Data are expressed as Chemotactic Index (CI) that is calculated as the number of cells that migrated towards the specific treatment over the number of cells that spontaneously migrated towards vehicle. In (B) cells were pretreated with PGD_2 receptor-specific antagonist alone or in combination before allowing the cells to migrate towards PGD_2-enriched media in the lower insert. For A and B , n=4-5, * $p<0.05$, ***$p<0.01$, ***$p<0.001$ as determined by Bonferonni's multiple comparison test. **(C)** Representative fluorescent micrographs showing migrated MDM on the lower surface of the DAPI-stained filter. Scale bar 50µm.

4.4 LPS-induced TNF-α secretion is modulated by PGD_2

Prompted by a report describing PGD_2 as being critical in mediating macrophage migration towards LPS, we hypothesized that other cellular functions in response to LPS were altered by PGD_2 treatment as well. We therefore examined the effect of PGD_2 in influencing TNF-α secretion induced by LPS. Human MDM were pretreated with PGD_2 or specific agonists followed by stimulation with LPS (100 ng/mL) and cell-free supernatants were collected. While vehicle-treated cells secreted no detectable amounts of TNFα, LPS treatment, as expected, induced production and secretion of the cytokine. This was markedly enhanced via both PGD_2 as well as the DP2 specific agonist DK-PGD_2, while the DP1 agonist BW245c did not enhance LPS-stimulated TNFα production. In support of the involvement of both PGD_2 receptors, PGD_2-induced enhancement of TNFα secretion was largely diminished by blocking DP1 or DP2 receptors by CAY10471 and MK0524, respectively, and could be abolished by simultaneous incubation with both DP1 and DP2 antagonists (Fig. 15A). We therefore hypothesize that there is a need for the DP1 receptor in mediating this process as well, despite the fact that the DP1 agonist alone was not able to induce an increase in the LPS-induced TNFα secretion.

As the NFκB pathway is critical for TNF-α production, we examined the effect of NFκB inhibitor IV, a resveratrol analogue, in the PGD_2-mediated enhancement of the LPS-induced TNF-α secretion. As shown before, LPS challenge alone led to increased production of TNF-α, which was even doubled when cells were pre-incubated with PGD_2. NFκB activation inhibitor IV at a concentration of 1 μM markedly inhibited the PGD_2 induced enhancement of TNF-α secretion. Noteworthy, at the concentration used, the NFκB inhibitor IV was not able to decrease TNF-α secretion induced by LPS alone (Fig. 15B). Taken together, these results suggests an involvement of PGD_2 in NFκB signaling that is likely mediated via both DP1 and DP2 receptors.

Prompted by a recently published report that activated Th2 cells in response to PGD_2 treatment react with increased secretion of IL-6 and granulocyte macrophage-colony stimulation factor (GM-CSF) (206) we activated macrophages with IL-4 and made a similar observation. IL-4-activated macrophages showed only minor secretion of TNF-α, while PGD_2 pretreatment markedly enhanced that process. In agreement with the LPS-activated MDM, NFκB inhibitor IV was able to reverse the PGD_2-mediated response.

Noteworthy, the response in the absolute amount of secreted TNF-α in the presence of IL-4 was much lower than upon LPS treatment.

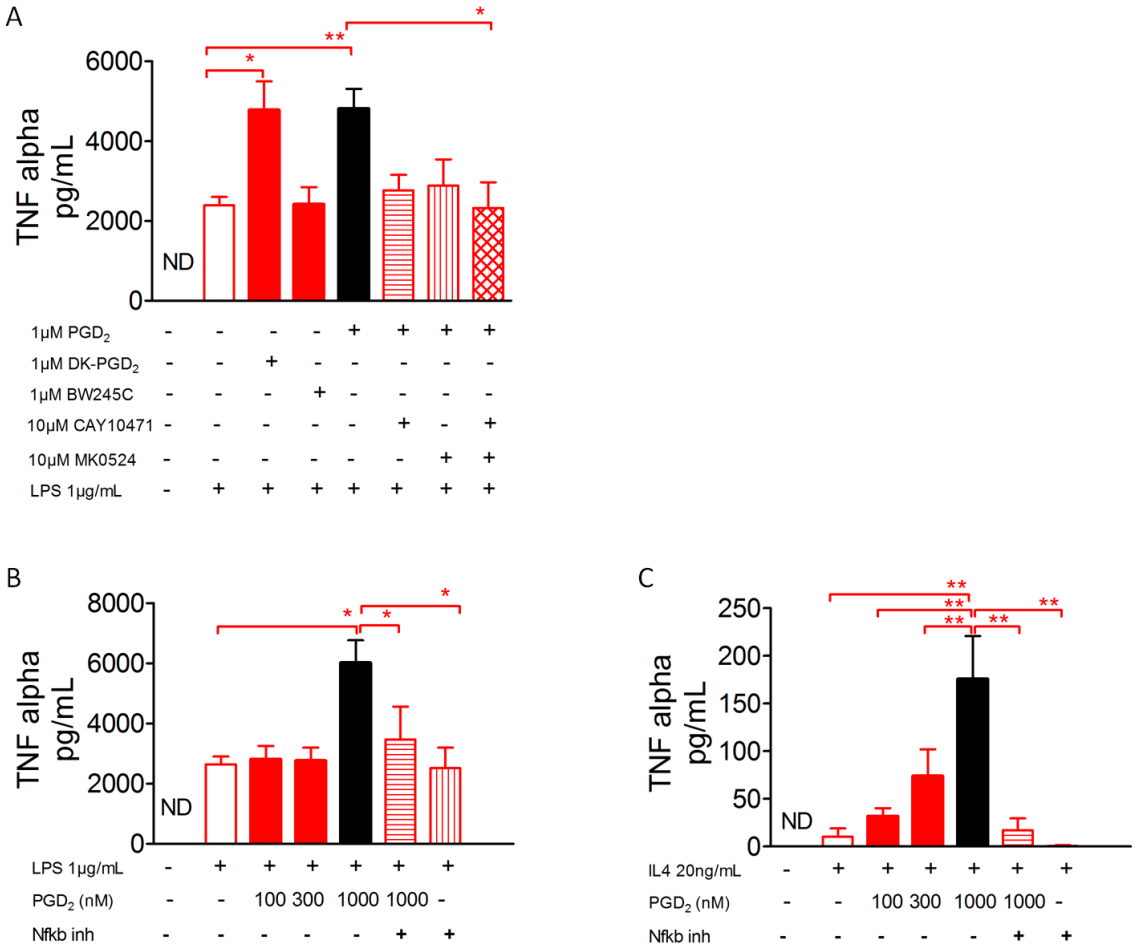

Figure 15. (A) Human MDM were pretreated with PGD_2, DK-PGD_2, BW245C or vehicle for 18 hours and then activated by 100 ng/mL LPS for 24 hours. Antagonists were added 30 min prior to PGD_2 treatment. TNF-α in supernatants was detected via ELISA, n=5 independent experiments performed in duplicates (* $p<0.05$, ** $p<0.01$ as determined by one-way ANOVA followed by Bonferonni's multiple comparison test). (B) Human MDM were pretreated with vehicle or NFκB -inhibitor IV with or without PGD_2 for 18 hours and then activated by 100ng/mL LPS for 24 hours. TNF-α in supernatants were detected via bead-based ELISA, n= 5 (* $p<0.05$ as determined by one-way ANOVA followed by Newman Keul's multiple comparison test). (C) Human MDM were pretreated with vehicle or NFκB-inhibitor IV with or without PGD_2 for 18 hours and then activated by 20 ng/mL IL-4 for 24 hours. TNF-α in supernatants was detected via bead-based ELISA, n= 3 (**$p<0.01$ as determined by one-way ANOVA followed by Newman Keul's multiple comparison test).

To further examine the involvement of NFκB signaling in PGD_2-mediated responses, we took use of a human monocytic U937- NFκB -GFP reporter cell line that upon activation of NFκB leads to induction of GFP that is detectable via flow cytometry. This cell line was kindly provided by the group of Herbert Strobl (Institute of Pathophysiology and Immunology, Medical University of Graz, Austria). U937 cells were preincubated with increasing concentrations of PGD_2, DK-PGD_2 and BW245C for 24 hours followed by 18 hours incubation with 100 ng/mL LPS. In fact we found that PGD_2 concentration-dependently increased the LPS induced increase in GFP fluorescence (Fig.16 and Fig. 17A).

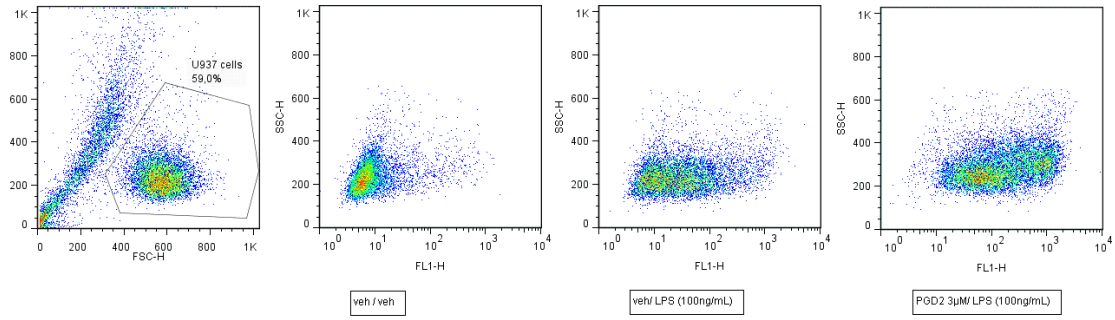

Figure 16. Typical flow cytometric plots of U937 cell lines reacting with increased fluorescent intensity in the FL1 channel due to increased expression of GFP after induction of NFκB pathway. LPS treatment leads to increased fluorescent intensity that is further enhanced by PGD_2 (starting at 3 µM) treatment.

Detailed examination of the contribution of DP1 and DP2 receptors showed that both selective agonists, DK-PGD_2 and BW245C, could significantly mimic these effects (Fig. 17B). While both specific agonists could mirror the PGD_2-mediated response, only preincubation with selective DP2 receptor antagonist, CAY10471 (10µM), could diminish the PGD_2 induced enhancement of NFκB activation. Nevertheless, we could observe the strongest inhibition when cells were incubated with both DP1 and DP2 receptor antagonists together, thus it is likely that DP receptors are implicated in this process (Fig. 17C). Monocytes treated with antagonists alone could not alter the LPS-induced NFκB

induction (Fig.17D). Taken together, these results suggest an involvement of PGD_2 in NFκB signaling that is likely mediated via both DP1 and DP2.

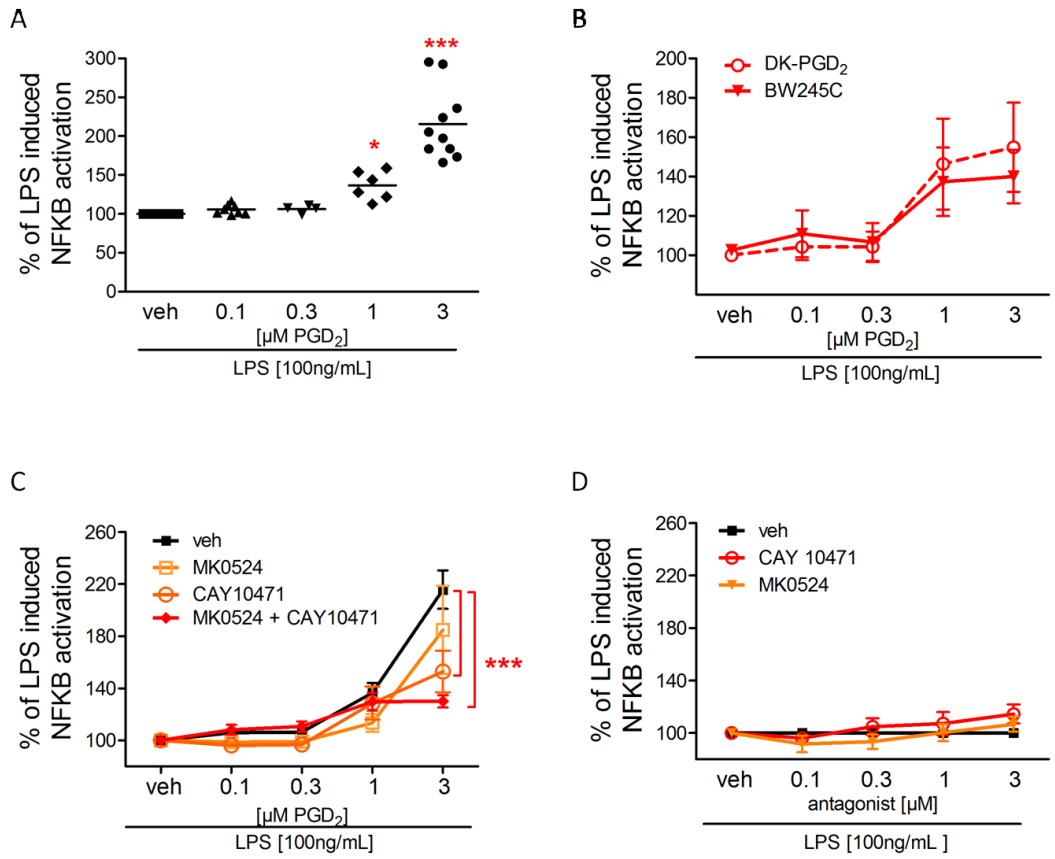

Figure 17. DP1 and DP2 activation enhances the LPS induced NF-KB pathway in human monocytic U937 cells. (**A** and **B**) U937 cells were pretreated with indicated concentrations of PGD_2 or selective agonists for 24 hours followed by incubation with 100ng/mL LPS for 18 hours (n= 5-9. *$p < 0.05$ ***$p < 0.001$ versus vehicle as determined by one-way ANOVA followed by Bonferroni's multiple comparison test). (**C** and **D**) In antagonist experiments, cells were treated with selective DP1 or DP2 antagonist alone or in combination with PGD_2 for 24 hours followed by LPS treatment for 18 hours. NFκB induction was measured on a FacsCalibur flow cytometer as an increase in GFP fluorescence. (n=5-10, ***$p < 0.001$ as versus vehicle as determined by two-way ANOVA followed by Bonferroni's post test).

As these responses were only visible upon higher concentrations of the DP1 and DP2 agonists than in primary human MDM – where Ca^{2+} flux was induced at 1 µM PGD_2 and the chemotactic maximum response was induced by 100 nM – we investigated the expression of DP1 and DP2 in these cell lines (Fig. 18A). And indeed we found that,

although both DP1 and DP2 receptors are expressed in U937 cells, expression is lower than in MDM (compare Fig. 18B and Fig. 7B).

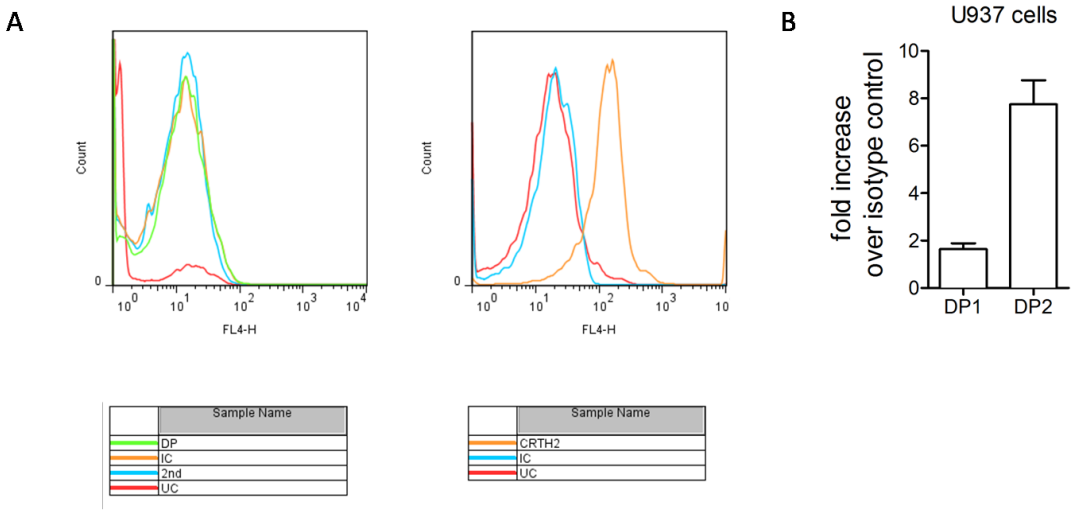

Figure 18. U937 monocytic cells express DP1 and DP2 PGD2 receptors. (A) representative flow cytometry histograms of DP1 and DP2 cell surface staining. (B) Quantification of DP1 and DP2 flow cytometric cell surface staining represented as fold increase over isotype control. DP2 is expressed more abundantly than DP1.

4.5 LPS treatment leads to a feedback loop of DP2 expression on MDM

Having shown that primary human MDM and the monocyte-macrophage cell line U937 are hyperreactive to LPS following PGD_2 receptor activation, we next wanted to evaluate whether LPS treatment also directly influences PGD_2 receptor expression. Since TNF-α secretion was likewise influenced by IL-4, we also activated macrophages with IL-4 and cell surface receptor expression was evaluated. To this end, MDM were activated with LPS (100 ng/mL) or IL-4 (20ng/mL), and cell surface receptor expression was investigated by flow cytometry. Analysis revealed that no difference in expression, when data was analyzed as fold increase over isotype control (Fig. 19A). When data was analyzed as % of expression with respect to vehicle-treated control MDM, we observed an upregulation of DP2 expression upon LPS activation (Fig. 19B). This discrepancy can be explained by the high variation in basal expression found in the different donors examined. This data suggests not only a hyperreactivity towards LPS treatment, but also a positive feedback

loop of LPS treatment in PGD_2 - DP2 receptor expression and further highlights the functional connection of LPS and PGD_2.

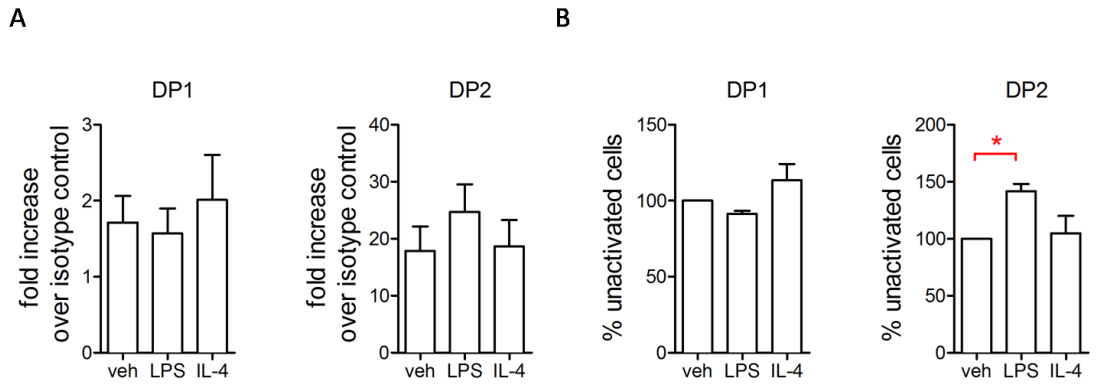

Figure 19. DP2 expression is enhanced following LPS treatment. Fully differentiated MDM were activated with LPS (100 ng/mL) or IL-4 (20 ng/mL) and cell surface receptor expression of PGD_2 receptors DP1 and DP2 was evaluated. (A) Data is presented as fold increase over isotype control (n=4-5, each from a different donor) (B) Same data as in (A) but data is presented as % in expression over vehicle-treated control MDM (n=4-5, *$p < 0.05$ versus veh as determined by two-way ANOVA followed by Dunnet's post test).

4.6 Endotoxin-induced lung injury is aggravated in mice with increased systemic PGD_2 levels

Given the strong capacity of PGD_2 to enhance LPS-induced macrophage activation, we next evaluated the effect of PGD_2 in an *in-vivo* model of LPS-induced acute lung injury (ALI). In this experimental model, acute inflammatory responses are induced by intranasal application of endotoxin (1 mg/kg). The concentrations used in this study are sufficient to induce all hallmarks of early ARDS, including neutrophilic infiltration, vascular leakage and edema formation, but are not lethal to mice. In LPS-induced ALI, neutrophil infiltration is a main characteristic but this early inflammatory response is highly dependent on macrophage function and reaction towards the injury (207). Since the role of macrophages in the resolution phase has already been assessed by various groups, we wanted to evaluate the effect of macrophages and PGD_2 receptor activation on macrophages on the early phase of ALI. To this end, mice were intranasally administered LPS and bronchoalveolar lavage was performed 4 hours following the LPS application.

Differential leukocyte staining was performed using multicolor flow cytometric staining (Fig. 20).

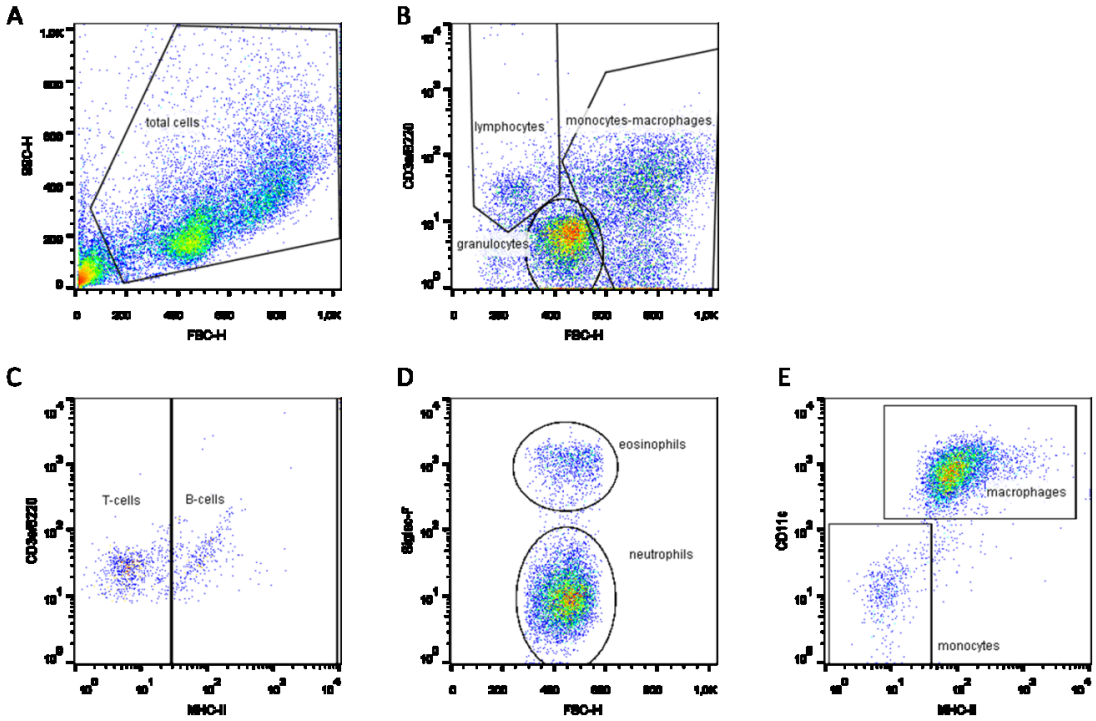

Figure 20. Gating strategy and flow cytometric staining pattern of BAL cells. Cells isolated by BAL from vehicle and LPS-treated animals were stained with FITC-conjugated MHC-II (2.5µg/mL), Siglec-F Ab (2µg/mL), PE-Cy5.5 conjugated CD3e Ab (2µg/mL), PE-Cy7 conjugated B220 Ab (2µg/mL) and APC conjugated CD11c Ab (2µg/mL) for 30 min at 4°C. Samples were washed once in PBS, 200µL fixative solution was added and samples were kept on ice until analyzed on a FACSCalibur flow cytometer. (A) BAL cells were identified on the basis of forward scatter (FSC) versus side scatter (SSC) parameters. (B) FSC versus CD3e/B220 (C) CD3e pos/B220 pos/ FSC low lymphocytes were further gated via their differential expression of MHC-II and (D) the granulocyte population from B was further divided into SiglecF negative neutrophils and SiglecF pos eosinophils. (E) Monocytes and macrophages were identified via their differential expression of MHC-II and CD11c.

As expected, intranasal application of LPS significantly increased neutrophilic influx into the alveolar space after 4 hours of LPS treatment. In accordance with our *in-vitro* data, this effect was almost doubled (increase by 186%) when mice were systemically administered PGD_2 (5 mg/kg) before LPS challenge (Fig. 21A). To delineate the involvement of the two main PGD_2 receptors in the enhancement of the LPS-induced neutrophilic influx, DP1 and

DP2 selective agonist were systemically applied before intranasal LPS administration. Interestingly, the increase in neutrophil recruitment compared to veh/LPS-treated animals, was even more pronounced with the selective DP2 agonist DK-PGD_2 being able to increase neutrophil influx by 253% and the selective DP1 agonist BW245c by 226% (Fig. 21B), which might be related to the higher metabolic resistance of these compounds as compared to PGD_2.

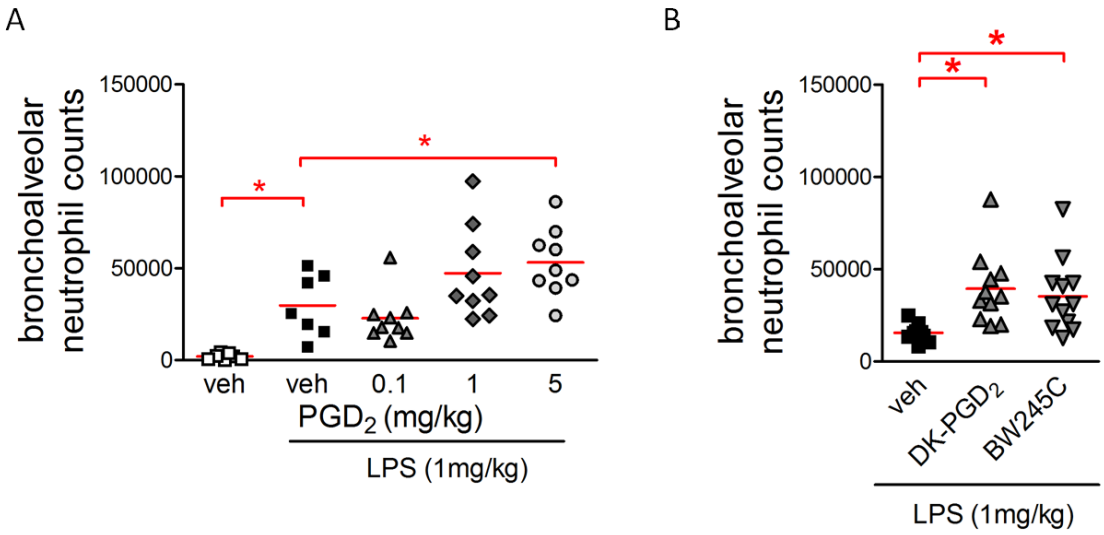

Figure 21. PGD_2 acting via both DP_1 and DP_2 receptors aggravates LPS-mediated recruitment of neutrophils in murine lungs. Mice were pretreated s.c. with PGD_2 at the indicated doses every 12 hours the day before intranasal LPS administration (1 mg/kg). After 4 hours, BAL was performed and cell populations were analyzed by flow cytometry. (A) Neutrophilic infiltration into the alveolar space following LPS administration was increased in PGD_2 pretreated animals. (* $p<0.05$ as determined by one-way ANOVA followed by Bonferonni's post test). (B) Selective agonists of DP2 (DK-PGD_2, 5 mg/kg) and DP1 (BW245C, 5 mg/kg) increased LPS-elicited neutrophil counts in the BAL (n =6-9, * $p<0.05$, versus vehicle/LPS as determined by one-way ANOVA followed by Dunnett's post test).

Other cell populations that were also measured by flow cytometry did not show a significant increase after LPS treatment alone (Fig. 22). This is not unusual, as this is mainly a neutrophilic-driven inflammation model. However, when PGD_2 (5mg/kg) was systemically applied before LPS administration, there was a marked increase in monocytic and lymphocytic populations found in the BAL (Fig. 22). These findings further

substantiate the hypothesis that PGD_2 receptor activation leads to an augmented inflammatory state.

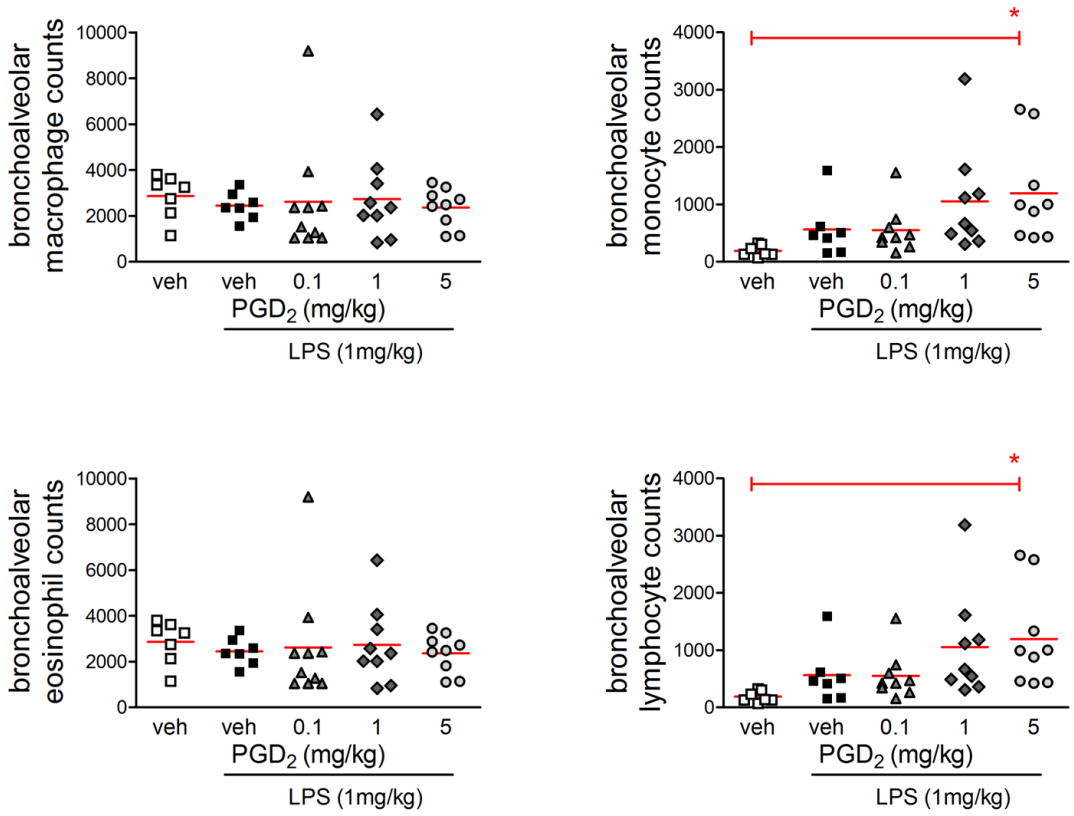

Figure 22. PGD_2 treatment does not alter macrophage, lymphocyte, eosinophil and monocyte influx in response to LPS treatment. Mice were pretreated s.c. with PGD_2 at the indicated doses every 12 hours the day before intranasal LPS administration (1 mg/kg). After 4 hours, BAL was performed and cell populations were analyzed by flow cytometry (n=6-9 * $p<0.05$ as determined by one-way ANOVA followed by Tukey‘s multiple comparison test).

Analyzing the effect of the specific PGD_2 receptor agonists, DK-PGD_2 and BW245C, on monocytes, macrophages, eosinophils and lymphocytes revealed a similar pattern. Solely, the DP2 receptor agonist DK-PGD_2 (5mg/kg) was able to alter monocyte migration into the lungs of the mice. While both PGD_2, as well as BW245C as a specific DP1 agonist, had no effect on monocyte migration, DP2 agonist DK-PGD_2 markedly enhanced monocyte recruitment (Fig. 23).

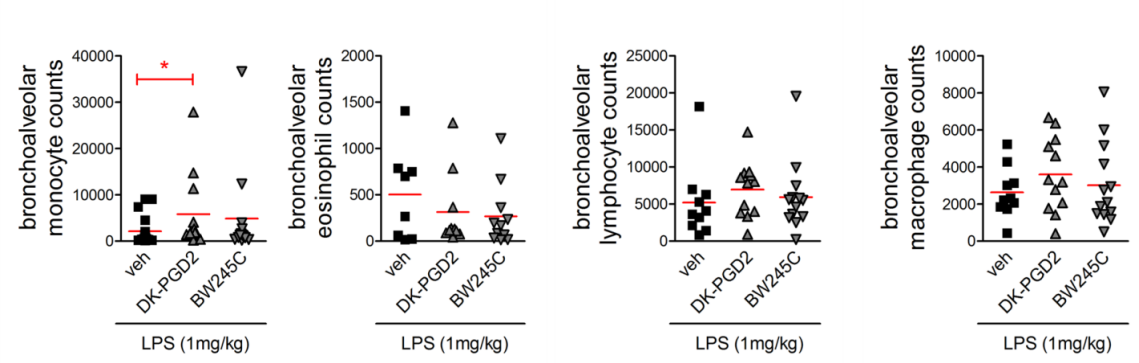

Figure 23. Effect of selective DP1 or DP2 receptor agonists on the LPS-induced recruitment of monocytes, eosinophils, lymphocytes and macrophages. Mice were pretreated s.c. with DK-PGD_2 or BW245c (5mg/kg) every 12 hours the day before intranasal LPS administration (1 mg/kg). After 4 hours, BAL was performed and cell populations were analyzed by flow cytometry (n=7-12, $p<0.05$ as determined by one-way ANOVA followed by Tukey's multiple comparison test).

We next set out to delineate whether the PGD_2-mediated enhancement was limited to the first 4 hours of inflammation, or whether the effect was sustained for a longer period of time. As we still were only interested in the acute, initial phase of the disease, we chose our next endpoint after 24 hours of LPS administration. This time-point is still characterized by neutrophilic infiltration and does not yet overlap with the resolution phase of the disease, which normally starts on around day 3 post injury.

Indeed, after 24 hours, there was still an ample influx of neutrophils into the alveolar space (Fig. 24). Furthermore, the time-course of recruitment of monocytes seems to be shifted to the right in comparison to neutrophils. The vast amount of monocytes appears to be recruited at time-points starting later than 4 hours post LPS treatment (Fig. 24). Importantly, the influx of neutrophils in PGD_2-treated animals was still markedly enhanced after 24 hours, suggesting a stable alteration in neutrophil recruitment after PGD_2 receptor activation.

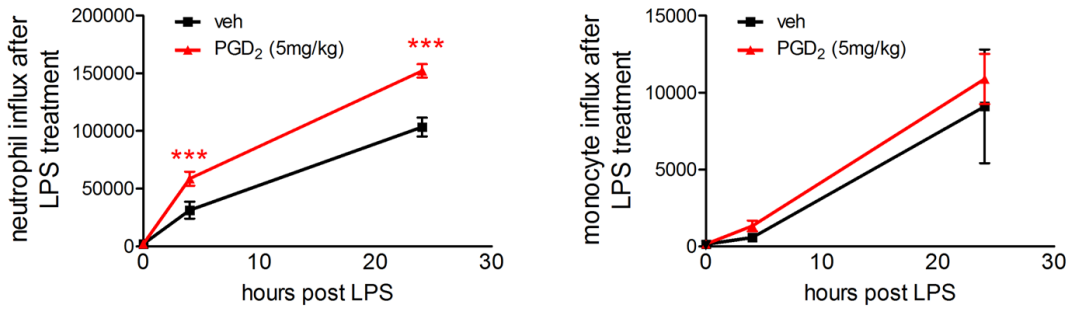

Figure 24. PGD_2-induced enhancement of neutrophil influx in response to LPS was stable for 24 hours, while recruitment of monocytes was not altered. Mice were pretreated s.c. with PGD_2 at the indicated doses every 12 hours the day before intranasal LPS administration (1 mg/kg). After 4 hours or 24 hours, respectively, BAL was performed and cell populations were analyzed by flow cytometry (n=4-9, *** $p<0.001$, versus vehicle, two-way ANOVA followed by Bonferroni's multiple comparison test).

Noteworthy, all effects of PGD_2 and specific agonists were dependent on a second inflammatory trigger – in this case LPS. Basal levels of neutrophils, monocytes, macrophages, eosinophils and lymphocytes in the alveolar space were not altered by systemic application of either PGD_2, DK-PGD_2 or BW245C (Fig. 25).

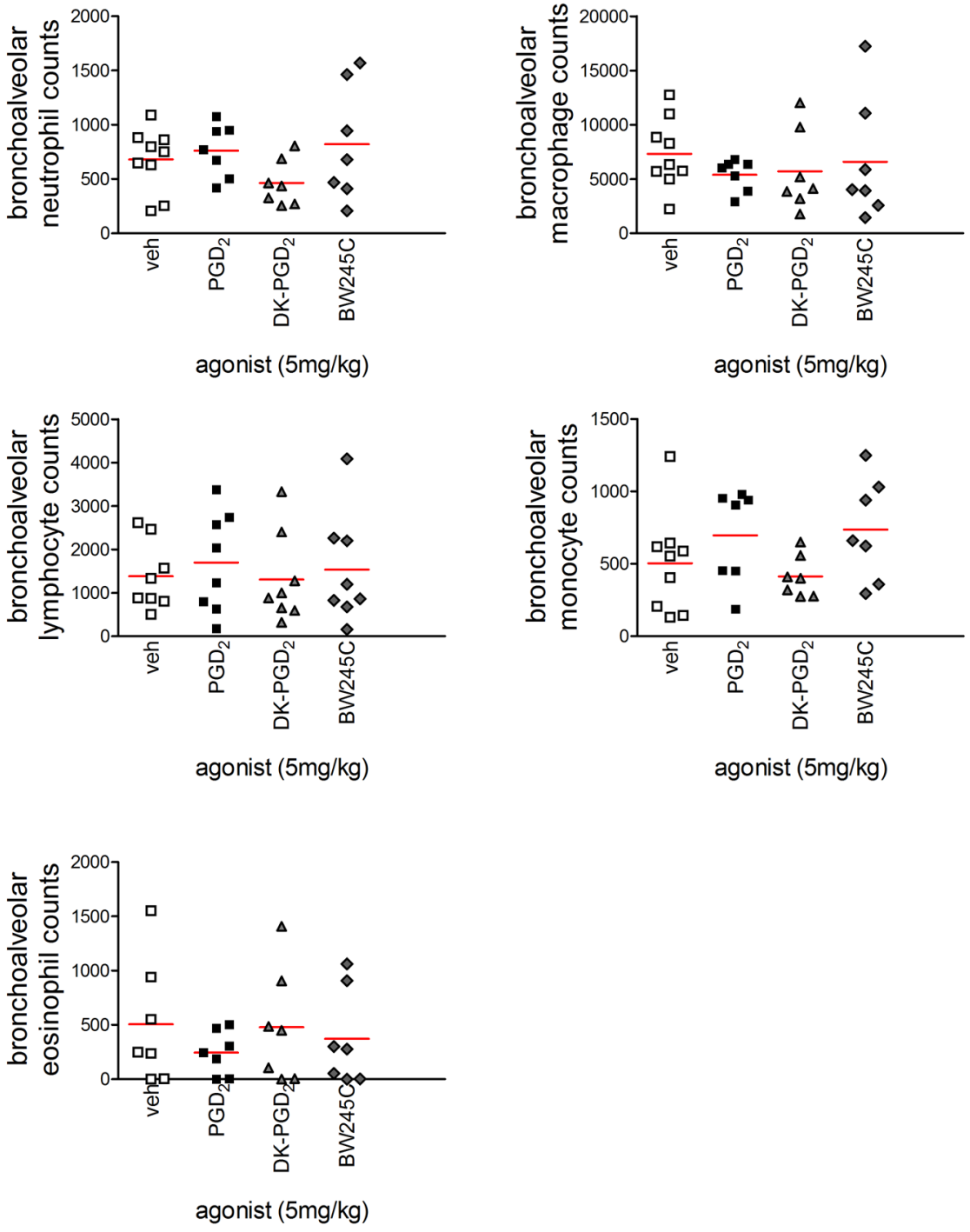

Figure 25. PGD_2 receptor activation without LPS challenge does not alter basal neutrophil, monocyte, macrophage, lymphocyte and macrophage distributions in the BAL. Mice were pretreated s.c. with PGD_2, DK-PGD_2 or BW245C (all 5mg/kg) every 12 hours the day before intranasal vehicle administration. After 4 hours, BAL was performed and cell populations were analyzed by flow cytometry.

4.7 Pulmonary inflammation is aggravated by increased systemic PGD_2

In addition to neutrophil infiltration into the bronchoalveolar space we also determined MPO activity in lung tissue samples as an indirect measure of interstitial pulmonary neutrophil counts. To this end, BAL was performed and lung tissue was collected. Following homogenisation, MPO activity was measured in supernatants with the use of the substrate O-dianosidine hydrochloride. Importantly, MPO activity directly correlates with disease severity. Concomitant with increased BAL neutrophil counts, MPO activity in BAL fluid-free wet lung tissue was also dose-dependently increased by systemic PGD_2 administered before LPS-induced lung injury (Fig. 26A). While both DP1 and DP2 receptor specific agonists induced an aggravated neutrophilic infiltration into the BAL, only DP2 specific DK-PGD_2 resembled the PGD_2-mediated increase in MPO activity compared to veh/LPS treatment. DP1 specific BW245C showed no difference in MPO activity compared to vehicle-treated mice (Fig. 26B). This data suggests a difference in the kinetics of neutrophil infiltration mediated by activation of DP1 or DP2 receptors.

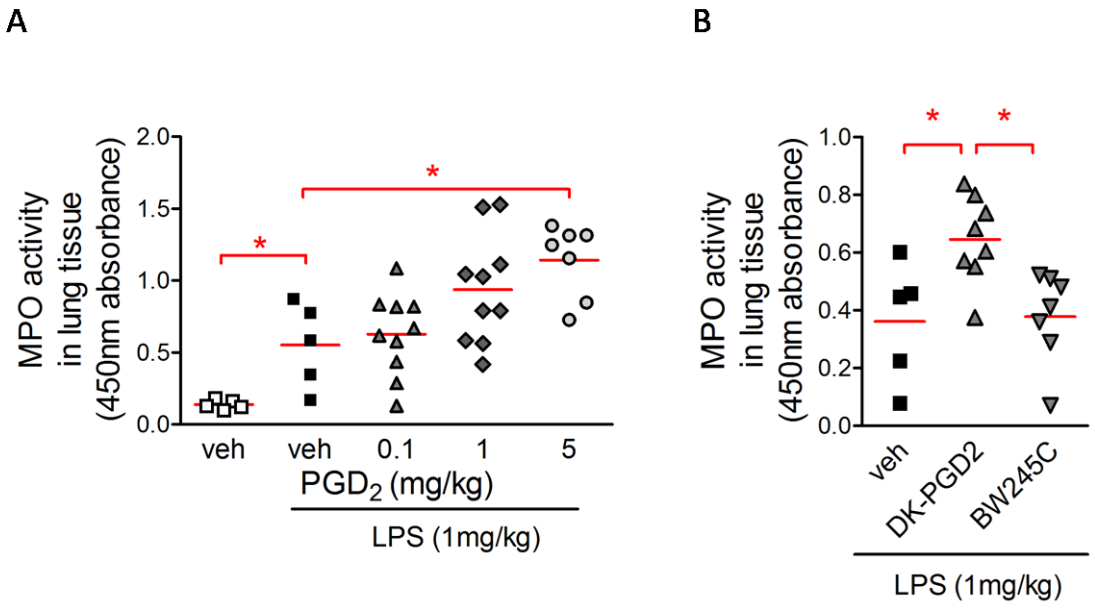

Figure 26. Enhanced MPO activity as an indirect measure of tissue neutrophils. Mice were pretreated s.c. with PGD_2 at the indicated doses or specific DP1 or DP2 specific agonists, DK-PGD_2 or BW245C, 5 mg/kg respectively, every 12 hours the day before intranasal LPS administration (1 mg/kg). After 4 hours, BAL was performed, and BALF free lung tissue was

collected. (A) MPO activity is elevated in lungs isolated from PGD_2-pretreated animals compared to veh/LPS treatment only (n=5-7, $p<0.05$ as determined by one-way ANOVA followed by Bonferonni's multiple comparison test). (B) DK-PGD_2 treatment mimics the PGD_2-mediated elevation of MPO activity in LPS-injured mice. (n=5-8, $p<0.05$ as determined by one-way ANOVA followed by Bonferonni's multiple comparison test).

4.8 PGD_2 worsens murine lung pathology

To further substantiate our findings of increased inflammatory responses upon high systemic PGD_2 levels, we histologically examined alterations in lung tissue. For these experiments, BAL was performed, followed by perfusion of the lungs with PBS/EDTA and by 4 % paraformaldehyde for fixation of tissue architecture. Paraffin-embedded lung tissue samples were consequently stained for H&E. Histologically, the worsened inflammatory state could be observed by dense infiltration of inflammatory cells with disturbed alveolar morphology in LPS-treated animals. When PGD_2 was systemically administered before LPS treatment, even more pronounced architectural destruction of the alveoli as well as injured epithelium was observed (Fig. 27).

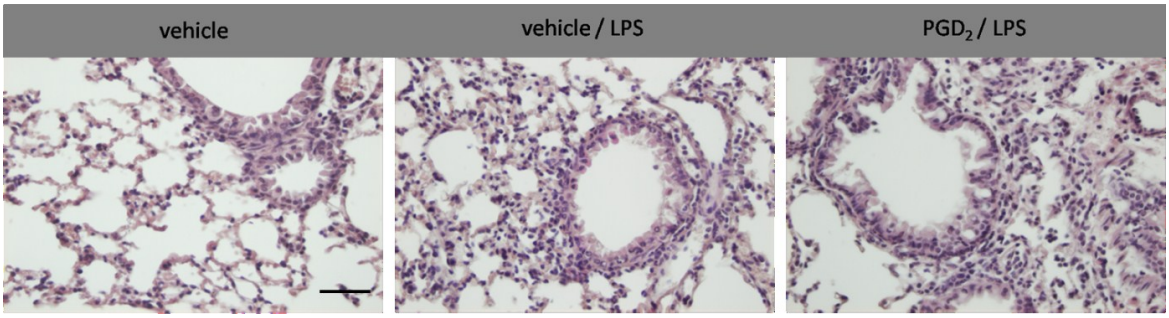

Figure 27. H&E staining of murine lungs shows disturbed architecture. Representative pictures of paraffin-embedded lung sections (5µm sections) stained with hematoxylin and eosin 4 hours post LPS treatment (n=3). Mice were either systemically pretreated with vehicle or 5 mg/kg PGD_2. Note the increased inflammatory cell infiltration in the peribronchial and alveolar space in PGD_2/LPS-treated mice. Scale bar 50 µm.

To confirm that the infiltration was in fact due to neutrophils, we immunohistochemically stained the paraffin tissue slides with an anti-Ly6G antibody, specifically for murine

neutrophils. Four hours of LPS treatment led to a marked infiltration of Ly6G positive cells, located mainly around the bronchi. Only minor Ly6G positive regions were found in the alveolar region afar from bronchi. When PGD_2 was administered systemically before LPS treatment, the Ly6G positive cell population was also found in increased amounts in the alveolar space together with an enhanced radius of positively stained cells found around the bronchi (Fig.28).

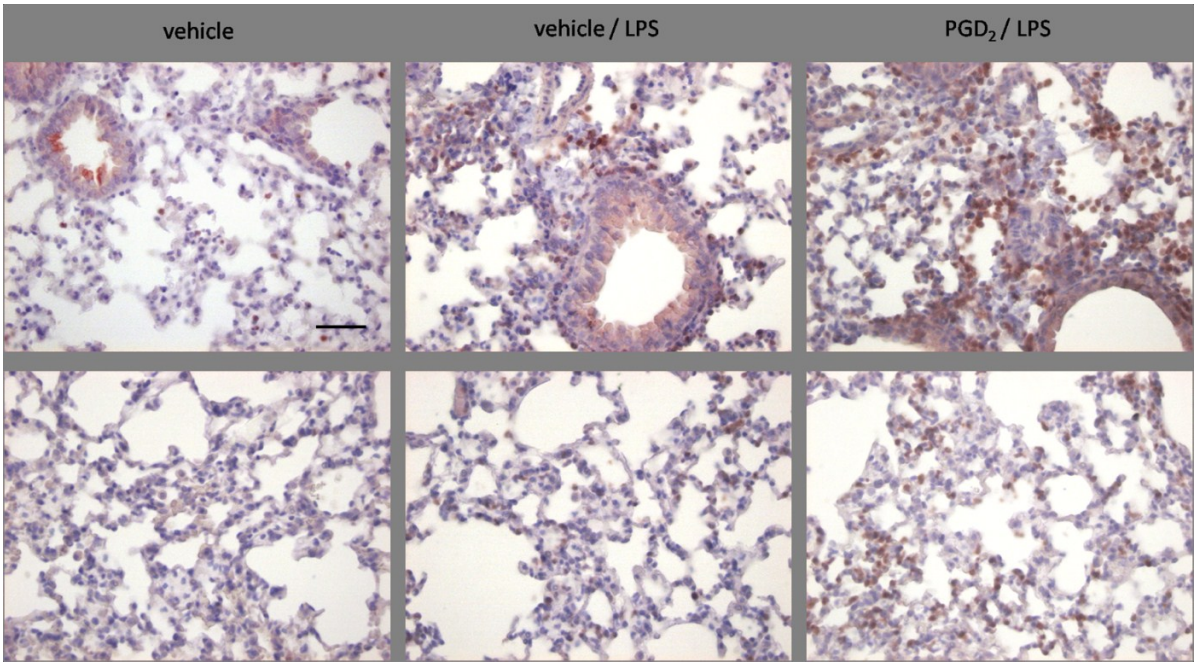

Figure 28. Ly6G-positive neutrophil infiltration in the peribronchial (upper panel) and alveolar space (lower panel). Immunohistochemistry of anti-Ly6G staining on paraffin embedded lung tissue samples from mice 4 hours post LPS or vehicle treatment. Mice were either systemically pretreated with vehicle or 5 mg/kg PGD_2. Representative pictures are shown. (n=3) Scale bar 50µm.

4.9 Increased neutrophilic infiltration is accompanied by protein extravasation into the lungs

Another hallmark of the early stages of acute lung injury is protein extravasation into the BAL and subsequent edema formation. To assess this process in our model, we took two approaches. First, we measured protein concentrations in the BALF. Second, we injected Evans blue intravenously and allowed to circulate for 60 min. Then, the amount of Evans blue found in the lungs of mice was measured. This extravasation from the circulation into the tissue is used as a measure of vascular permeability and edema formation. In our acute

model, LPS treatment caused only small alterations in protein concentrations in the BALF after 4 hours. The only measureable difference was observed between vehicle-treated mice not subjected to LPS treatment and mice treated with PGD_2 or DK-PGD_2 both at the dose 5mg/kg (Fig. 29A,B). Importantly, measurement of Evans blue dye extravasation appears more sensitive. As expected, the amount of dye found in the lungs of LPS treated mice was increased compared to vehicle treated mice. This effect was further enhanced by pretreatment with PGD_2, DK-PGD_2 and BW245C (Fig. 29C). This suggests, that both DP1 and DP2 activation leads to enhanced edema formation, independently of each other in the early stages of ALI.

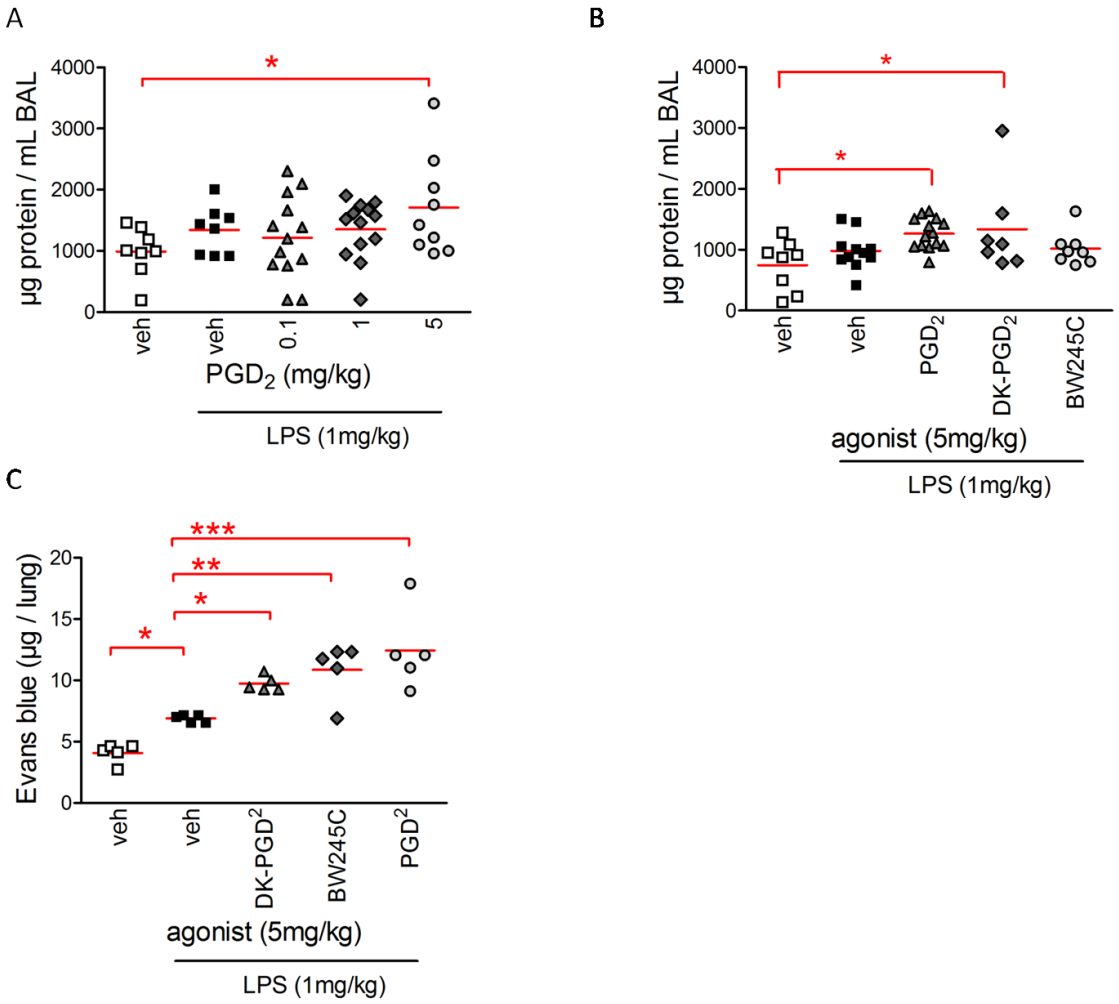

Figure 29. Protein extravasation is increased in PGD_2-treated mice. Mice were pretreated s.c. with PGD_2 or specific agonists at the indicated doses every 12 hours the day before intranasal LPS administration (1 mg/kg). (A) After 4 hours, BAL was performed and protein concentrations were measured (n=8-13, * $p<0.05$ as determined by one-way ANOVA followed by Bonferroni's multiple comparison test). (B) Specific DP2 agonist, DK-PGD_2, mimics the PGD_2-mediated

increase in BALF protein concentrations (n=7-10, * p<0.05 as determined by one-way ANOVA followed by Bonferroni's multiple comparison test). (C) Evans blue injected three hours post intranasal LPS administration and was allowed to circulate for 60 min before sacrificing mice. (n=5, * p<0.05, ** p<0.01, *** p<0.001 as determined by one-way ANOVA followed by Tukey's post test).

4.10 PGD_2 increases airway hyperresponsiveness

Finally, but most likely with the highest biological relevance, we tested for alterations in lung function following intranasal vehicle or LPS application in vehicle or PGD_2-treated mice. Using the flexiVent system, mice were mechanically ventilated and their bronchoconstrictor responses to aerosolized methacholine were measured. Airway resistance and compliance, as a measure of lung elasticity, were calculated. Here we observed that PGD_2-aggravated pulmonary inflammation after 4 hours of LPS treatment was further reflected by a decrease in lung function. While LPS application alone only increased responsiveness towards the highest concentration of methacholine (100 mg/mL), PGD_2-pretreated mice showed an aggravated response already to lower methacholine concentrations (Fig. 30 A, B). These data clearly suggested that exogenous and endogenous PGD_2 plays a pro-inflammatory role in the early state of endotoxin-induced lung injury.

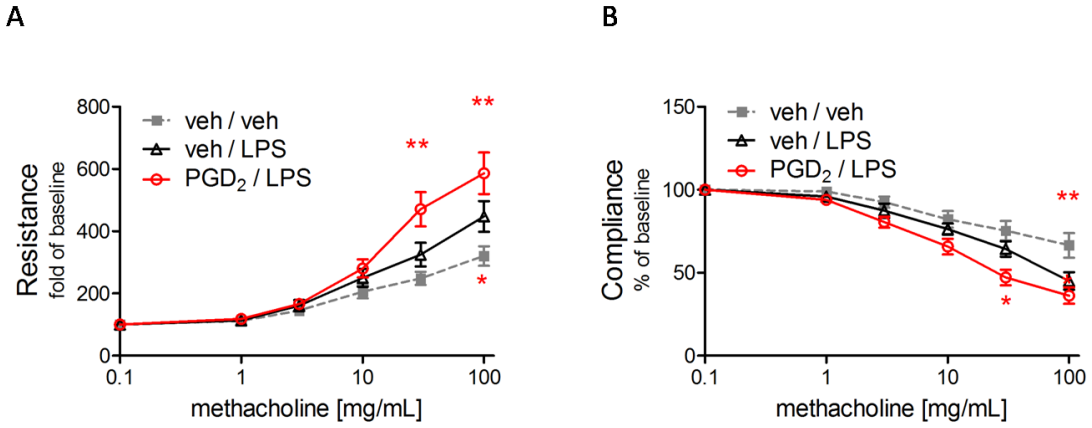

Figure 30. Hyperresponsiveness towards methacholine in PGD_2-treated animals. Mice were pretreated s.c. with PGD_2 (5mg/kg) every 12 hours the day before intranasal LPS administration (1 mg/kg). After 4 hours of LPS treatment mice were anesthetized and lung function parameters were measured using the FlexiVent system. (A) Resistance was calculated as $cmH_2O.s/mL$ and then normalized to basal levels (n=11-14, * p<0.05, ** p<0.01 compared to vehicle/LPS as determined

by one-way ANOVA followed by Dunnett's post test). (B) Compliance was calculated as mL/cmH_2O and then normalized to basal levels (n=11-14, * $p<0.05$, ** $p<0.01$ compared to vehicle/LPS as determined by one-way ANOVA followed by Dunnett's post test).

4.11 Endogenous levels of PGD_2 and other lipid mediators are increased upon intranasal LPS administration in the BALF

As all *in-vivo* experiments until this point involved the exogenous administration of PGD_2, we next wanted to investigate the role of endogenous PGD_2. A mass-spectrometric approach, performed by our collaborators at the Karolinska Institutet, revealed increased levels of PGD_2 in the BALF after 4 hours of LPS treatment. Furthermore, in agreement with previously published data (208)(4), PGE_2 was also enhanced after LPS challenge. Other lipid mediators, such as thromboxane (Tx) B_2 and 12-HHTrE were likewise elevated, while there we no detectable changes in PGI_2 (which was estimated via its metabolite 6-keto-$PGF_1\alpha$) (Fig. 31). These increased levels of PGD_2 point to a pathological role of endogenous PGD_2 in acute-lung injury.

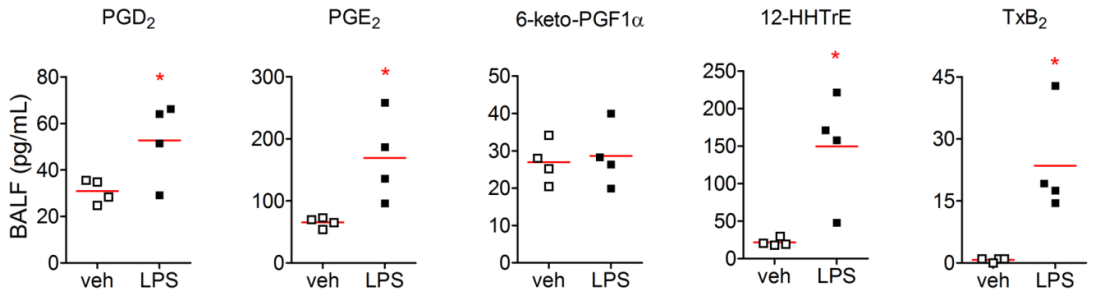

Figure 31. Increased levels of endogenous PGD_2 after LPS challenge. Lipid mediators in BAL fluid 4 hours after vehicle or LPS treatment were quantified by LC-MS/MS (n=4, * $p<0.05$, versus veh by Student's t-test).

4.12 Blocking endogenous PGD_2 improves lung inflammation

Next we set out to investigate whether blocking endogenous PGD_2 using DP1 or DP2 receptor specific antagonists would also improve disease activity. Therefore, mice were pretreated with DP1 or DP2 antagonist, CAY10471 and MK0524, respectively, followed by intranasal LPS administration. Both neutrophil infiltration into the alveolar and the interstitial space was evaluated. BALF neutrophil counts were reduced upon inhibition of

DP1 receptors, while stayed unaltered upon DP2 receptor blockade (Fig. 32A). In contrast, antagonism of DP2 receptor significantly decreased MPO activity, with no effect of DP1 receptor antagonism (Fig. 32B). Although inhibition of both receptors led to a decrease in neutrophil infiltration and thus reduced inflammation, it is likely that the two receptors act in a different anatomical compartments and/or at distinct kinetics.

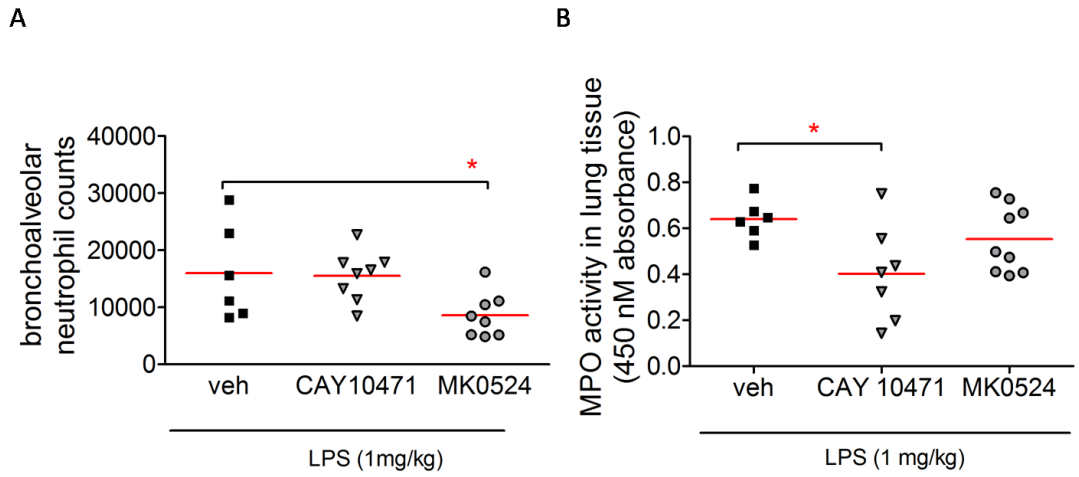

Figure 32. Inhibition of endogenous PGD_2 reduces lung inflammation. (A) Treatment of mice 24 hours before LPS with the DP1 antagonist, MK0524 (5 mg/kg s.c.) reduced neutrophil counts in the bronchoalveolar space while **(B)** MPO activity in lung tissue was reduced by the DP2 antagonist CAY10471 (5 mg/kg s.c.); * $p<0.05$ versus vehicle/LPS, one-way ANOVA followed Dunnett‘s post test.

While decreased neutrophil recruitment was apparent by blocking endogenous PGD_2, investigation of lung function in this setting did not reveal any effect on LPS-induced hyperreactivity towards methacholine with respect to resistance and compliance (Fig. 33A, B).

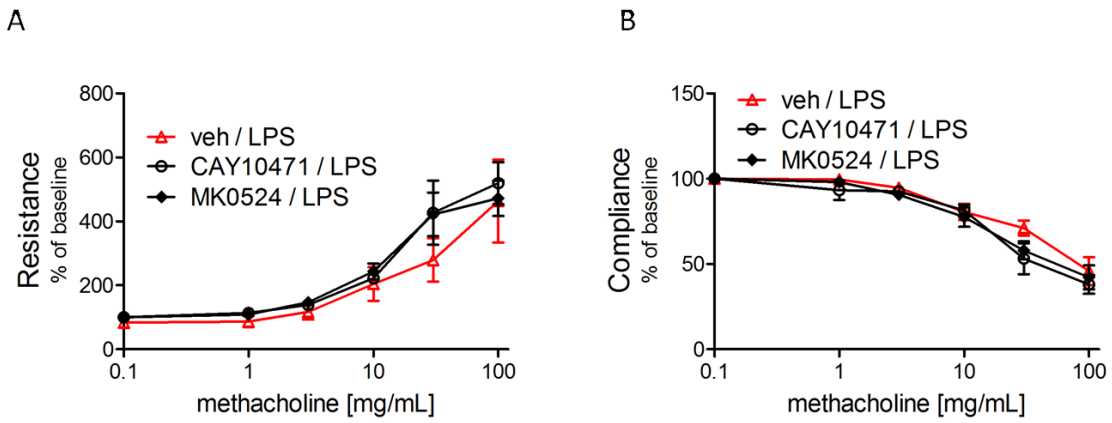

Figure 33. Unaltered responsiveness to methacholine after inhibition of PGD_2 receptors. Mice were treated with the DP1 antagonist, MK0524 (5 mg/kg s.c.) or DP2 antagonist, CAY10471 (5 mg/kg s.c.) 24 hours before LPS application. After 4 hours of LPS treatment mice were anesthetized and lung function measurements in response to aerosolized methacholine was measured using the flexiVent system (n=5).

4.13 Increased levels of inflammatory cytokines are found in the BALF

To determine the underlying cause for the increased inflammatory response and enhanced disease activity, we checked the levels of pro-inflammatory cytokines, keratinocyte-derived chemokine (KC), TNFα, macrophage chemotactic protein 1 (MCP1) and IL-6 in the cell free BALF from the treated animals. The highest response towards both LPS treatment alone and combined PGD_2/LPS treatment was observed in the levels of KC, which is a major chemoattractant for murine neutrophils. Although MCP1 levels, as well as TNF-α levels were increased compared to vehicle-only treated mice, these changes were minor compared to KC. Furthermore, as revealed above, monocyte migration – which would be mainly driven by MCP1 – appears at later stages after LPS treatment. BALF IL6 levels were not altered by either LPS or PGD_2/LPS treatment (Fig. 34).

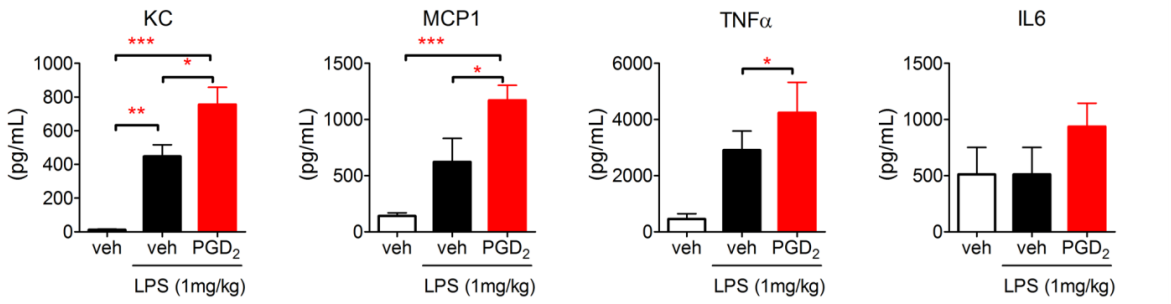

Figure 34. Levels of cytokines found in the BALF. Mice were pretreated s.c. with PGD_2 (5mg/kg) every 12 hours the day before intranasal LPS administration (1 mg/kg). After 4 hours of LPS treatment, BAL was performed. Cytokines were detected in cell-free supernatants of BAL fluid by commercially available ELISAs; n=6-12; * $p<0.05$ compared to veh/LPS, ** $p<0.01$ compared to veh as determined by one-way ANOVA followed by Dunnett's post test.

4.14 Macrophages are the source of increased KC levels in the lung

As macrophages are highly competent in early response to lung injury with the secretion of a variety of cytokines, we checked whether these cells are responsible for the increased levels of KC found in the BALF of PGD_2-pretreated mice. To this end, we isolated alveolar and interstitial pulmonary macrophages and mimicked the *in-vivo* model *in vitro*. First, macrophage purity was confirmed by immunofluorescent staining with anti-F4/80 antibody. In fact, isolated cells were 90% positive for the F4/80 macrophage marker. To further delineate if isolation was yielding an activated macrophage phenotype, we used both a marker for classically and alternatively activated macrophages (iNos and Relm-α). Both isolated alveolar and interstitial pulmonary macrophages expressed both markers. Therefore, no specific phenotype was observed. Representative fluorescent micrographs are shown in Figures 35 and 36.

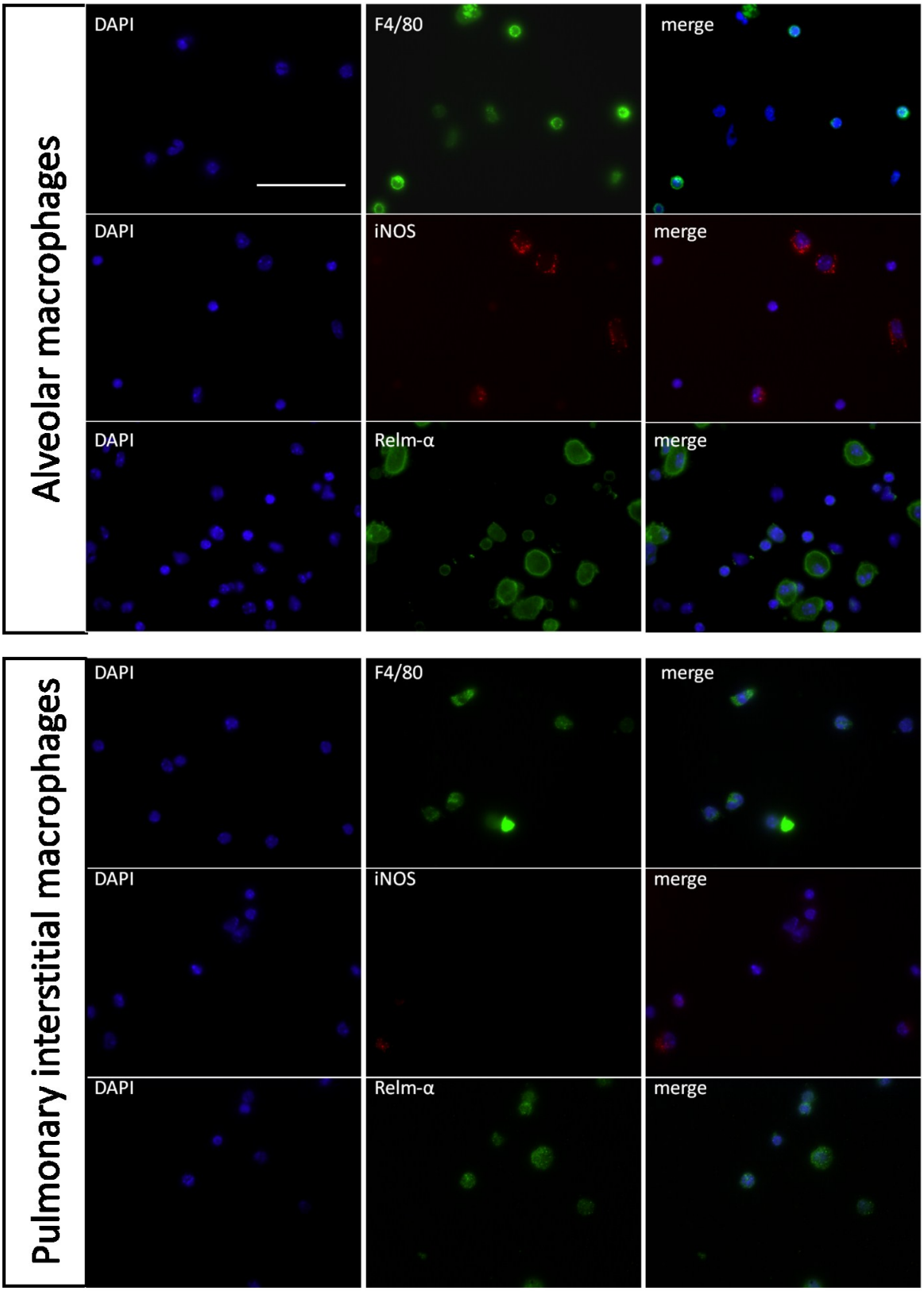

Figure 35. Characterization of isolated alveolar and interstitial pulmonary macrophages from mice. Purity of macrophages was confirmed by F4/80 staining. Both alveolar and intersititial macrophages were positive for iNOS and Relm-α. Representative pictures out of three independent isolations are shown. Bar 50µm.

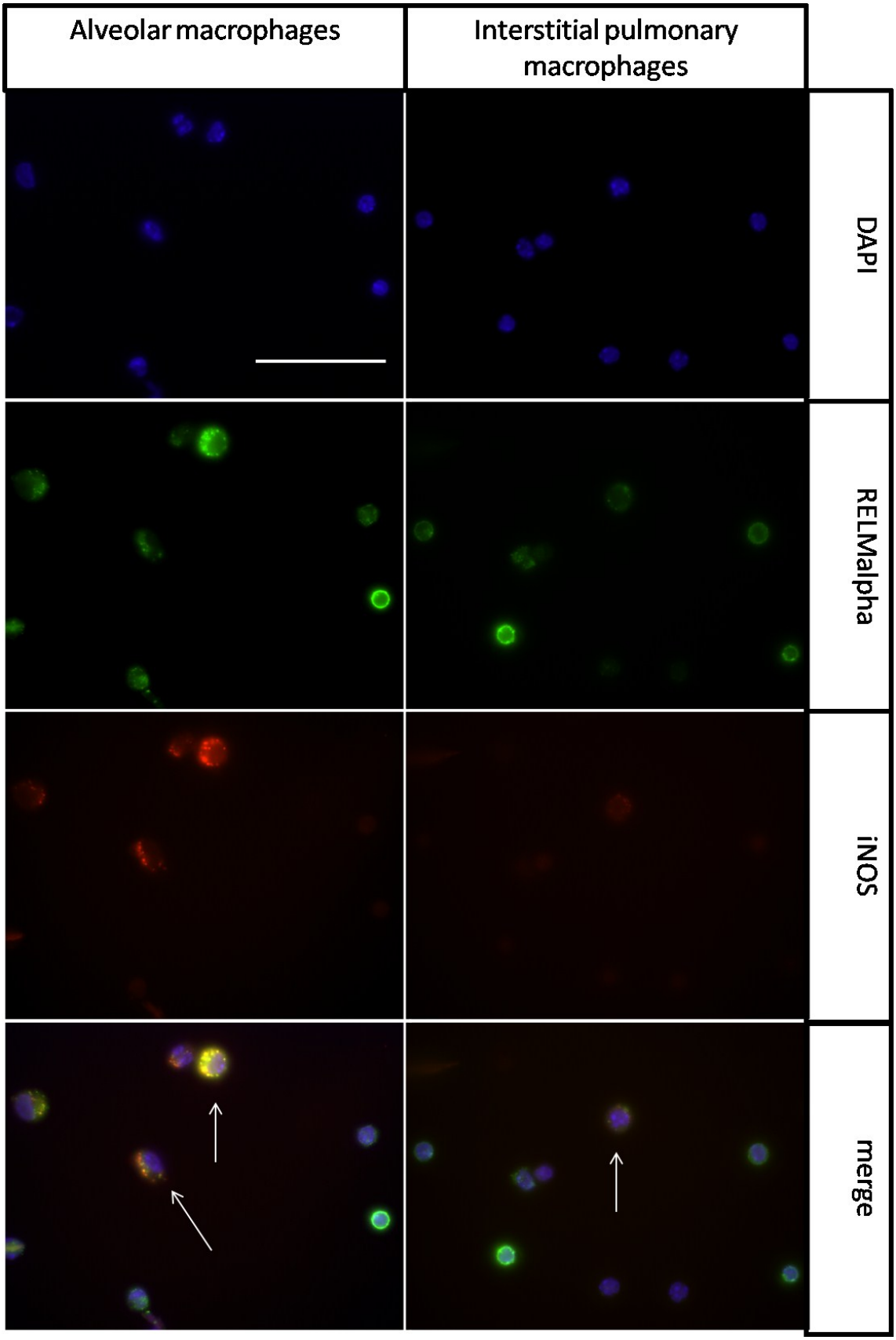
Alveolar macrophages
Interstitial pulmonary macrophages
DAPI
RELMalpha
iNOS
merge

Figure 36. Alveolar and interstitial pulmonary macrophages show a mixed phenotype. Both alveolar and interstitial macrophages cells co-expressing iNOS and Relm-α (white arrow). Representative pictures of three independent isolations are shown. Bar 50µm.

Having confirmed the purity of macrophages in the isolation process, we mimicked the *in-vivo* model, by pretreating cells with PGD_2 followed by LPS stimulation. In general, interstitial macrophages were less capable in the secretion of all investigated cytokines. Alveolar macrophages appeared more potent in both the secretion of basal levels of cytokines as well as in their response towards LPS. Solely, TNF-α secretion was induced by LPS treatment in pulmonary interstitial macrophages. LPS was not able to induce a significant increase in the cytokines KC, IL6, IL10 and MCP1 in interstitial pulmonary macrophages while, in contrast, alveolar macrophages enhanced their production in TNF-α, IL10, and most prominently, IL6 upon LPS treatment. Importantly, both types of pulmonary macrophages enhanced their secretion of KC upon combined PGD_2/LPS treatment, making it the cytokine that was most likely to be regulated by PGD_2 in our model. While BALF MCP1 levels were also increased in PGD_2-treated mice (Fig.37) both interstitial pulmonary macrophages, and alveolar macrophages showed no alterations in the secretion of MCP1 upon PGD_2 receptor activation. Thus, it is very likely, that a different cell type is responsible for the increased production of MCP1. Taken together, the increased secretion of the neutrophil chemoattractant KC by both interstitial pulmonary macrophages as well as alveolar macrophages upon PGD_2 treatment highly suggests that that macrophages are the cell type that mediate the enhanced neutrophil recruitment in this ALI model.

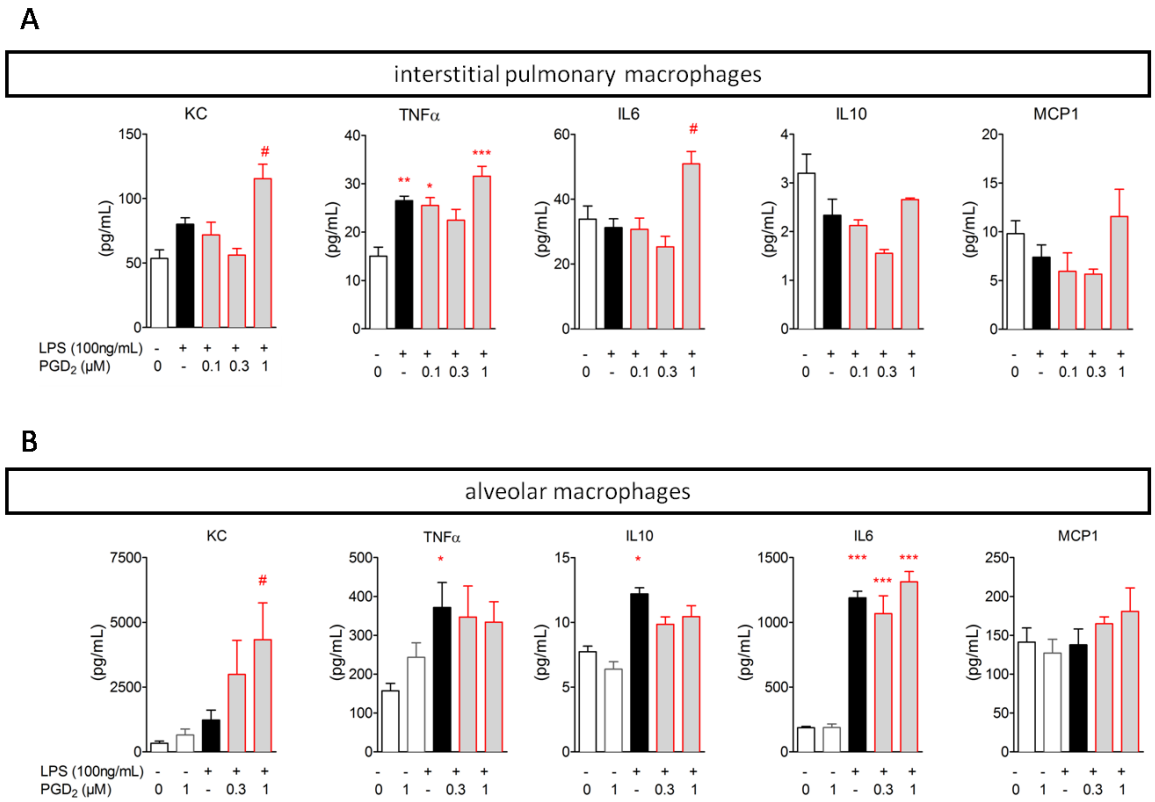

Figure 37. PGD_2 treatment stimulate the *in-vitro* cytokine secretion of (A) interstitial pulmonary macrophages and (B) alveolar macrophages as determined by bead-based ELISA (n= 3-5 independent experiments performed in triplicates; * p<0.05, **p<0.01 and ***p<0.001, compared to veh/veh, and #p<0.05 compared to veh/LPS as determined by one-way ANOVA followed by Bonferroni's post test).

4.15 Macrophage depletion inhibits the increased inflammatory response induced by PGD_2

To further investigate the role of macrophages in mediating PGD_2-dependent inflammatory cascade, we selectively depleted alveolar macrophages in the same experimental setup.

Preliminary experiments revealed that intranasal application of 300µg of clodronate liposomes led to a marked reduction of alveolar macrophages, which was consistent 24-72 hours after clodronate application (Fig. 38A). Liposomal control application did not alter alveolar macrophage counts. Both control as well as clodronate liposomes lead to an obvious increase in neutrophils recovered from BALF, suggesting that liposomes, when applied intranasally as a vehicle causes an injury to the lung and thus an inflammatory

response. Importantly, this enhanced neutrophil recruitment vanished 48 and 72 hours post liposomal administration (Fig. 38B).

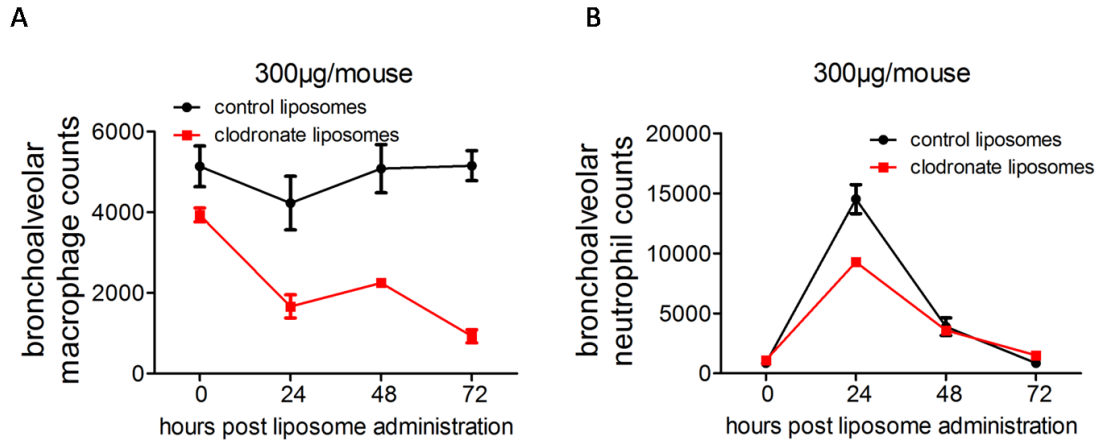

Figure 38. Clodronate-induced macrophage depletion. Mice were applied 300 µg clodronate intranasally and (A) alveolar macrophage and (B) bronchoalveolar neutrophil counts were evaluated at the given time-points (n=2 per timepoint).

Therefore, we chose our settings accordingly. LPS was applied 72 hours post liposomal control or clodronate treatment, to avoid any remaining effects on neutrophils. One day before LPS, agonists were applied s.c. every 12 **hours (Fig. 39).**

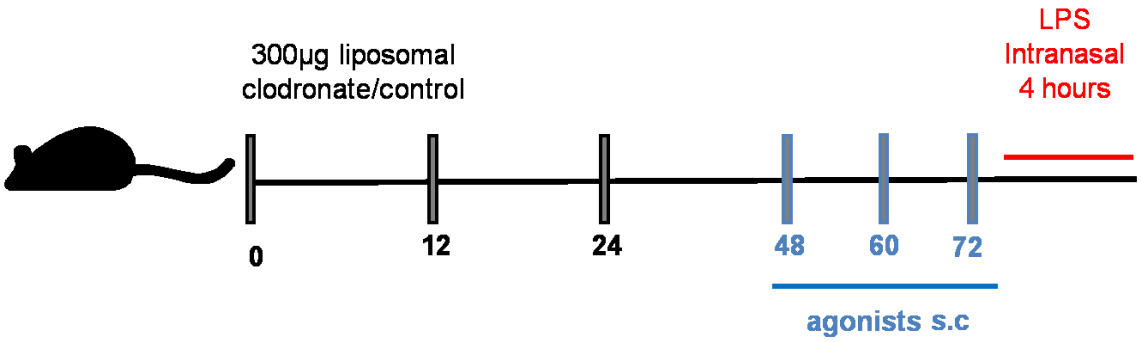

Figure 39. Scheme for *in-vivo* treatment. 48 hours post clodronate application mice were applied agonists s.c. every twelve hours. LPS was administered intranasally 72 hours after liposomal administration. Mice were sacrificed 4 hours post LPS treatment.

.

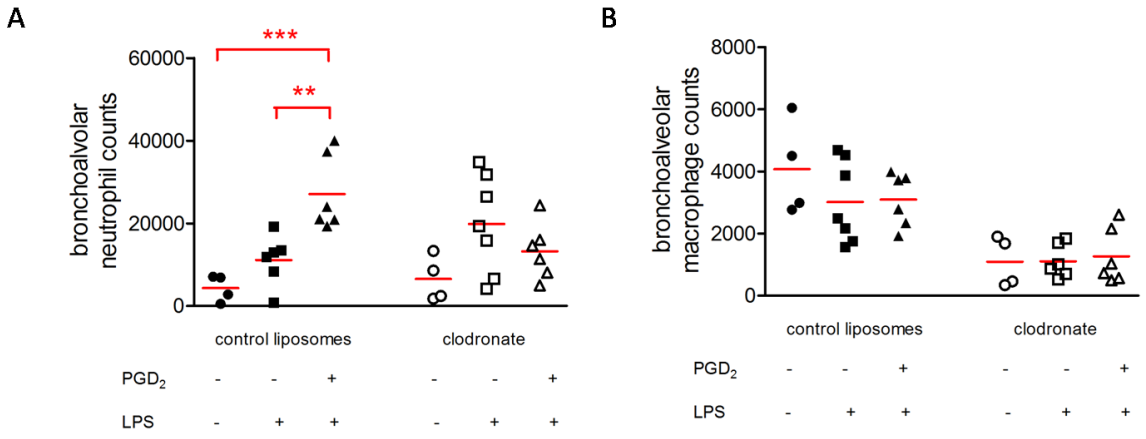

Figure 40. Macrophage reduction inhibits the proinflammatory effect of PGD_2 on neutrophil recruitment. Mice received 300 µg of clodronate in 60 µL liposomes or 60 µL control liposomes intranasally and were treated s.c. with vehicle or PGD_2 (5 mg/kg) 24 hours before LPS challenge. BALF was collected 4 hours after LPS treatment and (A) macrophage and (B) neutrophil numbers were analyzed by flow cytometry (* $p<0.05$, as determined by one-way ANOVA followed by Bonferonni‘s post test.).

Animals that had received liposomal control treatment showed effective neutrophil recruitment upon LPS stimulation, which was further enhanced by increased systemic PGD_2 levels (Fig. 40A). Clodronate-mediated reduction of macrophages (Fig. 40B) did not alter the LPS-mediated neutrophil infiltration into the alveolar space, but abolished the PGD_2-induced enhancement. Interestingly, even in reduced macrophage state – 30% of the macrophages in the lungs in control liposome-treated mice (Fig. 41) – LPS was still able to induce neutrophil recruitment.

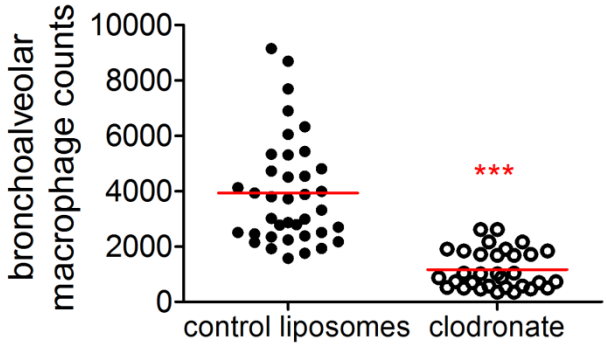

Figure 41. Reduced macrophage numbers after clodronate treatment. Mice were intranasally applied 300µg of clodronate in 60µL liposomes, or 60µL control liposomes. Depicted are macrophage numbers from the same animals as in Fig. 40 and Fig. 42 with pooled control and clodronate liposome groups; n= 32-38; *** $p<0.001$, compared to control liposomes as determined by student's t-test.

This also suggests, that only a minor population of macrophages in sufficient enough for mediating neutrophil infiltration.

We next wanted to elucidate the dependency of DP1- or DP2-mediated neutrophil recruitment on the presence of macrophages. Thus, selective DP1 receptor agonist BW245C or DP2 receptor agonist DK-PGD_2 was used subsequently following the scheme depicted in Fig.39. Independent activation of each receptor still mimicked the PGD_2-mediated effect in the liposomal-treated group, while – as for PGD_2 – this was abolished following macrophage depletion (Fig. 42A and B).

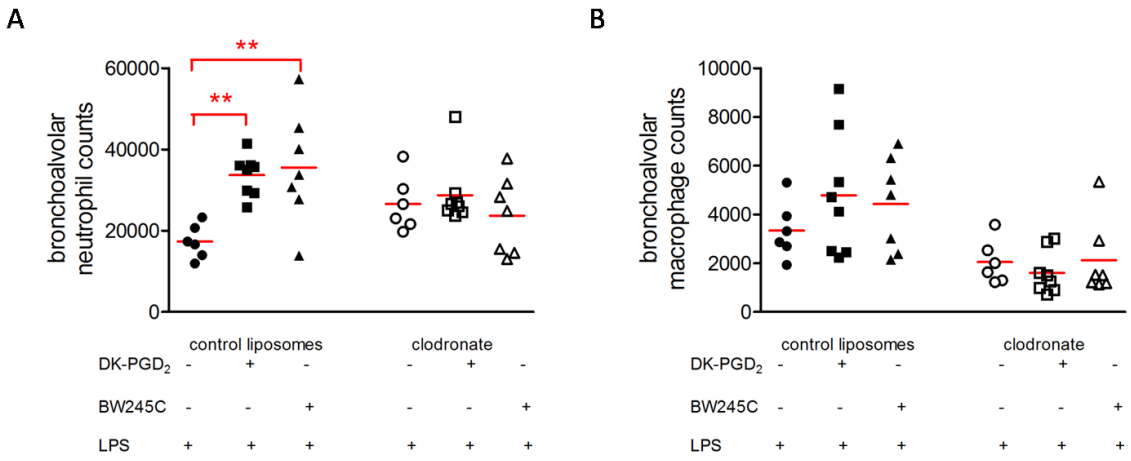

Figure 42. Enhancement of LPS-induced neutrophil recruitment mediated by DP1 or DP2 activation depends on the presence of macrophages. Mice received 300 µg of clodronate in 60 µL liposomes or 60 µL control liposomes intranasally and were treated s.c. with vehicle or PGD_2 (5 mg/kg) 24 hours before LPS challenge. BAL fluid was collected 4 hours after LPS treatment and (A) macrophage as well (B) neutrophil numbers were analyzed by flow cytometry (* $p<0.05$, as determined by one-way ANOVA followed by Bonferonni's post test).

When comparing the absolute numbers of recruited neutrophils as depicted in Fig. 40A and Fig. 42A directly across treatment groups, e.g. responses to LPS/PGD_2 in the liposomal control versus the clodronate group, we did not find statistical significant differences**.** This does not limit the conclusions drawn from the data, but we still performed additional statistical analyses of the same data. When normalizing neutrophil counts to the mean of the veh/LPS-treated animals in both the liposomal control and clodronate groups, the bias of a generally enhanced neutrophil infiltration due to clodronate treatment was diminished. In this analysis, a direct statistical significant difference between the aforementioned groups was observed (Fig. 43).

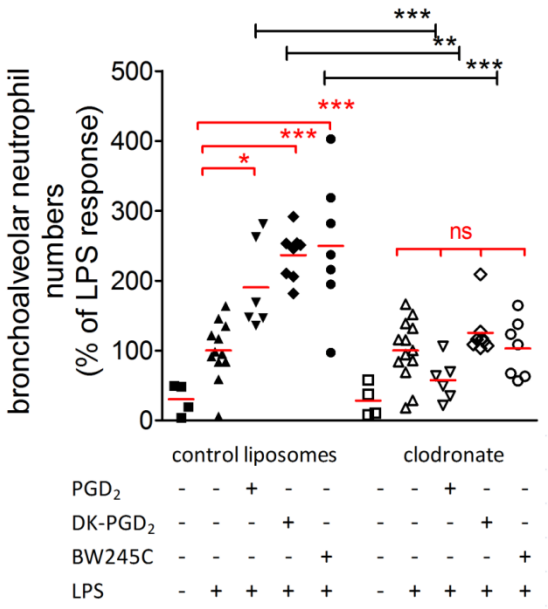

Figure 43. Bronchoalveolar neutrophil counts after treatment with control liposomes or clodronate-loaded liposomes. Depicted are the same animals as in **Fig.34 and Fig.36.** Here data is presented as % of the LPS response to the control liposome and the clodronate-treated group, respectively; * $p<0.05$, ** $p<0.01$, *** $p<0.001$ as determined by one-way ANOVA followed by Bonferroni‘s multiple comparison test.

The abolished effect after macrophage depletion was not solely limited to the recruitment of neutrophils into the alveolar space, but also to the interstitial pulmonary areas, as reflected by MPO activity. Following macrophage reduction, there was no enhancement of MPO activity in PGD_2-treated animals, which was in contrast to the liposomal control groups (Fig. 44).

Taken together, these data clearly argued in favor of a central role of PGD_2 as a modulator of macrophage function governing the neutrophil-mediated inflammatory response in the lung.

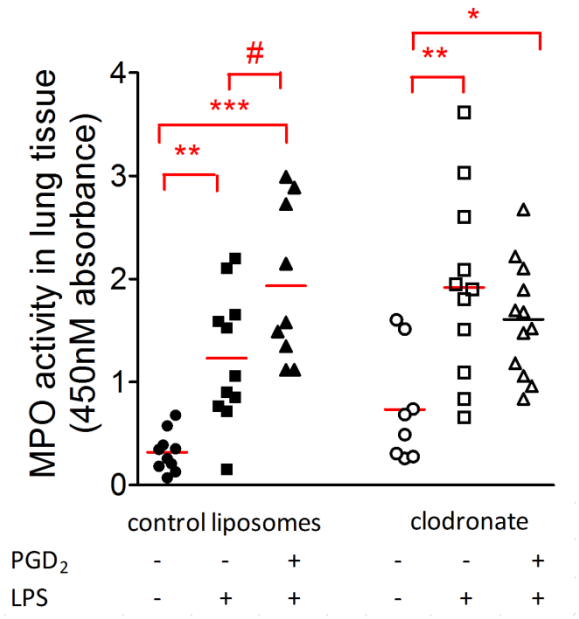

Figure 44. Macrophage depletion inhibits the increased MPO activity in PGD_2-treated animals. Mice received 300 µg of clodronate in 60 µL liposomes or 60 µL control liposomes intranasally and were treated s.c. with vehicle or PGD_2 (5 mg/kg) 24 hours before LPS challenge. MPO activity was determined in wet lung tissue following BAL; * $p<0.05$, **$p<0.01$, *** $p<0.001$ versus veh and # $p<0.05$ versus veh/LPS as determined by one-way ANOVA followed by Bonferonni‘s post test.

Finally, we investigated whether the inhibition of proinflammatory neutrophil recruitment would directly translate to improved lung function. While mice treated with PGD_2 in the liposomal group showed a clear hyperresponsiveness towards methacholine compared to veh/LPS treated animals both in resistance (Fig. 45A) and compliance (Fig. 45B), this was not the case anymore after macrophages depletion.

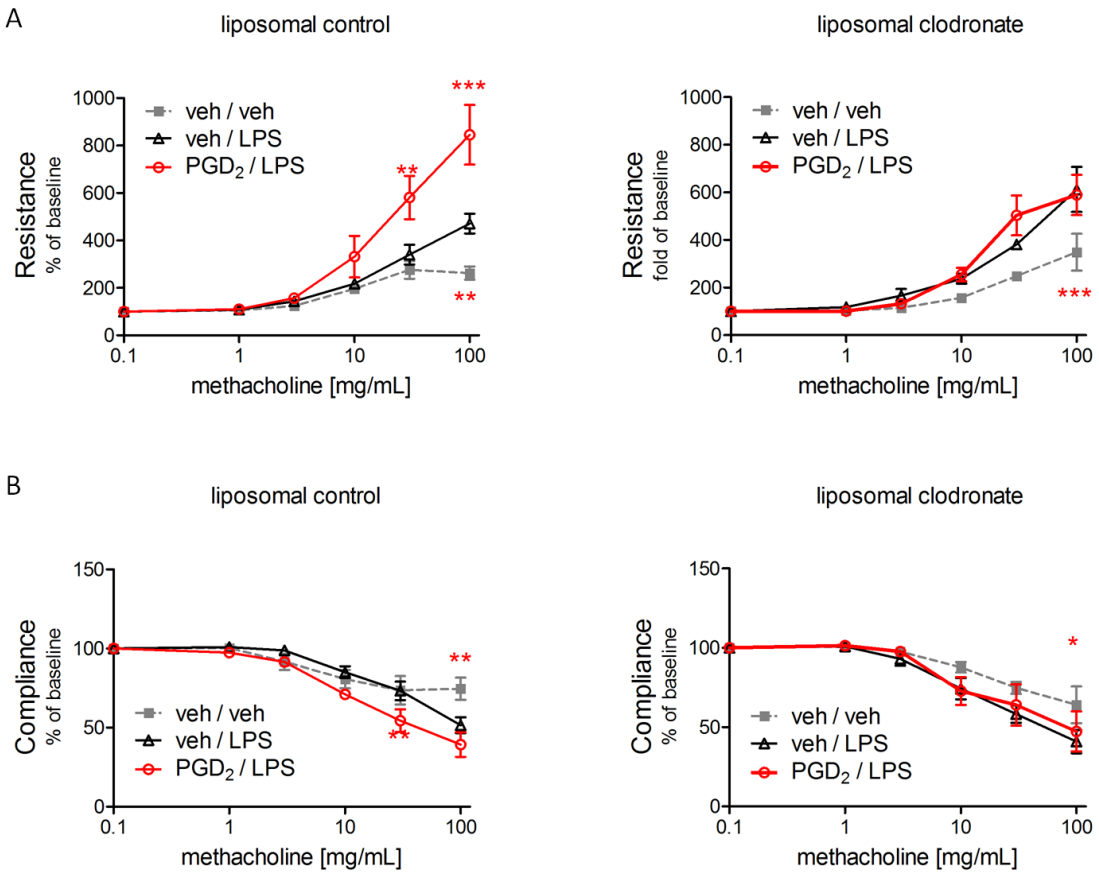

Figure 45. Hyperresponsiveness towards methacholine in PGD_2-treated animals is abolished in macrophage-reduced state. Mice were pretreated s.c. with PGD_2 (5mg/kg) every 12 hours the day before intranasal LPS administration (1 mg/kg). After 4 hours of LPS treatment mice were anesthetized and lung function parameters were measured using the Flexivent system. (A) Resistance was calculated as $cmH_2O.s/mL$ and then normalized to baseline levels (n=4-7, ** $p<0.01$, *** $p<0.001$ compared to vehicle/LPS as determined by one-way ANOVA followed by Dunnett's post test). (B) Compliance was calculated as mL/cmH_2O and then normalized to baseline levels; n=4-7, * $p<0.05$, ** $p<0.01$ compared to vehicle/LPS as determined by one-way ANOVA followed by Dunnett's post test.

4.16 PGD_2 receptor activation on macrophages enhances neutrophil migration

To investigate the mechanisms underlying the PGD_2-mediated effects on neutrophil recruitment, we performed *in-vitro* neutrophil migration assays. In these experiments, neutrophils were co-cultured with human MDM treated with vehicle or PGD_2 and allowed to migrate towards increasing concentrations of the neutrophil chemoattractant IL-8. This

migration assays were used to mimik the KC-induced neutrophil recruitment in the previous *in-vivo* experiments. Cells that migrated through the filter into the lower compartment of the Transwell chambers, were collected and enumerated by flow cytometry. When neutrophils were incubated with macrophages that had been pretreated with PGD_2, their responsiveness towards IL-8 was increased and their migration enhanced. Importantly, the underlying mechanism seems to be some kind of a priming effect, since basal neutrophil migration was already enhanced (Fig. 46A). When the data was normalized to each respective vehicle, there was no difference between the conditions (Fig. 46B). In contrast, when neutrophils were allowed to migrate in the absence of macrophages, their migratory responsiveness was left unaltered by PGD_2 (Fig. 46A, B). Therefore, the observed effect clearly depended on activated PGD_2 receptors on macrophages.

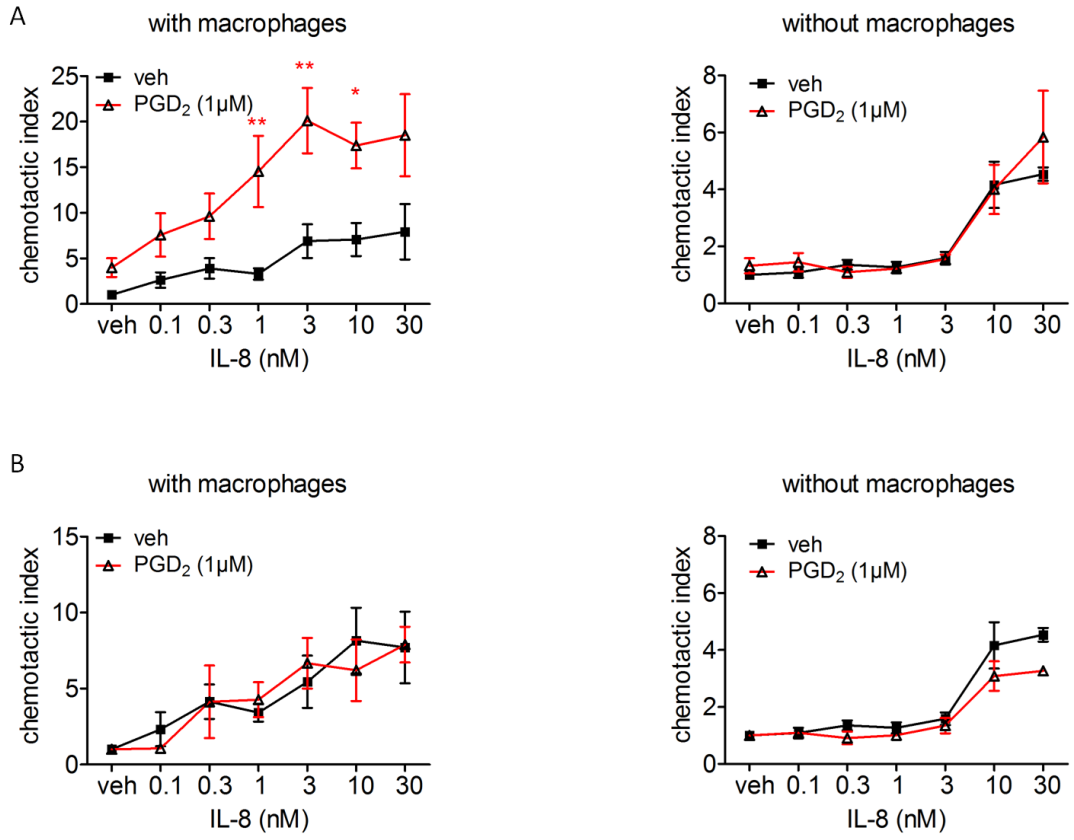

Figure 46. PGD_2 receptor activation on MDM enhances basal neutrophil migration. MDM were cultured on 5µm Transwell inserts and activated with PGD_2 for 60 min. Then neutrophils

were put on the upper insert and allowed to migrate towards a gradient of IL-8 in the lower compartment. Cells that migrated into the lower chamber were collected and enumerated by flow cytometry for 30 sec. (A) Neutrophil migration towards IL-8 was assessed in the presence of MDM treated with PGD_2 or vehicle; mean ± SEM, n= 5-10 independent experiments done in duplicates * $p<0.05$, ** $p<0.01$ versus vehicle, two-way ANOVA followed by Bonferroni's post test. The same experiment was also repeated in the absence of macrophages but in the presence of vehicle or PGD_2 (n= 3-5 independent experiments done in duplicates). Data were normalized to the basal migration of vehicle treated cells. (B) Same data as in (A) but normalized to the respective vehicle.

4.17 PGD_2 acting on MDM prolongs neutrophil survival

The effect of PGD_2 receptor activation on modulating neutrophil function was not limited to neutrophil migration, but could likewise be observed in neutrophil apoptosis. Here, neutrophils were co-cultivated with macrophages, which were treated with vehicle or PGD_2, and at given timepoints, cells were stained with Annexin V and PI. A hallmark of apoptosis is the exposure of phosphatidylserine on their cell surface, which in turn can be stained with Annexin V. Propidium iodide is a DNA-intercalating agent used to discriminate viable from dead cells. Thus, we evaluated the amount of viable cells, i.e. Annexin V- and PI-negative neutrophils, in the presence of macrophages treated with vehicle or PGD_2. Concomitant with increased neutrophil migration, activated PGD_2 receptors on macrophages induced prolonged survival of neutrophils over time (Fig. 47A). In agreement with above, neutrophils stimulated with PGD_2 in the absence of macrophages, showed unaltered AnnexinV/PI staining (Fig. 47B).

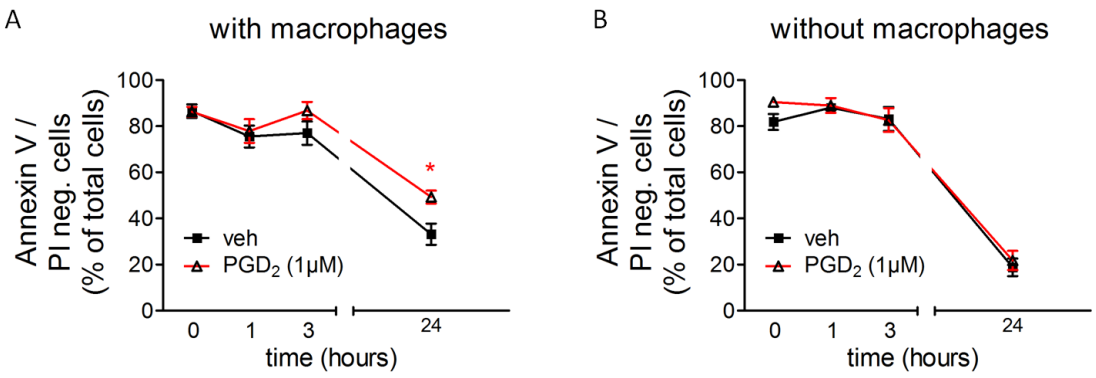

Figure 47. Prolonged survival of neutrophils in the presence of MDM with activated PGD_2 receptors. Neutrophils were cultured **(A)** in the presence of MDM that had been treated with PGD_2 or vehicle, or **(B)** in the absence of macrophages but in the presence of vehicle or PGD_2. Non-

apoptotic neutrophils were regarded as being negative for Annexin V/PI; n=5-10 independent experiments, * $p<0.05$ versus vehicle, two-way ANOVA followed by Bonferroni's post test.

Analysis of all population after Annexin V/PI staining (Fig. 48A,B) shows that it is clearly the viable population of Annnexin V-negative/PI-negative cells that is promoted by PGD_2 receptor activation on macrophages.

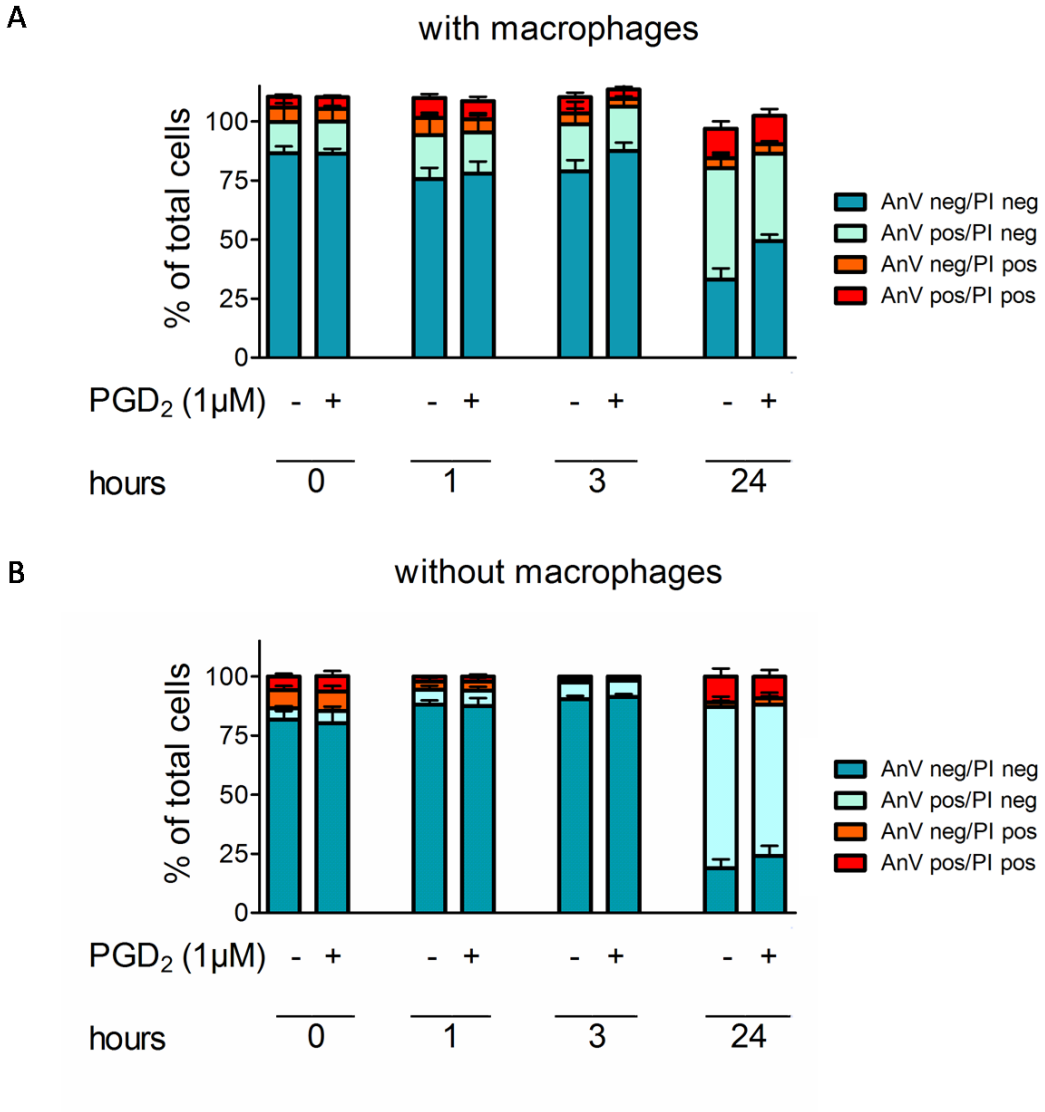

Figure 48. Annexin V/PI staining on neutrophils over time in the presence and absence of MDM. Same data as in **Fig.41.** (n=5-10 independent experiments).

To confirm, that it is truly a survival-prolonging effect that is observed here, we also assessed the cell numbers in each condition. Importantly, the numbers of neutrophils that were measured did not change throughout the experiment (Fig.49), suggesting that the described effects are not due to enhanced phagocytosis of neutrophils by macrophages. These data show that PGD_2 receptor activation on macrophages strongly alters neutrophil function by enhancing their migratory capacity and survival. It is likely that similar mechanisms are responsible for the observed *in-vivo* effects and can thus explain the increased inflammatory response in PGD_2 treated animals.

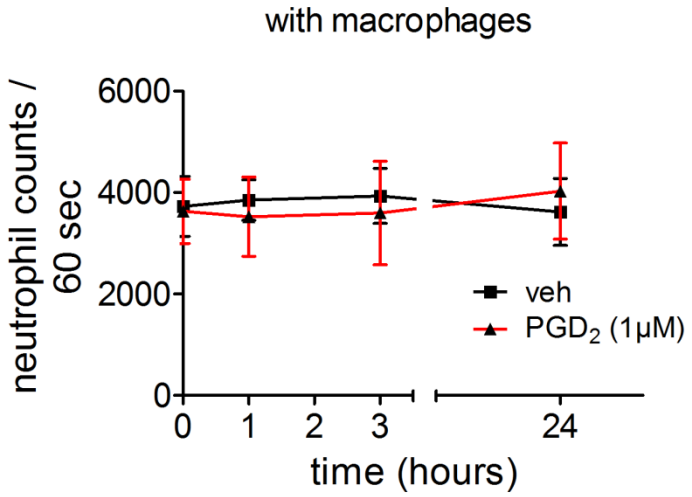

Figure 49. Co-culture of neutrophils with MDM, does not affect the numbers of neutrophils assessed in the experiments. Neutrophil counts in the same samples as in Fig.47 were determined per 60sec using flow cytometry (n=5).

4.18 Cells expressing hematopoietic PGD_2 synthase (HPGDS) are abundant in lungs of ARDS patients

Finally, we wanted to investigate which cells in the lung are responsible for PGD_2 production – i.e. express HPGDS - and assess whether levels of HPGDS are altered in patients suffering from ARDS. Indeed, after performing immunohistochemistry on tissue samples from ARDS and control lungs, we saw a clear increase in the amount of cells that are positive for HGPDS staining (Fig. 50A,B). Most interestingly, while we could confirm that mast cells expressed HPGDS (Fig. 50C), we found that in ARDS lung tissue it was

mainly macrophages that showed a profound expression of HPGDS. Quantitation revealed that all tryptase-positive mast cells express HPGDS in control and ARDS lungs, showing a constitutive expression. Interestingly, about 50-60% of alveolar macrophages were positive for HPGDS in control lungs, which was increased to 85-90% in lung samples derived from ARDS patients (Fig. 50D).

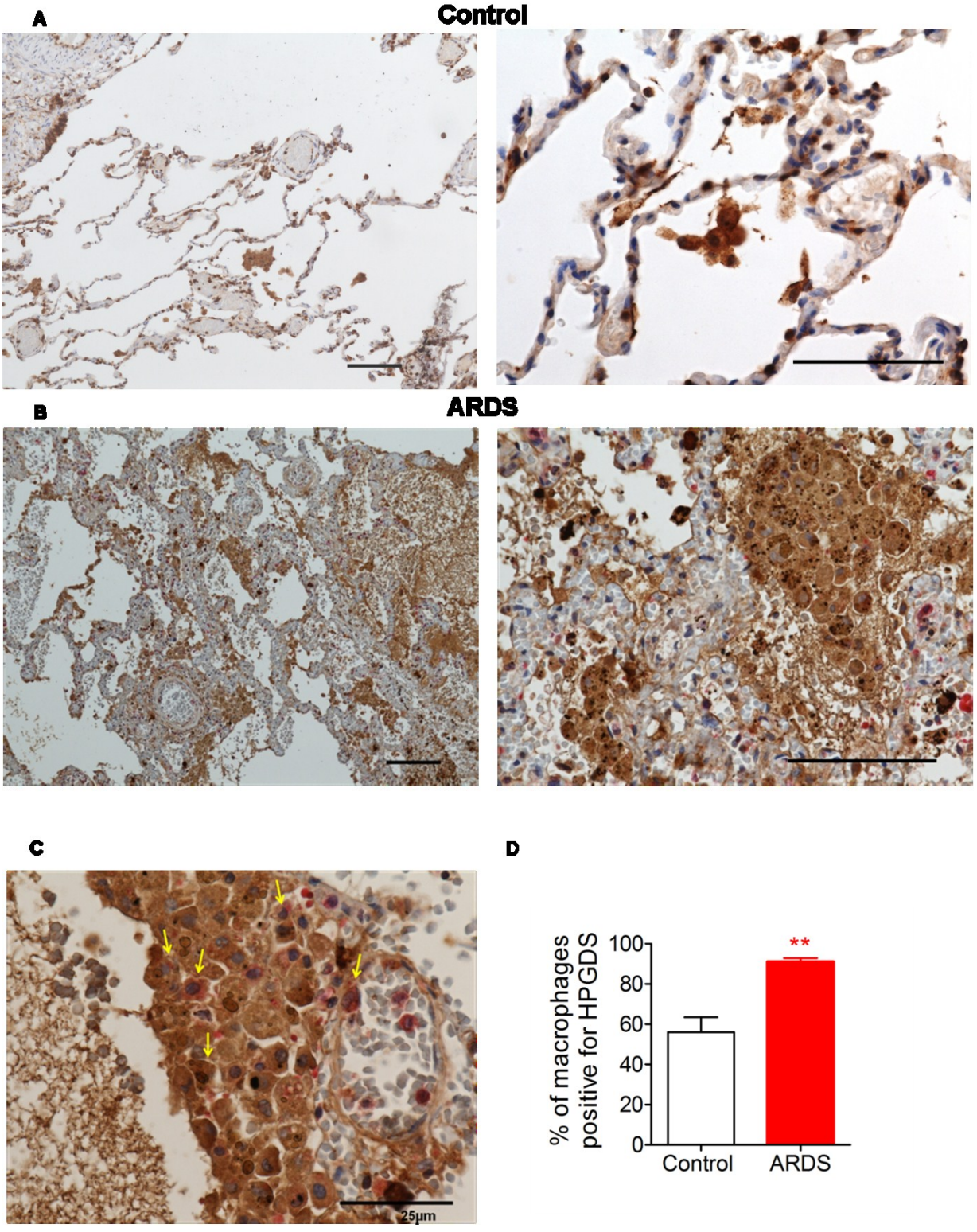

Figure 50. Increased numbers of HPGDS-expressing cells in lungs of ARDS patients. Micrographs show double staining for HPGDS (brown) and mast cell tryptase (red) in lung sections from a (A) control and (B) ARDS patient. Stainings are representative pictures of 5 patients and controls. Note the high amount of HPGDS found in alveolar macrophages. Bar 100µm. **(C)** Pictures under high magnification showing positive cells for HPGDS (brown) and mast cell tryptase (red) as indicated with arrows. Staining is a representative picture of 5 patients and controls. Bar 25µM. (D) Quantitation of macrophages stained positive for HPGDS in control and ARDS lungs (n=5, * $p<0.05$ versus vehicle, determined by student's t-test).

5. Discussion

During all stages of inflammatory responses, macrophages incorporate a key role.

First, macrophages – belonging to the innate immune system – can quickly react to pathogens or other inflammatory triggers because of the variety of cell surface receptors expressed by them. In their evolutionary development, macrophages have acquired receptors (pathogen recognition receptors, PPRs) that can bind to conserved structures on pathogens, the so-called pathogen-associated-molecular patterns (PAMPs). Binding quickly induces a well-defined signaling cascade that will polarize macrophages into the activation state that is required to protect their surroundings.

Second, after danger signals from their surroundings have been sensed, macrophages will acquire a phenotype switch from a resting / patrolling cell type towards an activated one. In the case of a type-1 inflammation, they release early phase mediators and cytokines such as TNF-α, TGF-β, IFN-γ, IL-8, or IL-1β in a NF-κb dependent manner. This initiates the acute phase of inflammation and triggers the influx of other peripheral blood granulocytes. The first recruited cells to arrive at the sites of inflammation are typically neutrophils, followed by monocytes, which – under specific conditions – can differentiate into macrophages. Recruited differentiated macrophages complete and/or even outcompete the resident macrophage population. This stage causes all the cardinal signs of inflammation.

Third, macrophages eliminate the noxious stimulus and undertake a phenotype switch once more. Regulatory mechanisms assure that inappropriate hyperactivation of macrophages is prevented and that macrophages initiate the resolution phase of inflammation. The desired outcome is a successful clearance of pathogens or damaging stimuli and a subsequent repair of the damaged tissue.

Amongst the early phase mediators, prostanoids take a central position. Rapidly after stimulation, their biosynthesis as well as release is rapidly enhanced in the inflamed tissue. Prostaglandin D_2 production has up to now mainly been attributed to mast cells, that – especially during allergic reaction – can release the D-type prostanoid in only a few minutes' time (209). But also macrophages are known for their potential of prostanoid synthesis in response to a variety of signals including stimulation by LPS. Human alveolar macrophages exhibit a marked increase in mRNA levels of COX-2– an enzyme

responsible for the generation of the precursor prostanoid PGH_2 – over a time-frame of 48 hours following the stimulus (210). Importantly, this precursor molecule will give rise to a collection of end-stage prostanoids all inhabiting distinct roles in inflammation.

In this study, I investigated in detail, the role of the inflammatory mediator, PGD_2, on modulating macrophage function. The presence of both PGD_2 receptors, DP1 and DP2 could be confirmed on human macrophages – be it derived from monocyte ontology or from resident macrophages in the lung. Importantly, on human pulmonary macrophages, both DP1 and DP2 were not regulated by any underlying pulmonary disease activity. PGD_2 could also shown to be an effective modulator in macrophage function, as it was able to induce both intracellular Ca^{2+} release and migration. PGD_2 influenced LPS-induced cytokine secretion, further undermining its role in type1 inflammation. In an acute-lung injury model, PGD_2 acting on macrophages worsened inflammatory parameters including neutrophil infiltration, cytokine secretion and lung function. A direct axis between stimulated PGD_2 receptors on macrophages and neutrophil activation was observed. Finally, we could determine alveolar macrophages as a potential direct source for PGD_2 production in human ARDS patients.

The first part of this thesis is concerned with PGD_2 receptor expression on human macrophages. Interestingly, although a reasonable amount of studies have investigated the expression of DP1 and DP2 on inflammatory cells, to our knowledge we are the first to report their existence on human macrophages. This is surprising as in 2003, Gosset and colleagues described DP1 and DP2 expression on human monocytes and monocyte-derived dendritic cells (162). Since we also investigated PGD_2 receptor expression on monocytes, we can confirm the presence of both receptors on monocytes. Furthermore, we could broaden the existing knowledge, as we evaluated the expression on protein levels – determined by flow cytometric analysis of cell surface receptor expression – compared to realtime-PCR analysis by the aforementioned study. Since then, only a limited number of investigations proposed a potential expression of DP1 and DP2 receptor expression on macrophages. In another study, immunohistochemical staining confirmed an increase in DP2-expressing cells in nasal mucosa of allergic patients compared to non-allergic subjects. The authors suggested macrophages amongst those positively stained cells (211). Indirectly, the importance of DP2 receptors on macrophages was described, when DP2 knock-out mice showed inhibition of macrophage infiltration into lung tissue in a model of helminth-induced pulmonary inflammation (212). Here, we could thoroughly describe that

in-vitro differentiated macrophages, which may represent the *in-vivo* situation of recruited monocyte-derived macrophages under inflammatory conditions, as well as resident human alveolar macrophages express both PGD_2 receptors.

Although both receptors are expressed, their expression degree varies. Surprisingly, this difference in expression levels does not directly translate to altered functional activity. Both receptors contributed equally to receptor-induced Ca^{2+} signaling. This can be explained by the fact that GPCRs can couple to more than one G-protein, thus GPCR expression may not be equal to the functional response. In neutrophils, for example, as little as 50 of the formyl peptide receptors that recognize and bind the bacteria-derive N-formylated peptides, are sufficient to induced a signal via Gαi (213,214). In human monocyte-derived macrophages, activation of both DP1 and DP2 receptors showed a pertussis toxin-sensitive Ca^{2+} signaling, suggesting that both receptors are coupled to Gαi. Gαi leads to Ca^{2+} signaling via activation of Phospholipase C that initiates the cleavage of phosphatidylinositol 4,5-biphosphate to inositol 1,4,5-phosphate that activates IP3-sensitive Ca^{2+} channels and diacylglycerol (DAG) stimulating protein kinase C. Whether or not the dissociation of the βγ-dimer subunit results in signaling via Rac or phosphatidylinostil 3-kinase we have not determined in our study, but might represent an interesting future question for investigation. DP2 receptor signaling is well established to be Gαi-dependent. In agreement with Th2 cells, eosinophils, basophils and a heterologous DP2/HEK293 system, DP2 receptor activation on macrophages relies on Gαi proteins (166,177). DP1 activation has been described to stimulate adenylyl cyclase in a Gαs-dependent way that results in the rise of intracellular cAMP. Interestingly, DP1 stimulation in the heterologous DP1/HEK293 expression system also leads to the release of intracellular Ca^{2+} but, in contrast to DP2, this increase was Gαq/11-mediated (150). To add more complexity to this question, DP1 and DP2 receptors are often co-expressed on cells and PGD_2 acts as an endogenous ligand for both receptors. In a heterologous system, in which both receptors are co-expressed in HEK-cells, DP1 and DP2 receptors show a cooperative manner of signal transduction. DP1 receptors cannot only augment DP2-mediated Ca^{2+} flux, but are further absolutely necessary for the latter (215). In several native systems, including eosinophils, Th2 cells and basophils, both receptors are co-expressed. This also accounts for macrophages. Therefore, although macrophages already differ from other cells types in regard to the Gαi-dependency of the DP1 receptors, we also investigated whether the two receptors likewise modulate each other's signaling capacities.

In contrast to the DP1- and DP2- coexpressing HEK cells, these receptors function independently from each other in macrophages. Activation of each receptor separately induced a prominent Ca^{2+} flux and blockade of one receptor attenuated the Ca^{2+} rise mediated by the other. Thus, in macrophages, DP1 and DP2 receptors can elicit the same underlying signaling mechanisms in an independent way. Therefore, it seems likely that the mode of cooperativity in DP1 and DP2 signaling is cell type specific.

Chemotactic responses elicited by PGD_2 are normally accounted to DP2 activation, but DP1 receptors have also been reported to be implicated in this process. For example, PGD_2-mediated release of eosinophils from the bone-marrow was inhibited by both DP1 and DP2 antagonists (216). In human macrophages, blockage of DP1 or DP2 receptors reduced the chemotactic potential of PGD_2 *in vitro*, which was almost reduced to baseline migration when both receptors were blocked. This finding is indeed interesting, as similar responses can be observed in eosinophils, which also express both PGD_2 receptors. DP1 blockade causes an alteration of PGD_2-mediated migration of eosinophils, by inducing a rightward shift of the concentration response-curve (216). Interestingly, other reports show opposing effects of DP1 in migratory processes. Gosset and colleagues observed that, while, PGD_2 and DP2 specific agonist DK-PGD_2 induced a chemotactic response of human mononcyte, the DP1 agonist BW245c failed to elicit a similar response. On the contrary, DP1 activation inhibited the migratory capacity of monocytes towards other well-established chemoattractants, such as CCL5 and CCL19 (162). In our study we have not examined chemotactic responses of monocytes towards PGD_2, because both the expression levels of DP1 and DP2 receptors, and Ca^{2+} flux elicited by PGD_2, appeared minor in comparison to macrophages.

In monocytic/macrophage-like cells, PGD_2 is implicated to influence cellular responses elicited by LPS. RAW264.7 cells showed reduced migration towards LPS after COX inhibition. The involvement of PGD_2 receptors was further corroborated when, in the same study, the same pattern of attenuated chemotaxis towards LPS was observed in both DP2- as well as HPGDS-deficient mice (163). Interestingly, although PGD_2 binds with equal affinity to both DP1 and DP2 receptors, it seems that the time-course of cellular responses after activation of either receptor is different. DP2 activation has mostly been associated with immediate responses, contributing the early recruitment. Interestingly, DP1 involvement in the modulation of LPS function has not been examined to date. In this study, we delineated the ability of PGD_2 to modulate LPS responses with regard to the

involvement of the distinct PGD_2 receptors. For the first time we could show that PGD_2 enhanced the LPS-induced TNF-α secretion from human monocyte-derived macrophages. While single activation of DP2 receptors mirrored PGD_2 responses, only the blockade of both receptors could inhibit the enhancement in TNF-α secretion elicited by PGD_2. In this process, DP2 receptors seem to be dominating, but PGD_2 responses still show a dependence on DP1 receptors. This pro-inflammatory phenotype was also observed when monocyte-derived macrophages were first activated with IL-4, a cytokine that is mainly associated with the activation of macrophages towards a type-2 like, anti-inflammatory state. On one hand, this effect is quite astonishing as under basal conditions IL-4 activated macrophages fail to secrete any measurable amounts of TNF-α. On the other hand, it was recently reported that Th2 cells reacted with increased secretion of the neutrophil-activator GM-CSF upon PGD_2 stimulation. Thus, type 2-like macrophages were highly suggestible to also show alterations in their cytokine profile. Importantly, stimulation by PGD_2 alone did not alter TNF-α production. This effect was always dependent on a prior activation trigger, such as LPS or IL-4. The underlying mechanisms by which PGD_2 modulates TNF-α release is likely to be NFκB-dependent, as NFκB inhibition reduced TNF-α secretion back to levels observed after LPS stimulation alone. To further delineate the NFκB -involvement in the PGD_2-PD1-DP2 axis in monocytic cells, we took use of the U937-NFκB reporter cell line. Selective stimulation of either receptor, as well as dual agonistic action by PGD_2, led to a concentration-dependent NFκB activation. Interestingly, to completely attenuate the PGD_2-mediated response, inhibition of both receptors was necessary. This, again emphasizes that DP2 might be a stronger driver of pro-inflammatory signaling capacities induced by PGD_2, but DP1 receptors are still needed in this process. Taken together, we could demonstrate an involvement of PGD_2 receptors in macrophage Ca^{2+} flux, migration and cytokine secretion. Underlying receptor involvement could demonstrate an independence from each other, as specific agonist of DP1 and DP2 were able to mimic PGD_2 responses, although sometimes to a lesser extent. Still, pro-inflammatory signaling of PGD_2 could only be attenuated via inhibition of both PGD_2 receptors simultaneously, suggesting a cooperative way of action for these two receptors.

Animal models are used to mimic human disease, and as such, they all come with certain caveats. In the case of LPS-induced ALI, the most prominent feature is neutrophilic alveolitis. Furthermore, it is also characterized by changes in epithelial permeability. Noteworthy, especially the initial phase of endotoxin-induced ALI represents the

pathological findings in human ALI/ARDS, whereas the later stages differs, as LPS-induced ALI in mice heals without fibrosis, which is in marked contrast to human ALI (217). We chose this model, because PGD_2 activates macrophages and alters LPS-mediated responses. Those responses were usually seen over a short period of time, thus overlapping with the initial phase of the ALI time-course. In ALI and ARDS, macrophages take a central role during the initial exsudative phase as well as during the regenerative fibro-proliferative phase. During the initial phase, appropriate macrophage activation is of most importance to avoid excessive inflammation and an over-complicated regenerative phase. We found that it is just this unwanted hyperreactivity of macrophages in response to the endotoxin trigger which is induced by PGD_2 receptor activation. Here we could demonstrate that activated PGD_2 receptors on macrophages worsen the initial phase of the ALI, by i) enhancing neutrophil recruitment into the bronchoalveolar space, ii) increasing neutrophil migration into the interstitial lung parenchyma, iii) inducing edema formation and iv) decreasing lung function. Therefore, PGD_2 alters and aggravates all pathological features that are characteristic for the acute phase of ALI. Most of the aforementioned actions were shown to be mediated via both receptors. Activation of either DP1 or DP2 receptors increased neutrophilic alveolitis and edema formation. Interestingly, PGD_2 or specific agonist treatment, showed no effect on the LPS-mediated recruitment of any other cell type measured with one exception. LPS-induced monocyte influx into the alveolar space was enhanced upon DP2 receptor stimulation, too. This observation is in line with the study by Gossett and colleagues who described a DP2-dependent recruitment of monocytes (162). Importantly, neutrophils are the first cell type to arrive at the site of inflammation and surely precede monocyte influx. Therefore, neutrophil counts were the only reliable, and probably most relevant, cell types to evaluate during the investigated time-course.

Interestingly, while other – mostly chronic – studies often showed opposing effects of the two PGD_2 receptors, this was not the case in our acute model that strongly relied on macrophage activation. In a chronic model of ulcerative colitis, DP1 receptor activation appears beneficial whereas DP2 activation induces a more severe phenotype of colitis (218,219). In chronic asthmatic models, the question whether PGD_2 acts pro- or anti-inflammatory is even more challenging to answer. DP1-deficient mice showed an ameliorated phenotype, suggesting that DP1 receptors enhance allergic airway inflammation (152), while administration of DP1 agonists proved to be beneficial in

ovalbumin-induced asthma in mice (156). Thus, even in similar inflammatory processes, the role of DP1 receptors has remained unclear. DP2 receptors, on the other hand, have consistently been associated with pro-inflammatory signaling capacities.

It seems that during long term models, the role of PGD_2 and PGD_2 receptor activation is complicated. This might be explained by the formation of metabolites which then might act on either receptor. Furthermore, long term stimulation of receptors can lead to a down-regulation / internalization particularly of DP2 (215) and can thus further influence the domination of one receptor over the other.

In short term models, the role of the PGD_2 receptors has not clearly been investigated. This is rather surprising as the D-type prostanoid is considered an early phase mediator that gets released by a variety of stimuli, including IgE, methylnicotinate, LPS and many more (134,184,220). And indeed, in our short term acute model, DP1 and DP2 receptors did not oppose each other but induced the same effector actions on cells with a similar underlying signal transduction pathway. Exogenous administration of PGD_2 enhanced neutrophil recruitment into the alveolar region and into the interstitial space, induced edema formation and decreased lung function in mice. DP1 receptor activation mimicked both neutrophilic alveolitis and edema formation induced by PGD_2. DP2 receptor activation, on the other hand, induced the same effects as DP1 receptor activation, with the addition of elevated MPO activity, reflecting increased neutrophils in lung parenchyma. Therefore, we found that DP2 receptor activation mirrored all effects induced by PGD_2 treatment. Again, it seems that both receptors lead to a similar pro-inflammatory phenotype, with the DP2 receptor maybe playing a more pronounced role.

Interestingly, it was recently shown that DP1-deficient mice show an aggravated phenotype in endotoxin-induced ALI (221). While on first glance this seems to contradict the results of our study, both studies show marked differences in experimental design and thus make a direct comparison hard to assess. First, as mentioned above, we focused on the early stages of ALI, Murata and colleagues investigated later stages of the disease model. This presents the aforementioned problem of long-term effects of PGD_2 receptor activation or inhibition. Second, the authors used endotoxin in concentrations that exceeded ours by four times. Third, the use of unconditional knock-out animals always poses the limitation of compensational mechanisms, such as increased levels of DP2 receptors that might drive inflammatory processes.

Prostanoids have already been implicated in injured lungs for a long time. Already 20 years ago, high levels of leukotrienes have been detected in the BAL fluid of ARDS patients (222). But pathogenesis will clearly depend on more than one prostanoid. Different prostanoids derived by different enzymes will exert both pro- und anti-inflammatory actions. For example, thromboxane synthase inhibition proved to be beneficial against lung injury, thus presenting a pro-inflammatory PG in ALI. Other PGs are reported to play anti-inflammatory roles, such as lipoxin A_4 and 15-deoxy-PGJ_2 (223,224). To add more complexity to this picture, the same prostanoid can differentially alter disease activity, by acting on specific receptors. PGE_2 acting on EP4 receptors can profoundly inhibit endotoxin-induced lung injury (225), while EP3-deficient mice are protected against lung edema (226). Importantly, in our study, we also assessed the role of endogenous PGD_2 in acute lung injury. We could confirm previous studies that described increased levels of PGE_2 found in the BAL fluid of animals with injured lungs (208,225) but also found increased levels of PGD_2 together with arachidonic acid metabolites 12-HHTrE and TxB_2. The latter is of special interest, as a metabolite of TxB_2 - 11-dehydro-TXB_2 – can act as a full agonist for DP2 (180). This further substantiates the critical involvement of the DP2 pathway in pulmonary inflammation. Importantly, the blockade of endogenous PGD_2 signaling could ameliorate the recruitment of neutrophils into both interstitial and alveolar space. Interestingly, the two PGD_2 receptors seem to take over a time and compartment specific role in neutrophil recruitment. Antagonism of DP1 receptors reduced alveolar neutrophil counts, whereas DP2 antagonism inhibited the pronounced interstitial inflammation. Therefore, DP2 receptors appear to direct peripheral blood neutrophils into the interstitial parenchyma, while DP1 receptors seem to be responsible for alveolar evasion of neutrophils. Furthermore, time-specific differences might represent another explanation, as DP2 activation seems to be responsible for more immediate effects than those elicited by DP1. When lung function parameters such as compliance and resistance were assessed, neither of the specific antagonists could ameliorate the LPS-induced hyperreactivity. This might not be surprising as, firstly, neutrophilic infiltration into alveolar and interstitial space was reduced, but not reversed to basal levels, and, secondly, other prostanoids, also acting pro-inflammatory, are released during endotoxin-induced lung injury as well. Furthermore, since both receptors seem to be involved during neutrophil recruitment after LPS administration, blockade of both receptors could have ameliorated lung function in mice. This will surely be part of future investigation.

In our study, we could confirm that macrophages represent key players that are responsible for the increased inflammatory state of mice upon high systemic PGD_2 levels. We have substantiated this statement, by showing that i) isolated alveolar and interstitial macrophages release increased amounts of the neutrophil chemoattractant KC, ii) reduction of alveolar macrophages inhibits PGD_2-worsened lung inflammation, and iii) activated PGD_2 receptor on human monocyte-derived macrophages lead to hyperreactivity of neutrophils with regard to migration and survival.

As described above, macrophages take over important tasks in the different stages of ALI. Therefore, it proved challenging during this study, to find a level of macrophages that was sufficient to induce neutrophilic infiltration but at the same time is adequately reduced to inhibit PGD_2-mediated responses by them. We found that a reduction of alveolar macrophages to a resting population of 30% worked best to answer the questions asked. In the presence of high endogenous PGD_2 levels, all hallmarks of LPS-induced lung injury – increased inflammation, neutrophilic alveolitis, edema formation and decreased lung function – could be restored to basal LPS-induced levels when macrophages were depleted. This highly suggests that the PGD_2-induced enhanced inflammatory state was indeed mediated by activation of its receptors on macrophages.

Finally, we could also propose a mechanism of action of the PGD_2-mediated neutrophil-macrophage crosstalk and could further show that our murine data can translate into human models as well. In *in-vitro* experiments with human monocyte-derived macrophages and peripheral blood neutrophils showed that PGD_2 receptor activation on macrophages leads to a hyperreactive neutrophil phenotype. First, in the presence of monocyte-derived macrophages that have been activated with PGD_2, neutrophils show an increased migratory capacity towards IL-8. Although we have not assessed migration towards other stimuli, it is tempting to hypothesize that this would also be enhanced, as not the chemotactic index towards IL-8 itself was altered, but the basal migratory capacity was enhanced. Second, neutrophils that were co-cultured with PGD_2-activated macrophages, presented with prolonged survival. These actions show an indirect mechanism of PGD_2, as direct PGD_2 treatment of neutrophils did not alter any of the assessed functions by them. Moreover, neutrophils themselves have only been described to express DP1 receptors, and lack DP2 receptors. Although we have not yet determined which factors released from activated macrophages drive neutrophilic hyperreactivity, some key candidates can be speculated. A recent study described that PGD_2-activated Th2 cells release increased levels of GM-CSF

that directly influence and enhance neutrophil function. This mechanism of action might not be restricted to Th2 cells, but could also apply for macrophages (227). This hypothesis can be further substantiated by our finding that IL-4 activated macrophages react with increased secretion of TNF-α upon PGD_2 treatment. Still, this remains a speculation and will need to be elucidated in future studies.

In the last part of the study, we found further evidence for the importance of PGD_2 in ARDS, when we observed that macrophages not only express DP1 and DP2 receptors, but also HPGDS, the rate-limiting enzyme of PGD_2 production. This presents a direct loop of HPGDS-PGD_2-DP1-DP2 on human macrophages. Although macrophages have been described to be a source for PGD_2 production, this is – to our account – the first time that HPGDS expression was described on human alveolar macrophages. Interestingly, although a basal expression of HPGDS is observed in alveolar macrophages in healthy subjects, the percentage of HPGDS-positive macrophages increases in ARDS patients. Thus, macrophages probably are the driving source of increased levels of PGD_2 found in acute lung injury and PGD_2 acting on macrophages worsens pulmonary inflammatory. Drugs targeting this direct feed-back loop could prove beneficial in the treatment of ARDS.

Importantly, there is a clear need for pharmacological treatments in ARDS. If drugs could reduce the initial inflammation, the events in the fibro-proliferative late-stage would not be as severe. Up to now, ARDS is mainly treated using ventilator strategies, mainly by applying low tidal volume ventilation with high levels of applied positive end-expiratory pressure (PEEP) to avoid collapse of lung parenchyma (228,229). These mechanical treatments are known to improve mortality rate in ARDS but up to now, no drug has proven useful in the treatment of ARDS. Other potential targets that have been investigated in clinical trials including administration of glucocorticoids, ibuprofen, inhaled synthetic surfactant or antibody-mediated blocking of endotoxin have failed to ameliorate the outcome of the disease (230).

Single DP2 antagonists, such as OC000459 or BI 671800, have recently been assessed in clinical trials for the treatment of asthma. The DP2 antagonist OC000459 slightly improved the forced expiratory volume in the asthmatic group as compared to the placebo group (231). The other DP2 antagonists that has recently been under clinical investigation, BI 671800, could slightly improve lung function in controller-naïve asthmatic patients, as well as in patients that were taking inhaled corticosteroids (232).

Taken together, DP2 antagonists have the potential of improving pulmonary inflammation, although this might be limited if DP1 receptors are also involved in pro-inflammatory signaling. Whether these patients represent a specific cohort still remains unclear. Dual DP1-DP2 antagonists or even multiple prostanoid receptor antagonists can represent a more promising pharmacological tool. Recently, a new multiple antagonist has been introduced, AGN 211377, that targets PGD_2 receptors DP1 and DP2, PGE_2 receptors EP1 and EP4, $PGF_2\alpha$ receptor, and TxA_2 receptor, without any antagonist action on EP2, EP3, and the prostacyclin receptor, IP (233). Interestingly this compound could inhibit pro-inflammatory macrophage actions induced by LPS. Thus this compound might prove beneficial in LPS-induced lung injury, and should be subject to future studies. Further implication of the future importance of multiple prostanoid receptor targeting, without the need of blocking upstream mechanisms such as cyclooxygenase inhibition, is given by increasing evidence of synergistic action of prostanoids (215,227)

Collectively, we could demonstrate a pivotal role of the PGD_2-DP1-DP2 axis on macrophages in the regulation of pulmonary inflammation. Hyperreactivity of neutrophils induced by activated macrophages, as well as tissue damage and an inappropriate pro-inflammatory environment due to activation of the latter, present them as promising therapeutic targets. Recently developed dual DP1/DP2 antagonists, might prove beneficial in regulating macrophage activation in diseases with increased endogenous PGD_2.

REFERENCES

1. Stefater III JA, Ren S, Lang RA, Duffield JS. Metchnikoff's policemen: macrophages in development, homeostasis and regeneration. Trends Mol Med. 2011 Dec;17(12):743–52.

2. Epelman S, Lavine KJ, Randolph GJ. Origin and Functions of Tissue Macrophages. Immunity. 2014 Jul 17;41(1):21–35.

3. Cooper MD, Alder MN. The Evolution of Adaptive Immune Systems. Cell. 2006 Feb 24;124(4):815–22.

4. Tauber AI. Metchnikoff and the phagocytosis theory. Nat Rev Mol Cell Biol. 2003 Nov;4(11):897–901.

5. Cavaillon J-M. The historical milestones in the understanding of leukocyte biology initiated by Elie Metchnikoff. J Leukoc Biol. 2011 Sep;90(3):413–24.

6. van Furth R, Cohn ZA. THE ORIGIN AND KINETICS OF MONONUCLEAR PHAGOCYTES. J Exp Med. 1968 Sep 1;128(3):415–35.

7. Epelman S, Lavine KJ, Beaudin AE, Sojka DK, Carrero JA, Calderon B, et al. Embryonic and Adult-Derived Resident Cardiac Macrophages Are Maintained through Distinct Mechanisms at Steady State and during Inflammation. Immunity. 2014 Jan 16;40(1):91–104.

8. Guilliams M, Kleer ID, Henri S, Post S, Vanhoutte L, Prijck SD, et al. Alveolar macrophages develop from fetal monocytes that differentiate into long-lived cells in the first week of life via GM-CSF. J Exp Med. 2013 Sep 23;210(10):1977–92.

9. Ginhoux F, Greter M, Leboeuf M, Nandi S, See P, Gokhan S, et al. Fate Mapping Analysis Reveals That Adult Microglia Derive from Primitive Macrophages. Science. 2010 Nov 5;330(6005):841–5.

10. Schulz C, Perdiguero EG, Chorro L, Szabo-Rogers H, Cagnard N, Kierdorf K, et al. A Lineage of Myeloid Cells Independent of Myb and Hematopoietic Stem Cells. Science. 2012 Apr 6;336(6077):86–90.

11. McKercher SR, Torbett BE, Anderson KL, Henkel GW, Vestal DJ, Baribault H, et al. Targeted disruption of the PU.1 gene results in multiple hematopoietic abnormalities. EMBO J. 1996 Oct 15;15(20):5647–58.

12. DeKoter RP, Walsh JC, Singh H. PU.1 regulates both cytokine-dependent proliferation and differentiation of granulocyte/macrophage progenitors. EMBO J. 1998 Aug 3;17(15):4456–68.

13. Nottingham WT, Jarratt A, Burgess M, Speck CL, Cheng J-F, Prabhakar S, et al. Runx1-mediated hematopoietic stem-cell emergence is controlled by a Gata/Ets/SCL-regulated enhancer. Blood. 2007 Dec 15;110(13):4188–97.

14. Boyer SW, Schroeder AV, Smith-Berdan S, Forsberg EC. All hematopoietic cells develop from hematopoietic stem cells through Flk2/Flt3-positive progenitor cells. Cell Stem Cell. 2011 Jul 8;9(1):64–73.

15. Italiani P, Boraschi D. New Insights Into Tissue Macrophages: From Their Origin to the Development of Memory. Immune Netw. 2015 Aug;15(4):167–76.

16. van Furth R, Cohn ZA, Hirsch JG, Humphrey JH, Spector WG, Langevoort HL. The mononuclear phagocyte system: a new classification of macrophages, monocytes, and their precursor cells. Bull World Health Organ. 1972;46(6):845–52.

17. Mildner A, Yona S, Jung S. A close encounter of the third kind: monocyte-derived cells. Adv Immunol. 2013;120:69–103.

18. Varol C, Mildner A, Jung S. Macrophages: Development and Tissue Specialization. Annu Rev Immunol. 2015;33(1):643–75.

19. Passlick B, Flieger D, Ziegler-Heitbrock HW. Identification and characterization of a novel monocyte subpopulation in human peripheral blood. Blood. 1989 Nov 15;74(7):2527–34.

20. Ziegler-Heitbrock L, Ancuta P, Crowe S, Dalod M, Grau V, Hart DN, et al. Nomenclature of monocytes and dendritic cells in blood. Blood. 2010 Oct 21;116(16):e74-80.

21. Zanoni I, Ostuni R, Marek LR, Barresi S, Barbalat R, Barton GM, et al. CD14 controls the LPS-induced endocytosis of Toll-like receptor 4. Cell. 2011 Nov 11;147(4):868–80.

22. Wright SD, Ramos RA, Tobias PS, Ulevitch RJ, Mathison JC. CD14, a receptor for complexes of lipopolysaccharide (LPS) and LPS binding protein. Science. 1990 Sep 21;249(4975):1431–3.

23. Cros J, Cagnard N, Woollard K, Patey N, Zhang S-Y, Senechal B, et al. Human CD14dim monocytes patrol and sense nucleic acids and viruses via TLR7 and TLR8 receptors. Immunity. 2010 Sep 24;33(3):375–86.

24. Xu H, Manivannan A, Crane I, Dawson R, Liversidge J. Critical but divergent roles for CD62L and CD44 in directing blood monocyte trafficking in vivo during inflammation. Blood. 2008 Aug 15;112(4):1166–74.

25. Tarzi RM, Liu J, Schneiter S, Hill NR, Page TH, Cook HT, et al. CD14 expression is increased on monocytes in patients with anti-neutrophil cytoplasm antibody (ANCA)-associated vasculitis and correlates with the expression of ANCA autoantigens. Clin Exp Immunol. 2015 Jul 1;181(1):65–75.

26. Boruchov AM, Heller G, Veri M-C, Bonvini E, Ravetch JV, Young JW. Activating and inhibitory IgG Fc receptors on human DCs mediate opposing functions. J Clin Invest. 2005 Oct;115(10):2914–23.

27. Mayer A, Hiebl B, Lendlein A, Jung F. Support of HUVEC proliferation by pro-angiogenic intermediate CD163+ monocytes/macrophages: a co-culture experiment. Clin Hemorheol Microcirc. 2011;49(1–4):423–30.

28. Stansfield BK, Ingram DA. Clinical significance of monocyte heterogeneity. Clin Transl Med [Internet]. 2015 Feb 14 [cited 2016 Feb 18];4. Available from: http://www.ncbi.nlm.nih.gov/pmc/articles/PMC4384980/

29. Ingersoll MA, Spanbroek R, Lottaz C, Gautier EL, Frankenberger M, Hoffmann R, et al. Comparison of gene expression profiles between human and mouse monocyte subsets. Blood. 2010 Jan 21;115(3):e10-19.

30. Nockher WA, Scherberich JE. Expanded CD14+ CD16+ monocyte subpopulation in patients with acute and chronic infections undergoing hemodialysis. Infect Immun. 1998 Jun;66(6):2782–90.

31. Saionji K, Ohsaka A. Expansion of CD4+CD16+ blood monocytes in patients with chronic renal failure undergoing dialysis: possible involvement of macrophage colony-stimulating factor. Acta Haematol. 2001;105(1):21–6.

32. Emminger W, Zlabinger GJ, Fritsch G, Urbanek R. CD14(dim)/CD16(bright) monocytes in hemophagocytic lymphohistiocytosis. Eur J Immunol. 2001 Jun;31(6):1716–9.

33. Belge K-U, Dayyani F, Horelt A, Siedlar M, Frankenberger M, Frankenberger B, et al. The proinflammatory CD14+CD16+DR++ monocytes are a major source of TNF. J Immunol Baltim Md 1950. 2002 Apr 1;168(7):3536–42.

34. Skrzeczyńska-Moncznik J, Bzowska M, Lo˝seke S, Grage-Griebenow E, Zembala M, Pryjma J. Peripheral Blood CD14high CD16+ Monocytes are Main Producers of IL-10. Scand J Immunol. 2008 Feb 1;67(2):152–9.

35. Yang J, Zhang L, Yu C, Yang X-F, Wang H. Monocyte and macrophage differentiation: circulation inflammatory monocyte as biomarker for inflammatory diseases. Biomark Res. 2014 Jan 7;2:1.

36. Korkosz M, Bukowska-Strakova K, Sadis S, Grodzicki T, Siedlar M. Monoclonal antibodies against macrophage colony-stimulating factor diminish the number of circulating intermediate and nonclassical (CD14++CD16+/CD14+CD16++) monocytes in rheumatoid arthritis patient. Blood. 2012 May 31;119(22):5329–30.

37. Burbano C, Vasquez G, Rojas M. Modulatory Effects of CD14+CD16++ Monocytes on CD14++CD16− Monocytes: A Possible Explanation of Monocyte Alterations in Systemic Lupus Erythematosus. Arthritis Rheumatol. 2014 Dec 1;66(12):3371–81.

38. Ancuta P, Rao R, Moses A, Mehle A, Shaw SK, Luscinskas FW, et al. Fractalkine preferentially mediates arrest and migration of CD16+ monocytes. J Exp Med. 2003 Jun 16;197(12):1701–7.

39. Imaizumi T, Yoshida H, Satoh K. Regulation of CX3CL1/fractalkine expression in endothelial cells. J Atheroscler Thromb. 2004;11(1):15–21.

40. Italiani P, Boraschi D. From Monocytes to M1/M2 Macrophages: Phenotypical vs. Functional Differentiation. Front Immunol. 2014;5:514.

41. Gautier EL, Shay T, Miller J, Greter M, Jakubzick C, Ivanov S, et al. Gene-expression profiles and transcriptional regulatory pathways that underlie the identity and diversity of mouse tissue macrophages. Nat Immunol. 2012 Nov;13(11):1118–28.

42. Davalos D, Grutzendler J, Yang G, Kim JV, Zuo Y, Jung S, et al. ATP mediates rapid microglial response to local brain injury in vivo. Nat Neurosci. 2005 Jun;8(6):752–8.

43. Stuart LM, Ezekowitz RAB. Phagocytosis: elegant complexity. Immunity. 2005 May;22(5):539–50.

44. Bogdan C, Vodovotz Y, Nathan C. Macrophage deactivation by interleukin 10. J Exp Med. 1991 Dec 1;174(6):1549–55.

45. Zigmond E, Bernshtein B, Friedlander G, Walker CR, Yona S, Kim K-W, et al. Macrophage-restricted interleukin-10 receptor deficiency, but not IL-10 deficiency, causes severe spontaneous colitis. Immunity. 2014 May 15;40(5):720–33.

46. Butovsky O, Jedrychowski MP, Moore CS, Cialic R, Lanser AJ, Gabriely G, et al. Identification of a unique TGF-β-dependent molecular and functional signature in microglia. Nat Neurosci. 2014 Jan;17(1):131–43.

47. Snelgrove RJ, Goulding J, Didierlaurent AM, Lyonga D, Vekaria S, Edwards L, et al. A critical function for CD200 in lung immune homeostasis and the severity of influenza infection. Nat Immunol. 2008 Sep;9(9):1074–83.

48. Hoek RM, Ruuls SR, Murphy CA, Wright GJ, Goddard R, Zurawski SM, et al. Down-regulation of the macrophage lineage through interaction with OX2 (CD200). Science. 2000 Dec 1;290(5497):1768–71.

49. Murray PJ, Allen JE, Biswas SK, Fisher EA, Gilroy DW, Goerdt S, et al. Macrophage activation and polarization: nomenclature and experimental guidelines. Immunity. 2014 Jul 17;41(1):14–20.

50. Xue J, Schmidt SV, Sander J, Draffehn A, Krebs W, Quester I, et al. Transcriptome-Based Network Analysis Reveals a Spectrum Model of Human Macrophage Activation. Immunity. 2014 Feb 20;40(2):274–88.

51. Hussell T, Bell TJ. Alveolar macrophages: plasticity in a tissue-specific context. Nat Rev Immunol. 2014 Feb;14(2):81–93.

52. Morales-Nebreda L, Misharin AV, Perlman H, Budinger GRS. The heterogeneity of lung macrophages in the susceptibility to disease. Eur Respir Rev. 2015 Sep 1;24(137):505–9.

53. Gordon SB, Read RC. Macrophage defences against respiratory tract infections. Br Med Bull. 2002;61:45–61.

54. Schneberger D, Aharonson-Raz K, Singh B. Monocyte and macrophage heterogeneity and Toll-like receptors in the lung. Cell Tissue Res. 2010 Sep 8;343(1):97–106.

55. Lemke G. Biology of the TAM Receptors. Cold Spring Harb Perspect Biol. 2013 Nov 1;5(11):a009076.

56. Seitz HM, Camenisch TD, Lemke G, Earp HS, Matsushima GK. Macrophages and dendritic cells use different Axl/Mertk/Tyro3 receptors in clearance of apoptotic cells. J Immunol Baltim Md 1950. 2007 May 1;178(9):5635–42.

57. Choi J-Y, Park H-J, Lee Y-J, Byun J, Youn Y-S, Choi JH, et al. Upregulation of Mer Receptor Tyrosine Kinase Signaling Attenuated Lipopolysaccharide-Induced Lung Inflammation. J Pharmacol Exp Ther. 2013 Feb 1;344(2):447–58.

58. Hiraiwa K, van Eeden SF. Contribution of lung macrophages to the inflammatory responses induced by exposure to air pollutants. Mediators Inflamm. 2013;2013:619523.

59. Palecanda A, Paulauskis J, Al-Mutairi E, Imrich A, Qin G, Suzuki H, et al. Role of the scavenger receptor MARCO in alveolar macrophage binding of unopsonized environmental particles. J Exp Med. 1999 May 3;189(9):1497–506.

60. Arredouani MS, Yang Z, Imrich A, Ning Y, Qin G, Kobzik L. The macrophage scavenger receptor SR-AI/II and lung defense against pneumococci and particles. Am J Respir Cell Mol Biol. 2006 Oct;35(4):474–8.

61. Guth AM, Janssen WJ, Bosio CM, Crouch EC, Henson PM, Dow SW. Lung environment determines unique phenotype of alveolar macrophages. Am J Physiol Lung Cell Mol Physiol. 2009 Jun;296(6):L936-946.

62. von Garnier C, Filgueira L, Wikstrom M, Smith M, Thomas JA, Strickland DH, et al. Anatomical location determines the distribution and function of dendritic cells and other APCs in the respiratory tract. J Immunol Baltim Md 1950. 2005 Aug 1;175(3):1609–18.

63. Kaku Y, Imaoka H, Morimatsu Y, Komohara Y, Ohnishi K, Oda H, et al. Overexpression of CD163, CD204 and CD206 on Alveolar Macrophages in the Lungs of Patients with Severe Chronic Obstructive Pulmonary Disease. PLoS ONE [Internet]. 2014 Jan 30 [cited 2016 Mar 24];9(1). Available from: http://www.ncbi.nlm.nih.gov/pmc/articles/PMC3907529/

64. Bharat A, Bhorade SM, Morales-Nebreda L, McQuattie-Pimentel AC, Soberanes S, Ridge K, et al. Flow Cytometry Reveals Similarities Between Lung Macrophages in Humans and Mice. Am J Respir Cell Mol Biol. 2015 Aug 14;54(1):147–9.

65. Blumenthal RL, Campbell DE, Hwang P, DeKruyff RH, Frankel LR, Umetsu DT. Human alveolar macrophages induce functional inactivation in antigen-specific CD4 T cells. J Allergy Clin Immunol. 2001 Feb;107(2):258–64.

66. Roth, Michael D. SHG. Human pulmonary macrophages utilize prostaglandins and transforming growth factor beta 1 to suppress lymphocyte activation. J Leukoc Biol. 1993;53(4):366–371.

67. Melgert BN, Hacken NH ten, Rutgers B, Timens W, Postma DS, Hylkema MN. More alternative activation of macrophages in lungs of asthmatic patients. J Allergy Clin Immunol. 2011 Mar 1;127(3):831–3.

68. Pechkovsky DV, Prasse A, Kollert F, Engel KMY, Dentler J, Luttmann W, et al. Alternatively activated alveolar macrophages in pulmonary fibrosis-mediator production and intracellular signal transduction. Clin Immunol Orlando Fla. 2010 Oct;137(1):89–101.

69. Murray PJ. Understanding and exploiting the endogenous interleukin-10/STAT3-mediated anti-inflammatory response. Curr Opin Pharmacol. 2006 Aug;6(4):379–86.

70. Murray PJ. The primary mechanism of the IL-10-regulated antiinflammatory response is to selectively inhibit transcription. Proc Natl Acad Sci U S A. 2005 Jun 14;102(24):8686–91.

71. Derynck R, Zhang YE. Smad-dependent and Smad-independent pathways in TGF-beta family signalling. Nature. 2003 Oct 9;425(6958):577–84.

72. Yona S, Kim K-W, Wolf Y, Mildner A, Varol D, Breker M, et al. Fate Mapping Reveals Origins and Dynamics of Monocytes and Tissue Macrophages under Homeostasis. Immunity. 2013 Jan 24;38(1):79–91.

73. Hashimoto D, Chow A, Noizat C, Teo P, Beasley MB, Leboeuf M, et al. Tissue-Resident Macrophages Self-Maintain Locally throughout Adult Life with Minimal Contribution from Circulating Monocytes. Immunity. 2013 Apr 18;38(4):792–804.

74. Hopkins HA, Monick MM, Hunninghake GW. Lipopolysaccharide upregulates surface expression of CD14 on human alveolar macrophages. Am J Physiol. 1995 Dec;269(6 Pt 1):L849-854.

75. Landmann R, Knopf HP, Link S, Sansano S, Schumann R, Zimmerli W. Human monocyte CD14 is upregulated by lipopolysaccharide. Infect Immun. 1996 May;64(5):1762–9.

76. Colonna M. TREMs in the immune system and beyond. Nat Rev Immunol. 2003 Jun;3(6):445–53.

77. Fernandez S, Jose P, Avdiushko MG, Kaplan AM, Cohen DA. Inhibition of IL-10 receptor function in alveolar macrophages by Toll-like receptor agonists. J Immunol Baltim Md 1950. 2004 Feb 15;172(4):2613–20.

78. Islam MA, Pröll M, Hölker M, Tholen E, Tesfaye D, Looft C, et al. Alveolar macrophage phagocytic activity is enhanced with LPS priming, and combined stimulation of LPS and lipoteichoic acid synergistically induce pro-inflammatory cytokines in pigs. Innate Immun. 2013 Dec;19(6):631–43.

79. Steinmüller C, Franke-Ullmann G, Lohmann-Matthes ML, Emmendörffer A. Local activation of nonspecific defense against a respiratory model infection by application of interferon-gamma: comparison between rat alveolar and interstitial lung macrophages. Am J Respir Cell Mol Biol. 2000 Apr;22(4):481–90.

80. Högner K, Wolff T, Pleschka S, Plog S, Gruber AD, Kalinke U, et al. Macrophage-expressed IFN-β Contributes to Apoptotic Alveolar Epithelial Cell Injury in Severe Influenza Virus Pneumonia. PLOS Pathog. 2013 Feb 28;9(2):e1003188.

81. Herold S, Steinmueller M, Wulffen W von, Cakarova L, Pinto R, Pleschka S, et al. Lung epithelial apoptosis in influenza virus pneumonia: the role of macrophage-expressed TNF-related apoptosis-inducing ligand. J Exp Med. 2008 Dec 22;205(13):3065–77.

82. Gwyer Findlay E, Hussell T. Macrophage-mediated inflammation and disease: a focus on the lung. Mediators Inflamm. 2012;2012:140937.

83. Bonfield TL, Panuska JR, Konstan MW, Hilliard KA, Hilliard JB, Ghnaim H, et al. Inflammatory cytokines in cystic fibrosis lungs. Am J Respir Crit Care Med. 1995 Dec;152(6 Pt 1):2111–8.

84. Palfreyman RW, Watson ML, Eden C, Smith AW. Induction of biologically active interleukin-8 from lung epithelial cells by Burkholderia (Pseudomonas) cepacia products. Infect Immun. 1997 Feb;65(2):617–22.

85. De Soyza A, Ellis CD, Khan CMA, Corris PA, Demarco de Hormaeche R. Burkholderia cenocepacia lipopolysaccharide, lipid A, and proinflammatory activity. Am J Respir Crit Care Med. 2004 Jul 1;170(1):70–7.

86. Martinet Y, Rom WN, Grotendorst GR, Martin GR, Crystal RG. Exaggerated Spontaneous Release of Platelet-Derived Growth Factor by Alveolar Macrophages from Patients with Idiopathic Pulmonary Fibrosis. N Engl J Med. 1987 Jul 23;317(4):202–9.

87. Wynn TA. Integrating mechanisms of pulmonary fibrosis. J Exp Med. 2011 Jul 4;208(7):1339–50.

88. Song E, Ouyang N, Hörbelt M, Antus B, Wang M, Exton MS. Influence of alternatively and classically activated macrophages on fibrogenic activities of human fibroblasts. Cell Immunol. 2000 Aug 25;204(1):19–28.

89. Ghosh S, Gregory D, Smith A, Kobzik L. MARCO regulates early inflammatory responses against influenza: a useful macrophage function with adverse outcome. Am J Respir Cell Mol Biol. 2011 Nov;45(5):1036–44.

90. Tate MD, Pickett DL, van Rooijen N, Brooks AG, Reading PC. Critical role of airway macrophages in modulating disease severity during influenza virus infection of mice. J Virol. 2010 Aug;84(15):7569–80.

91. Kim HM, Lee Y-W, Lee K-J, Kim HS, Cho SW, van Rooijen N, et al. Alveolar macrophages are indispensable for controlling influenza viruses in lungs of pigs. J Virol. 2008 May;82(9):4265–74.

92. Byrne AJ, Mathie SA, Gregory LG, Lloyd CM. Pulmonary macrophages: key players in the innate defence of the airways. Thorax. 2015 Dec;70(12):1189–96.

93. Chacón-Salinas R, Serafín-López J, Ramos-Payán R, Méndez-Aragón P, Hernández-Pando R, Van Soolingen D, et al. Differential pattern of cytokine expression by macrophages infected in vitro with different Mycobacterium tuberculosis genotypes. Clin Exp Immunol. 2005 Jun;140(3):443–9.

94. Medeiros AI, Serezani CH, Lee SP, Peters-Golden M. Efferocytosis impairs pulmonary macrophage and lung antibacterial function via PGE2/EP2 signaling. J Exp Med. 2009 Jan 16;206(1):61–8.

95. Traves SL, Culpitt SV, Russell REK, Barnes PJ, Donnelly LE. Increased levels of the chemokines GROalpha and MCP-1 in sputum samples from patients with COPD. Thorax. 2002 Jul;57(7):590–5.

96. Eltboli O, Bafadhel M, Hollins F, Wright A, Hargadon B, Kulkarni N, et al. COPD exacerbation severity and frequency is associated with impaired macrophage efferocytosis of eosinophils. BMC Pulm Med. 2014;14:112.

97. Hodge S, Hodge G, Scicchitano R, Reynolds PN, Holmes M. Alveolar macrophages from subjects with chronic obstructive pulmonary disease are deficient in their ability to phagocytose apoptotic airway epithelial cells. Immunol Cell Biol. 2003 Aug;81(4):289–96.

98. Taylor AE, Finney-Hayward TK, Quint JK, Thomas CMR, Tudhope SJ, Wedzicha JA, et al. Defective macrophage phagocytosis of bacteria in COPD. Eur Respir J. 2010 May;35(5):1039–47.

99. Bang B-R, Chun E, Shim E-J, Lee H-S, Lee S-Y, Cho S-H, et al. Alveolar macrophages modulate allergic inflammation in a murine model of asthma. Exp Mol Med. 2011 May 31;43(5):275–80.

100. Careau E, Bissonnette EY. Adoptive transfer of alveolar macrophages abrogates bronchial hyperresponsiveness. Am J Respir Cell Mol Biol. 2004 Jul;31(1):22–7.

101. Upham JW, Strickland DH, Bilyk N, Robinson BW, Holt PG. Alveolar macrophages from humans and rodents selectively inhibit T-cell proliferation but permit T-cell activation and cytokine secretion. Immunology. 1995 Jan;84(1):142–7.

102. Holt PG, Oliver J, Bilyk N, McMenamin C, McMenamin PG, Kraal G, et al. Downregulation of the antigen presenting cell function(s) of pulmonary dendritic cells in vivo by resident alveolar macrophages. J Exp Med. 1993 Feb 1;177(2):397–407.

103. Zasłona Z, Przybranowski S, Wilke C, van Rooijen N, Teitz-Tennenbaum S, Osterholzer JJ, et al. Resident alveolar macrophages suppress while recruited monocytes promote allergic lung inflammation in murine models of asthma. J Immunol Baltim Md 1950. 2014 Oct 15;193(8):4245–53.

104. Moon K-A, Kim SY, Kim T-B, Yun ES, Park C-S, Cho YS, et al. Allergen-induced CD11b+ CD11c(int) CCR3+ macrophages in the lung promote eosinophilic airway inflammation in a mouse asthma model. Int Immunol. 2007 Dec;19(12):1371–81.

105. Nomura H, Sato E, Koyama S, Haniuda M, Kubo K, Nagai S, et al. Histamine stimulates alveolar macrophages to release neutrophil and monocyte chemotactic activity. J Lab Clin Med. 2001 Oct;138(4):226–35.

106. Balhara J, Gounni AS. The alveolar macrophages in asthma: a double-edged sword. Mucosal Immunol. 2012 Nov;5(6):605–9.

107. Huynh M-LN, Malcolm KC, Kotaru C, Tilstra JA, Westcott JY, Fadok VA, et al. Defective apoptotic cell phagocytosis attenuates prostaglandin E2 and 15-hydroxyeicosatetraenoic acid in severe asthma alveolar macrophages. Am J Respir Crit Care Med. 2005 Oct 15;172(8):972–9.

108. Fitzpatrick AM, Holguin F, Teague WG, Brown LAS. Alveolar macrophage phagocytosis is impaired in children with poorly controlled asthma. J Allergy Clin Immunol. 2008 Jun;121(6):1372–1378.e3.

109. Ware LB, Matthay MA. The acute respiratory distress syndrome. N Engl J Med. 2000 May 4;342(18):1334–49.

110. Dushianthan A, Grocott MPW, Postle AD, Cusack R. Acute respiratory distress syndrome and acute lung injury. Postgrad Med J. 2011 Sep 1;87(1031):612–22.

111. The ARDS Definition Task Force*. Acute respiratory distress syndrome: The berlin definition. JAMA. 2012 Jun 20;307(23):2526–33.

112. Ely EW, Wheeler AP, Thompson BT, Ancukiewicz M, Steinberg KP, Bernard GR. Recovery rate and prognosis in older persons who develop acute lung injury and the acute respiratory distress syndrome. Ann Intern Med. 2002 Jan 1;136(1):25–36.

113. Wheeler AP, Bernard GR. Acute lung injury and the acute respiratory distress syndrome: a clinical review. The Lancet. 2007 May;369(9572):1553–64.

114. Bellani G, Laffey JG, Pham T, Fan E, Brochard L, Esteban A, et al. Epidemiology, Patterns of Care, and Mortality for Patients With Acute Respiratory Distress Syndrome in Intensive Care Units in 50 Countries. JAMA. 2016 Feb 23;315(8):788–800.

115. Orme J, Romney JS, Hopkins RO, Pope D, Chan KJ, Thomsen G, et al. Pulmonary function and health-related quality of life in survivors of acute respiratory distress syndrome. Am J Respir Crit Care Med. 2003 Mar 1;167(5):690–4.

116. Wiener-Kronish JP, Albertine KH, Matthay MA. Differential responses of the endothelial and epithelial barriers of the lung in sheep to Escherichia coli endotoxin. J Clin Invest. 1991 Sep;88(3):864–75.

117. Ware LB, Matthay MA. Alveolar fluid clearance is impaired in the majority of patients with acute lung injury and the acute respiratory distress syndrome. Am J Respir Crit Care Med. 2001 May;163(6):1376–83.

118. Pugin J, Verghese G, Widmer MC, Matthay MA. The alveolar space is the site of intense inflammatory and profibrotic reactions in the early phase of acute respiratory distress syndrome. Crit Care Med. 1999 Feb;27(2):304–12.

119. Rosseau S, Hammerl P, Maus U, Walmrath HD, Schütte H, Grimminger F, et al. Phenotypic characterization of alveolar monocyte recruitment in acute respiratory distress syndrome. Am J Physiol Lung Cell Mol Physiol. 2000 Jul;279(1):L25-35.

120. Nakata K, Akagawa KS, Fukayama M, Hayashi Y, Kadokura M, Tokunaga T. Granulocyte-macrophage colony-stimulating factor promotes the proliferation of human alveolar macrophages in vitro. J Immunol Baltim Md 1950. 1991 Aug 15;147(4):1266–72.

121. Aggarwal NR, King LS, D'Alessio FR. Diverse macrophage populations mediate acute lung inflammation and resolution. Am J Physiol - Lung Cell Mol Physiol. 2014 Apr 15;306(8):L709–25.

122. Matute-Bello G, Liles WC, Radella F, Steinberg KP, Ruzinski JT, Hudson LD, et al. Modulation of neutrophil apoptosis by granulocyte colony-stimulating factor and granulocyte/macrophage colony-stimulating factor during the course of acute respiratory distress syndrome. Crit Care Med. 2000 Jan;28(1):1–7.

123. Paine R, Standiford TJ, Dechert RE, Moss M, Martin GS, Rosenberg AL, et al. A randomized trial of recombinant human granulocyte-macrophage colony stimulating factor for patients with acute lung injury. Crit Care Med. 2012 Jan;40(1):90–7.

124. Herold S, Mayer K, Lohmeyer J. Acute Lung Injury: How Macrophages Orchestrate Resolution of Inflammation and Tissue Repair. Front Immunol [Internet]. 2011 Nov 24 [cited 2014 May 6];2. Available from: http://www.ncbi.nlm.nih.gov/pmc/articles/PMC3342347/

125. Landsman L, Jung S. Lung macrophages serve as obligatory intermediate between blood monocytes and alveolar macrophages. J Immunol Baltim Md 1950. 2007 Sep 15;179(6):3488–94.

126. Srivastava M, Jung S, Wilhelm J, Fink L, Bühling F, Welte T, et al. The inflammatory versus constitutive trafficking of mononuclear phagocytes into the alveolar space of mice is associated with drastic changes in their gene expression profiles. J Immunol Baltim Md 1950. 2005 Aug 1;175(3):1884–93.

127. Gordon S, Martinez FO. Alternative activation of macrophages: mechanism and functions. Immunity. 2010 May 28;32(5):593–604.

128. Maus UA, Janzen S, Wall G, Srivastava M, Blackwell TS, Christman JW, et al. Resident Alveolar Macrophages Are Replaced by Recruited Monocytes in Response to Endotoxin-Induced Lung Inflammation. Am J Respir Cell Mol Biol. 2006 Aug 1;35(2):227–35.

129. Barr LC, Brittan M, Morris AC, McAuley DF, McCormack C, Fletcher AM, et al. A randomized controlled trial of peripheral blood mononuclear cell depletion in experimental human lung inflammation. Am J Respir Crit Care Med. 2013 Aug 15;188(4):449–55.

130. Dhaliwal K, Scholefield E, Ferenbach D, Gibbons M, Duffin R, Dorward DA, et al. Monocytes Control Second-Phase Neutrophil Emigration in Established

Lipopolysaccharide-induced Murine Lung Injury. Am J Respir Crit Care Med. 2012 Sep 15;186(6):514–24.

131. Tasaka S, Ishizaka A, Urano T, Sayama K, Sakamaki F, Nakamura H, et al. BCG priming enhances endotoxin-induced acute lung injury independent of neutrophils. Am J Respir Crit Care Med. 1995 Sep 1;152(3):1041–9.

132. Ricciotti E, FitzGerald GA. Prostaglandins and Inflammation. Arterioscler Thromb Vasc Biol. 2011 May;31(5):986–1000.

133. Kawata R, Reddy ST, Wolner B, Herschman HR. Prostaglandin synthase 1 and prostaglandin synthase 2 both participate in activation-induced prostaglandin D2 production in mast cells. J Immunol Baltim Md 1950. 1995 Jul 15;155(2):818–25.

134. Murakami M, Bingham CO, Matsumoto R, Austen KF, Arm JP. IgE-dependent activation of cytokine-primed mouse cultured mast cells induces a delayed phase of prostaglandin D2 generation via prostaglandin endoperoxide synthase-2. J Immunol Baltim Md 1950. 1995 Nov 1;155(9):4445–53.

135. Matsumoto H, Naraba H, Murakami M, Kudo I, Yamaki K, Ueno A, et al. Concordant induction of prostaglandin E2 synthase with cyclooxygenase-2 leads to preferred production of prostaglandin E2 over thromboxane and prostaglandin D2 in lipopolysaccharide-stimulated rat peritoneal macrophages. Biochem Biophys Res Commun. 1997 Jan 3;230(1):110–4.

136. Joo M, Sadikot RT, Joo M, Sadikot RT. PGD Synthase and PGD2 in Immune Resposne, PGD Synthase and PGD2 in Immune Resposne. Mediat Inflamm Mediat Inflamm. 2012 Jun 25;2012, 2012:e503128.

137. Lee S, Jang E, Kim J-H, Kim J-H, Lee W-H, Suk K. Lipocalin-type Prostaglandin D2 Synthase Protein Regulates Glial Cell Migration and Morphology through Myristoylated Alanine-rich C-Kinase Substrate PROSTAGLANDIN D2-INDEPENDENT EFFECTS. J Biol Chem. 2012 Mar 16;287(12):9414–28.

138. Kanaoka Y, Ago H, Inagaki E, Nanayama T, Miyano M, Kikuno R, et al. Cloning and Crystal Structure of Hematopoietic Prostaglandin D Synthase. Cell. 1997 Sep 19;90(6):1085–95.

139. Grill M, Heinemann A, Hoefler G, Peskar BA, Schuligoi R. Effect of endotoxin treatment on the expression and localization of spinal cyclooxygenase, prostaglandin synthases, and PGD2 receptors. J Neurochem. 2008 Mar;104(5):1345–57.

140. Mahmud I, Ueda N, Yamaguchi H, Yamashita R, Yamamoto S, Kanaoka Y, et al. Prostaglandin D Synthase in Human Megakaryoblastic Cells. J Biol Chem. 1997 Nov 7;272(45):28263–6.

141. Inoue T, Irikura D, Okazaki N, Kinugasa S, Matsumura H, Uodome N, et al. Mechanism of metal activation of human hematopoietic prostaglandin D synthase. Nat Struct Biol. 2003 Apr;10(4):291–6.

142. Fukushima M. Biological activities and mechanisms of action of PGJ2 and related compounds: an update. Prostaglandins Leukot Essent Fatty Acids. 1992 Sep;47(1):1–12.

143. Ray DM, Akbiyik F, Phipps RP. The Peroxisome Proliferator-Activated Receptor γ (PPARγ) Ligands 15-Deoxy-Δ12,14-Prostaglandin J2 and Ciglitazone Induce Human B

Lymphocyte and B Cell Lymphoma Apoptosis by PPARγ-Independent Mechanisms. J Immunol. 2006 Oct 15;177(8):5068–76.

144. Russel F, Koenderink J, Masereeuw R. Multidrug resistance protein 4 (MRP4/ABCC4): a versatile efflux transporter for drugs and signalling molecules. Trends Pharmacol Sci. 2008 Apr;29(4):200–7.

145. Schuster VL. Prostaglandin transport. Prostaglandins Other Lipid Mediat. 2002 Aug;68–69:633–47.

146. Coleman RA, Sheldrick RL. Prostanoid-induced contraction of human bronchial smooth muscle is mediated by TP-receptors. Br J Pharmacol. 1989 Mar;96(3):688–92.

147. Takeda S, Kadowaki S, Haga T, Takaesu H, Mitaku S. Identification of G protein-coupled receptor genes from the human genome sequence. FEBS Lett. 2002 Jun 5;520(1–3):97–101.

148. De Lean A, Stadel JM, Lefkowitz RJ. A ternary complex model explains the agonist-specific binding properties of the adenylate cyclase-coupled beta-adrenergic receptor. J Biol Chem. 1980 Aug 10;255(15):7108–17.

149. Hirata M, Kakizuka A, Aizawa M, Ushikubi F, Narumiya S. Molecular characterization of a mouse prostaglandin D receptor and functional expression of the cloned gene. Proc Natl Acad Sci U S A. 1994 Nov 8;91(23):11192–6.

150. Boie Y, Sawyer N, Slipetz DM, Metters KM, Abramovitz M. Molecular Cloning and Characterization of the Human Prostanoid DP Receptor. J Biol Chem. 1995 Aug 11;270(32):18910–6.

151. Whittle BJ, Moncada S, Mullane K, Vane JR. Platelet and cardiovascular activity of the hydantoin BW245C, a potent prostaglandin analogue. Prostaglandins. 1983 Feb;25(2):205–23.

152. Matsuoka T. Prostaglandin D2 as a Mediator of Allergic Asthma. Science. 2000 Mar 17;287(5460):2013–7.

153. Hirano Y, Shichijo M, Ikeda M, Kitaura M, Tsuchida J, Asanuma F, et al. Prostanoid DP receptor antagonists suppress symptomatic asthma-like manifestation by distinct actions from a glucocorticoid in rats. Eur J Pharmacol. 2011 Sep;666(1–3):233–41.

154. Gervais FG, Cruz RP, Chateauneuf A, Gale S, Sawyer N, Nantel F, et al. Selective modulation of chemokinesis, degranulation, and apoptosis in eosinophils through the PGD2 receptors CRTH2 and DP. J Allergy Clin Immunol. 2001 Dec;108(6):982–8.

155. Yoshimura-Uchiyama C, Iikura M, Yamaguchi M, Nagase H, Ishii A, Matsushima K, et al. Differential modulation of human basophil functions through prostaglandin D2 receptors DP and chemoattractant receptor-homologous molecule expressed on Th2 cells/DP2. Clin Exp Allergy J Br Soc Allergy Clin Immunol. 2004 Aug;34(8):1283–90.

156. Hammad H, Kool M, Soullié T, Narumiya S, Trottein F, Hoogsteden HC, et al. Activation of the D prostanoid 1 receptor suppresses asthma by modulation of lung dendritic cell function and induction of regulatory T cells. J Exp Med. 2007 Feb 19;204(2):357–67.

157. Isidoro-García M, Sanz C, García-Solaesa V, Pascual M, Pescador DB, Lorente F, et al. PTGDR gene in asthma: a functional, genetic, and epigenetic study. Allergy. 2011 Dec 1;66(12):1553–62.

158. Zhu G, Vestbo J, Lenney W, Silverman M, Whyte M, Helms P, et al. Association of PTGDR gene polymorphisms with asthma in two Caucasian populations. Genes Immun. 2007 Jul;8(5):398–403.

159. Marchese A, Sawzdargo M, Nguyen T, Cheng R, Heng HH, Nowak T, et al. Discovery of three novel orphan G-protein-coupled receptors. Genomics. 1999 Feb 15;56(1):12–21.

160. Nagata K, Tanaka K, Ogawa K, Kemmotsu K, Imai T, Yoshie O, et al. Selective expression of a novel surface molecule by human Th2 cells in vivo. J Immunol Baltim Md 1950. 1999 Feb 1;162(3):1278–86.

161. Nagata K, Hirai H. The second PGD2 receptor CRTH2: structure, properties, and functions in leukocytes. Prostaglandins Leukot Essent Fatty Acids. 2003 Aug 1;69(2):169–77.

162. Gosset P, Bureau F, Angeli V, Pichavant M, Faveeuw C, Tonnel A-B, et al. Prostaglandin D2 affects the maturation of human monocyte-derived dendritic cells: consequence on the polarization of naive Th cells. J Immunol Baltim Md 1950. 2003 May 15;170(10):4943–52.

163. Tajima T, Murata T, Aritake K, Urade Y, Hirai H, Nakamura M, et al. Lipopolysaccharide induces macrophage migration via prostaglandin D(2) and prostaglandin E(2). J Pharmacol Exp Ther. 2008 Aug;326(2):493–501.

164. Monneret G, Gravel S, Diamond M, Rokach J, Powell WS. Prostaglandin D2 is a potent chemoattractant for human eosinophils that acts via a novel DP receptor. Blood. 2001 Sep 15;98(6):1942–8.

165. Mesquita-Santos FP, Bakker-Abreu I, Luna-Gomes T, Bozza PT, Diaz BL, Bandeira-Melo C. Co-operative signalling through DP(1) and DP(2) prostanoid receptors is required to enhance leukotriene C(4) synthesis induced by prostaglandin D(2) in eosinophils. Br J Pharmacol. 2011 Apr;162(8):1674–85.

166. Hirai H, Tanaka K, Yoshie O, Ogawa K, Kenmotsu K, Takamori Y, et al. Prostaglandin D2 selectively induces chemotaxis in T helper type 2 cells, eosinophils, and basophils via seven-transmembrane receptor CRTH2. J Exp Med. 2001 Jan 15;193(2):255–61.

167. Almishri W, Cossette C, Rokach J, Martin JG, Hamid Q, Powell WS. Effects of prostaglandin D2, 15-deoxy-Delta12,14-prostaglandin J2, and selective DP1 and DP2 receptor agonists on pulmonary infiltration of eosinophils in Brown Norway rats. J Pharmacol Exp Ther. 2005 Apr;313(1):64–9.

168. Shiraishi Y, Asano K, Nakajima T, Oguma T, Suzuki Y, Shiomi T, et al. Prostaglandin D2-induced eosinophilic airway inflammation is mediated by CRTH2 receptor. J Pharmacol Exp Ther. 2005 Mar;312(3):954–60.

169. Spik I, Brénuchon C, Angéli V, Staumont D, Fleury S, Capron M, et al. Activation of the prostaglandin D2 receptor DP2/CRTH2 increases allergic inflammation in mouse. J Immunol Baltim Md 1950. 2005 Mar 15;174(6):3703–8.

170. Tanaka K, Hirai H, Takano S, Nakamura M, Nagata K. Effects of prostaglandin D2 on helper T cell functions. Biochem Biophys Res Commun. 2004 Apr 16;316(4):1009–14.

171. Uller L, Mathiesen JM, Alenmyr L, Korsgren M, Ulven T, Högberg T, et al. Antagonism of the prostaglandin D2 receptor CRTH2 attenuates asthma pathology in mouse eosinophilic airway inflammation. Respir Res. 2007;8:16.

172. Lukacs NW, Berlin AA, Franz-Bacon K, Sásik R, Sprague LJ, Ly TW, et al. CRTH2 antagonism significantly ameliorates airway hyperreactivity and downregulates inflammation-induced genes in a mouse model of airway inflammation. Am J Physiol Lung Cell Mol Physiol. 2008 Nov;295(5):L767-779.

173. Oiwa M, Satoh T, Watanabe M, Niwa H, Hirai H, Nakamura M, et al. CRTH2-dependent, STAT6-independent induction of cedar pollen dermatitis. Clin Exp Allergy J Br Soc Allergy Clin Immunol. 2008 Aug;38(8):1357–66.

174. Shiraishi Y, Asano K, Niimi K, Fukunaga K, Wakaki M, Kagyo J, et al. Cyclooxygenase-2/prostaglandin D2/CRTH2 pathway mediates double-stranded RNA-induced enhancement of allergic airway inflammation. J Immunol Baltim Md 1950. 2008 Jan 1;180(1):541–9.

175. Boehme SA, Chen EP, Franz-Bacon K, Sásik R, Sprague LJ, Ly TW, et al. Antagonism of CRTH2 ameliorates chronic epicutaneous sensitization-induced inflammation by multiple mechanisms. Int Immunol. 2009 Jan;21(1):1–17.

176. Sturm EM, Radnai B, Jandl K, Stančić A, Parzmair GP, Högenauer C, et al. Opposing Roles of Prostaglandin D2 Receptors in Ulcerative Colitis. J Immunol. 2014 Jul 15;193(2):827–39.

177. Sawyer N, Cauchon E, Chateauneuf A, Cruz RPG, Nicholson DW, Metters KM, et al. Molecular pharmacology of the human prostaglandin D2 receptor, CRTH2. Br J Pharmacol. 2002 Dec;137(8):1163–72.

178. Schuligoi R, Schmidt R, Geisslinger G, Kollroser M, Peskar BA, Heinemann A. PGD2 metabolism in plasma: kinetics and relationship with bioactivity on DP1 and CRTH2 receptors. Biochem Pharmacol. 2007 Jun 30;74(1):107–17.

179. Schuligoi R, Sedej M, Waldhoer M, Vukoja A, Sturm EM, Lippe IT, et al. Prostaglandin H2 induces the migration of human eosinophils through the chemoattractant receptor homologous molecule of Th2 cells, CRTH2. J Leukoc Biol. 2009 Jan;85(1):136–45.

180. Böhm E, Sturm GJ, Weiglhofer I, Sandig H, Shichijo M, McNamee A, et al. 11-Dehydro-thromboxane B2, a stable thromboxane metabolite, is a full agonist of chemoattractant receptor-homologous molecule expressed on TH2 cells (CRTH2) in human eosinophils and basophils. J Biol Chem. 2004 Feb 27;279(9):7663–70.

181. Lewis RA, Soter NA, Diamond PT, Austen KF, Oates JA, Roberts LJ 2nd. Prostaglandin D2 generation after activation of rat and human mast cells with anti-IgE. J Immunol Baltim Md 1950. 1982 Oct;129(4):1627–31.

182. Luna-Gomes T, Magalhães KG, Mesquita-Santos FP, Bakker-Abreu I, Samico RF, Molinaro R, et al. Eosinophils as a novel cell source of prostaglandin D2: autocrine role in allergic inflammation. J Immunol Baltim Md 1950. 2011 Dec 15;187(12):6518–26.

183. Tanaka K, Ogawa K, Sugamura K, Nakamura M, Takano S, Nagata K. Cutting edge: differential production of prostaglandin D2 by human helper T cell subsets. J Immunol Baltim Md 1950. 2000 Mar 1;164(5):2277–80.

184. Zhao G, Yu R, Deng J, Zhao Q, Li Y, Joo M, et al. Pivotal role of reactive oxygen species in differential regulation of lipopolysaccharide-induced prostaglandins production in macrophages. Mol Pharmacol. 2013 Jan;83(1):167–78.

185. Hardy CC, Robinson C, Tattersfield AE, Holgate ST. The bronchoconstrictor effect of inhaled prostaglandin D2 in normal and asthmatic men. N Engl J Med. 1984 Jul 26;311(4):209–13.

186. Liu MC, Bleecker ER, Lichtenstein LM, Kagey-Sobotka A, Niv Y, McLemore TL, et al. Evidence for elevated levels of histamine, prostaglandin D2, and other bronchoconstricting prostaglandins in the airways of subjects with mild asthma. Am Rev Respir Dis. 1990 Jul;142(1):126–32.

187. Fajt ML, Gelhaus SL, Freeman B, Uvalle CE, Trudeau JB, Holguin F, et al. Prostaglandin D_2 pathway upregulation: relation to asthma severity, control, and TH2 inflammation. J Allergy Clin Immunol. 2013 Jun;131(6):1504–12.

188. Stinson SE, Amrani Y, Brightling CE. D prostanoid receptor 2 (chemoattractant receptor–homologous molecule expressed on TH2 cells) protein expression in asthmatic patients and its effects on bronchial epithelial cells. J Allergy Clin Immunol [Internet]. [cited 2015 Jan 26]; Available from: http://www.sciencedirect.com/science/article/pii/S0091674914012007

189. Fuentes-Duculan J, Suárez-Fariñas M, Zaba LC, Nograles KE, Pierson KC, Mitsui H, et al. A subpopulation of CD163-positive macrophages is classically activated in psoriasis. J Invest Dermatol. 2010 Oct;130(10):2412–22.

190. Bouhlel MA, Derudas B, Rigamonti E, Dièvart R, Brozek J, Haulon S, et al. PPARγ Activation Primes Human Monocytes into Alternative M2 Macrophages with Anti-inflammatory Properties. Cell Metab. 2007 Aug 8;6(2):137–43.

191. Bernard GR, Artigas A, Brigham KL, Carlet J, Falke K, Hudson L, et al. The American-European Consensus Conference on ARDS. Definitions, mechanisms, relevant outcomes, and clinical trial coordination. Am J Respir Crit Care Med. 1994 Mar;149(3 Pt 1):818–24.

192. Travis WD, Costabel U, Hansell DM, King TE, Lynch DA, Nicholson AG, et al. An Official American Thoracic Society/European Respiratory Society Statement: Update of the International Multidisciplinary Classification of the Idiopathic Interstitial Pneumonias. Am J Respir Crit Care Med. 2013 Sep 15;188(6):733–48.

193. Grill M, Heinemann A, Hoefler G, Peskar BA, Schuligoi R. Effect of endotoxin treatment on the expression and localization of spinal cyclooxygenase, prostaglandin synthases, and PGD2 receptors. J Neurochem. 2008 Mar;104(5):1345–57.

194. Vong L, Ferraz JGP, Panaccione R, Beck PL, Wallace JL. A pro-resolution mediator, prostaglandin D(2), is specifically up-regulated in individuals in long-term remission from ulcerative colitis. Proc Natl Acad Sci U S A. 2010 Jun 29;107(26):12023–7.

195. Schuligoi R, Sedej M, Waldhoer M, Vukoja A, Sturm EM, Lippe IT, et al. Prostaglandin H2 induces the migration of human eosinophils through the chemoattractant receptor homologous molecule of Th2 cells, CRTH2. J Leukoc Biol. 2008 Oct 23;85(1):136–45.

196. Heinemann A, Schuligoi R, Sabroe I, Hartnell A, Peskar BA. Delta 12-prostaglandin J2, a plasma metabolite of prostaglandin D2, causes eosinophil mobilization from the bone marrow and primes eosinophils for chemotaxis. J Immunol Baltim Md 1950. 2003 May 1;170(9):4752–8.

197. Grynkiewicz G, Poenie M, Tsien RY. A New Generation of Ca2+ Indicators with Greatly Improved Fluorescence Properties. J Biol Chem. 1985 Mar 25;260(6):3440–50.

198. Bálint Z, Zabini D, Konya V, Nagaraj C, Végh AG, Váró G, et al. Double-Stranded RNA Attenuates the Barrier Function of Human Pulmonary Artery Endothelial Cells. PLoS ONE. 2013 Jun 3;8(6):e63776.

199. Jörgl A, Platzer B, Taschner S, Heinz LX, Höcher B, Reisner PM, et al. Human Langerhans-cell activation triggered in vitro by conditionally expressed MKK6 is counterregulated by the downstream effector RelB. Blood. 2007 Jan 1;109(1):185–93.

200. van Rijt LS, Kuipers H, Vos N, Hijdra D, Hoogsteden HC, Lambrecht BN. A rapid flow cytometric method for determining the cellular composition of bronchoalveolar lavage fluid cells in mouse models of asthma. J Immunol Methods. 2004 May;288(1–2):111–21.

201. Schicho R, Storr M. Topical and Systemic Cannabidiol Improves Trinitrobenzene Sulfonic Acid Colitis in Mice. Pharmacology. 2012 Apr;89(3–4):149–55.

202. Peng X, Hassoun PM, Sammani S, McVerry BJ, Burne MJ, Rabb H, et al. Protective Effects of Sphingosine 1-Phosphate in Murine Endotoxin-induced Inflammatory Lung Injury. Am J Respir Crit Care Med. 2004 Jun 1;169(11):1245–51.

203. Reutershan J, Chang D, Hayes JK, Ley K. Protective effects of isoflurane pretreatment in endotoxin-induced lung injury. Anesthesiology. 2006 Mar;104(3):511–7.

204. Balgoma D, Larsson J, Rokach J, Lawson JA, Daham K, Dahlén B, et al. Quantification of Lipid Mediator Metabolites in Human Urine from Asthma Patients by Electrospray Ionization Mass Spectrometry: Controlling Matrix Effects. Anal Chem. 2013 Aug 20;85(16):7866–74.

205. Jandl K, Stacher E, Bálint Z, Sturm EM, Maric J, Peinhaupt M, et al. Activated prostaglandin D2 receptors on macrophages enhance neutrophil recruitment into the lung. J Allergy Clin Immunol [Internet]. [cited 2016 Jan 18]; Available from: http://www.sciencedirect.com/science/article/pii/S0091674915017388

206. Xue L, Fergusson J, Salimi M, Panse I, Ussher JE, Hegazy AN, et al. Prostaglandin D2 and leukotriene E4 synergize to stimulate diverse TH2 functions and TH2 cell/neutrophil crosstalk. J Allergy Clin Immunol. 2015 May;135(5):1358–1366.e11.

207. Beck-Schimmer B, Schwendener R, Pasch T, Reyes L, Booy C, Schimmer RC. Alveolar macrophages regulate neutrophil recruitment in endotoxin-induced lung injury. Respir Res. 2005;6(1):61.

208. Alba-Loureiro TC, Martins EF, Miyasaka CK, Lopes LR, Landgraf RG, Jancar S, et al. Evidence that arachidonic acid derived from neutrophils and prostaglandin E2 are associated with the induction of acute lung inflammation by lipopolysaccharide of Escherichia coli. Inflamm Res Off J Eur Histamine Res Soc Al. 2004 Dec;53(12):658–63.

209. Ennis M, Barrow SE, Blair IA. Prostaglandin and histamine release from stimulated rat peritoneal mast cells. Agents Actions. 1984 Apr;14(3–4):397–400.

210. Hempel SL, Monick MM, Hunninghake GW. Lipopolysaccharide induces prostaglandin H synthase-2 protein and mRNA in human alveolar macrophages and blood monocytes. J Clin Invest. 1994 Jan;93(1):391–6.

211. Shirasaki H, Kikuchi M, Kanaizumi E, Himi T. Accumulation of CRTH2-positive leukocytes in human allergic nasal mucosa. Ann Allergy Asthma Immunol Off Publ Am Coll Allergy Asthma Immunol. 2009 Feb;102(2):110–5.

212. Tait Wojno ED, Monticelli LA, Tran SV, Alenghat T, Osborne LC, Thome JJ, et al. The prostaglandin D2 receptor CRTH2 regulates accumulation of group 2 innate lymphoid cells in the inflamed lung. Mucosal Immunol. 2015 Nov;8(6):1313–23.

213. Hoffman JF, Linderman JJ, Omann GM. Receptor up-regulation, internalization, and interconverting receptor states. Critical components of a quantitative description of N-formyl peptide-receptor dynamics in the neutrophil. J Biol Chem. 1996 Aug 2;271(31):18394–404.

214. Sklar LA, Finney DA, Oades ZG, Jesaitis AJ, Painter RG, Cochrane CG. The dynamics of ligand-receptor interactions. Real-time analyses of association, dissociation, and internalization of an N-formyl peptide and its receptors on the human neutrophil. J Biol Chem. 1984 May 10;259(9):5661–9.

215. Sedej M, Schröder R, Bell K, Platzer W, Vukoja A, Kostenis E, et al. D-type prostanoid receptor enhances the signaling of chemoattractant receptor-homologous molecule expressed on T(H)2 cells. J Allergy Clin Immunol. 2012 Feb;129(2):492–500, 500-9.

216. Schratl P, Royer JF, Kostenis E, Ulven T, Sturm EM, Waldhoer M, et al. The role of the prostaglandin D2 receptor, DP, in eosinophil trafficking. J Immunol Baltim Md 1950. 2007 Oct 1;179(7):4792–9.

217. Matute-Bello G, Frevert CW, Martin TR. Animal models of acute lung injury. Am J Physiol Lung Cell Mol Physiol. 2008 Sep;295(3):L379-399.

218. Sturm EM, Radnai B, Jandl K, Stančić A, Parzmair GP, Högenauer C, et al. Opposing roles of prostaglandin d2 receptors in ulcerative colitis. J Immunol Baltim Md 1950. 2014 Jul 15;193(2):827–39.

219. Zamuner SR, Bak AW, Devchand PR, Wallace JL. Predisposition to colorectal cancer in rats with resolved colitis: role of cyclooxygenase-2-derived prostaglandin d2. Am J Pathol. 2005 Nov;167(5):1293–300.

220. Papaliodis D, Boucher W, Kempuraj D, Michaelian M, Wolfberg A, House M, et al. Niacin-induced “flush” involves release of prostaglandin D2 from mast cells and serotonin from platelets: evidence from human cells in vitro and an animal model. J Pharmacol Exp Ther. 2008 Dec;327(3):665–72.

221. Murata T, Aritake K, Tsubosaka Y, Maruyama T, Nakagawa T, Hori M, et al. Anti-inflammatory role of PGD2 in acute lung inflammation and therapeutic application of its signal enhancement. Proc Natl Acad Sci U S A. 2013 Mar 26;110(13):5205–10.

222. Frank JA, Matthay MA. Leukotrienes in Acute Lung Injury. Am J Respir Crit Care Med. 2005 Aug 1;172(3):261–2.

223. Fukunaga K, Kohli P, Bonnans C, Fredenburgh LE, Levy BD. Cyclooxygenase 2 Plays a Pivotal Role in the Resolution of Acute Lung Injury. J Immunol. 2005 Apr 15;174(8):5033–9.

224. Mochizuki M, Ishii Y, Itoh K, Iizuka T, Morishima Y, Kimura T, et al. Role of 15-deoxy delta(12,14) prostaglandin J2 and Nrf2 pathways in protection against acute lung injury. Am J Respir Crit Care Med. 2005 Jun 1;171(11):1260–6.

225. Konya V, Maric J, Jandl K, Luschnig P, Aringer I, Lanz I, et al. Activation of EP4 receptors prevents endotoxin-induced neutrophil infiltration into the airways and enhances microvascular barrier function. Br J Pharmacol. 2015 Jun 23;

226. Göggel R, Hoffman S, Nüsing R, Narumiya S, Uhlig S. Platelet-activating factor-induced pulmonary edema is partly mediated by prostaglandin E(2), E-prostanoid 3-receptors, and potassium channels. Am J Respir Crit Care Med. 2002 Sep 1;166(5):657–62.

227. Xue L, Fergusson J, Salimi M, Panse I, Ussher JE, Hegazy AN, et al. Prostaglandin D2 and leukotriene E4 synergize to stimulate diverse TH2 functions and TH2 cell/neutrophil crosstalk. J Allergy Clin Immunol. 2015 May;135(5):1358–1366.e11.

228. Baron RM, Levy BD. Recent advances in understanding and treating ARDS. F1000Research. 2016;5.

229. Briel M, Meade M, Mercat A, Brower RG, Talmor D, Walter SD, et al. Higher versus lower positive end-expiratory pressure in patients with acute lung injury and acute respiratory distress syndrome: systematic review and meta-analysis. JAMA. 2010 Mar 3;303(9):865–73.

230. Raghavendran K, Pryhuber GS, Chess PR, Davidson BA, Knight PR, Notter RH. Pharmacotherapy of acute lung injury and acute respiratory distress syndrome. Curr Med Chem. 2008;15(19):1911–24.

231. Barnes N, Pavord I, Chuchalin A, Bell J, Hunter M, Lewis T, et al. A randomized, double-blind, placebo-controlled study of the CRTH2 antagonist OC000459 in moderate persistent asthma. Clin Exp Allergy J Br Soc Allergy Clin Immunol. 2012 Jan;42(1):38–48.

232. Hall IP, Fowler AV, Gupta A, Tetzlaff K, Nivens MC, Sarno M, et al. Efficacy of BI 671800, an oral CRTH2 antagonist, in poorly controlled asthma as sole controller and in the presence of inhaled corticosteroid treatment. Pulm Pharmacol Ther. 2015 Jun;32:37–44.

233. Wang JW, Woodward DF, Martos JL, Cornell CL, Carling RW, Kingsley PJ, et al. Multitargeting of selected prostanoid receptors provides agents with enhanced anti-inflammatory activity in macrophages. FASEB J. 2015 Sep 29;fj.15-275610.